

## 17. SITE 227

The Shipboard Scientific Party<sup>1</sup>

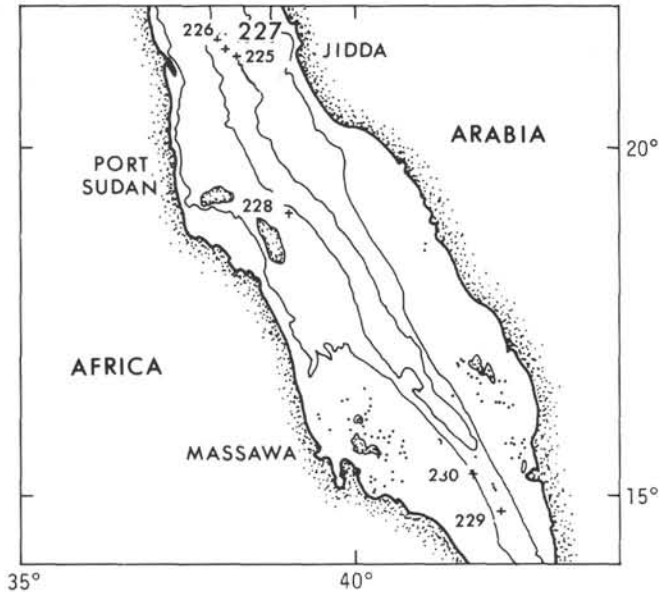


Figure 1. Bathymetric chart showing the position of Site 227 and other Leg 23 sites in the Red Sea. Contours at 500 and 1000 fathoms, from Laughton (1970).

### SITE DATA

Dates: 1320 18 Apr-1605 21 Apr 72

Time: 75 hours

Position (Figure 1): 21°19.86'N, 38°07.97'E

Holes Drilled: 1

Water Depth by Echo-Sounder: 1795 corr. meters

Total Penetration: 359 meters

Total Core Recovered: 123.5 meters from 45 cores

Age of Oldest Sediment: Late Miocene

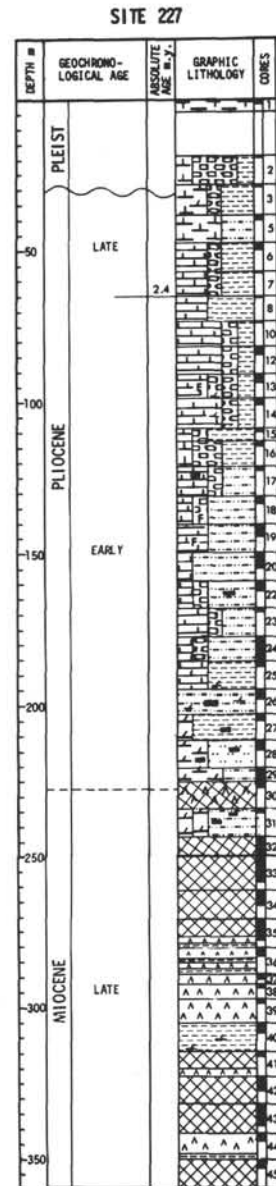
Basement: Not reached

### ABSTRACT

Site 227 was drilled on the edge of the axial trough about 5 km east of Site 226 and the Atlantis II Deep. The hole was drilled to a depth of 350 meters and was terminated 133 meters into a Late Miocene evaporite sequence. Four distinct lithological units were identified which are similar to, and apparently correlatable with, sedimentary units penetrated at Site 225.

Lithologic and paleontologic data suggest restricted evaporite conditions during the Miocene gradually evolving to more open ocean conditions which persisted in the Pliocene and Pleistocene.

Interstitial water salinities, as at Sites 225 and 228, indicated the presence of the evaporites before they were



<sup>1</sup>Robert B. Whitmarsh, National Institute of Oceanography, Wormley, Godalming, Surrey, United Kingdom; David A. Ross, Woods Hole Oceanographic Institution, Woods Hole, Massachusetts; Syed Ali, State University of New York, Stony Brook, New York; Joseph E. Boudreaux, Texaco, Inc., New Orleans, Louisiana; Robert Coleman, U. S. Geological Survey, Menlo Park, California; Robert L. Fleisher, University of Southern California, Los Angeles, California; Ronald W. Girdler, The University, Newcastle-upon-Tyne, United Kingdom; Frank T. Manheim, U. S. Geological Survey, Woods Hole, Massachusetts; Albert Matter, Geologisches Institut, Universität, Bern, Switzerland; Catherine Nigrini, Lexington, Massachusetts; Peter Stoffers, Laboratorium für Sedimentforschung, Universität Heidelberg, Heidelberg, Germany; Peter R. Supko, Scripps Institution of Oceanography, La Jolla, California

reached by the drill. Variations of water content combined with geochemical data of other workers suggest occasional influxes of salt or fresh water during the Late Miocene evaporite period.

As at Sites 225 and 228, the dark muds and shales in, and overlying, the evaporite sequence are occasionally enriched in vanadium, molybdenum, copper, and iron. This enrichment, so close to the hot brine area, suggests a close relationship—perhaps these sediments serve as a source for some of the heavy metals in the hot brine area (see Site Summary).

## BACKGROUND AND OBJECTIVES

The Red Sea is of considerable importance in the recent concepts of sea-floor spreading. Physiographically, the Red Sea consists of a large main trough between the coastal shelves of Saudi Arabia and Yemen on the east and Egypt, Sudan, and Ethiopia on the west (Allen, 1966; Laughton, 1970). The main trough is best developed in the southern and central portions of the sea and usually has a deep intensely deformed axial trough (Figure 2). In some areas the axial trough is displaced due to fracture zones or is topographically indistinct. The latter is especially true in the southern part of the Red Sea.

Geophysical data indicate that the axial trough is underlain by oceanic crust (basalt); the composition of the material underlying the other parts of the main trough and the shelf is probably both basaltic and continental (granite?). Magnetic anomalies from the axial trough and parts of the main trough have been interpreted in terms of sea-floor spreading (Vine, 1966). The spreading rate for the last 3 m.y. has been about 1 cm/year. High heat flow (Erickson and Simmons, 1969; Girdler, 1970) and seismicity (Fairhead and Girdler, 1970) are common in the axial trough. Seismic profiles generally indicate mildly deformed and uniformly thick postevaporitic sediment layers in the marginal zone with highly disturbed structure and generally little, if any, sediment in the axial trough (Phillips and Ross, 1970). A distinct seismic reflector (S) has been mapped over most of the Red Sea (Knott et al., 1966; Ross et al., 1969; Phillips and Ross, 1970) and is observed at depths up to 500 meters beneath the main trough, but is absent from the axial trough. This reflector is thought to represent an unconformity of late Miocene to early Pliocene age.

Three small pools containing hot salty water have been found within a small area (around 21°N) of the axial trough (Degens and Ross, 1969). Sediments underlying the brines are enriched in numerous heavy metals, such as copper, lead, zinc, silver, and gold and may be of economic importance (Bischoff and Manheim, 1969).

Site 227 is situated on the edge of the marginal zone about 5 km east of Site 226. Our objectives at this site were similar to those at Site 225:

- 1) Determine if there has been any effect of the nearby brines, during their migration, on the surrounding rocks.
- 2) Determine if ancient brine deposits are to be found in this locality which may have once been part of the axial trough.
- 3) Determine if other areas of enrichment of shales and mud occur similar to those found at Site 225.

4) Determine from the sedimentary record past connections of the Red Sea with the Mediterranean and Arabian seas.

5) Sample and date reflector S.

6) Determine the chronology and composition of the evaporite deposits and their relationship to sea-floor spreading.

The JOIDES Advisory Panel on Pollution Prevention and Safety made several recommendations for the Red Sea drilling; the most important ones were to core continuously and to monitor downhole temperatures.

## OPERATIONS

Site 227 was approached from the west on 18 Apr 72 along a track passing directly over the Site 226 beacon (Figure 3). This site was identified primarily on the basis of the water depth since we had previously obtained a reflection profile along this track during the approach to Site 226. A 16-kHz beacon was dropped under way at 5 knots, and the ship returned to the site after all gear had been recovered. As for the Site 226 survey, a 5- and a 10-cubic inch airgun were used with a 4-sec repetition rate. This arrangement, as an alternative to using a larger airgun with the 5-cubic inch gun, proved satisfactory for the water depth and penetration available in the area.

Drilling at Site 227 proceeded without major difficulty. Following the Safety Panel's recommendations, we cored continuously (except for a 15-m interval 3 to 18 m below the surface). The hole ended at a subbottom depth of 359 meters and produced a total of 45 cores (Table 1). For the 344-meter cored interval, we recovered 123.5 meters of core (35.9%).

Minor problems occurred in the upper 20-30 meters where hard lithic carbonate layers were found—this is the depth where we drilled 15 meters. Drilling time generally averaged about 30 minutes/core for the upper part of the section. Occasional hard mud layers required as much as 50 minutes to cut. Drilling times increased with Core 30 when we entered the evaporite sequence—in some instances over 2 hours were needed to cut a core.

Bit weight was between 5-8,000 lb for the first 12 cores; 10-12,000 lb for Cores 12 to 17. From Core 18, bit weight was increased to about 18-20,000 lb for the rest of the sequence.

Drilling was stopped at 1500 hours on 21 Apr 72 at a depth of 359 meters below the bottom and at a total depth below the drill floor of 2171 meters. The hole was filled with 150 barrels of 8.6 lb/gallon mud.

*Glomar Challenger* left Site 227 at 1940 hours on 21 Apr 72. The ship steamed to the north northeast while gear was streamed and then returned over the beacon at 8 knots on a course of 210°. This course, parallel to the inferred sea-floor spreading direction, was maintained across the whole width of the axial valley. When the far side of the valley was reached, a course was set at full speed for the next site. Originally, a third low priority site just west of Discovery Deep has been proposed, but after drilling two holes with similar sections to the east of the axial trough, there was obviously no advantage in drilling yet another hole nearby. Therefore, *Glomar Challenger* set off for the next nearest site at 19°06.0'N, 38°58.5'E.

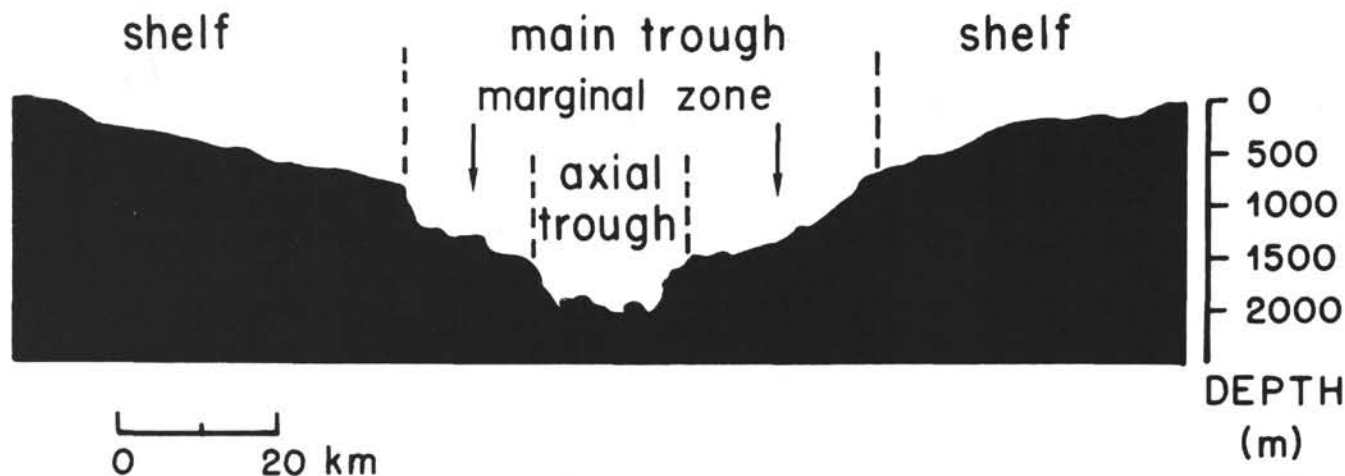


Figure 2. Typical physiographic profile across the Red Sea.

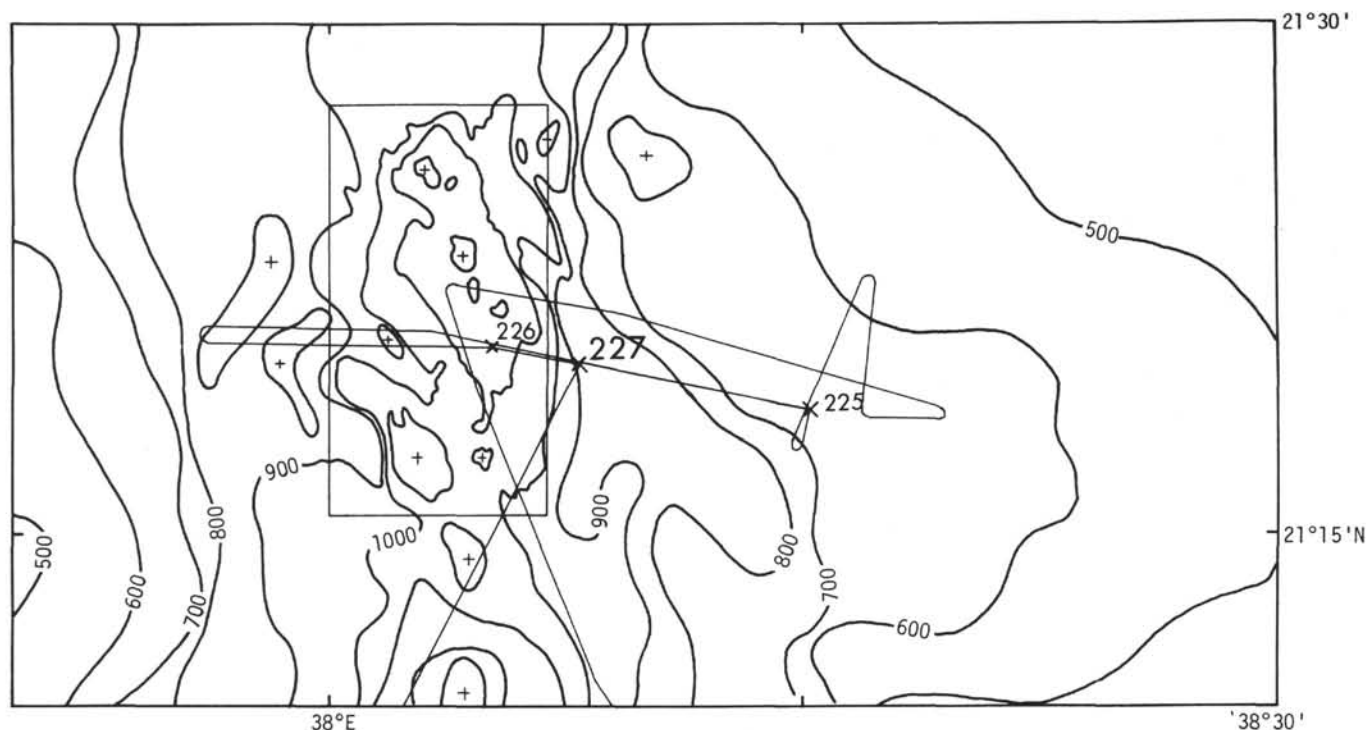


Figure 3. Bathymetric chart of the area around Sites 225, 226, and 227 with the tracks of Glomar Challenger. Contour interval 100 fathoms, depths in corrected fathoms. Contours within box from Amann (1972), other contours based on collected soundings too numerous to show clearly (after Laughton, unpublished).

### LITHOLOGY

The stratigraphic section penetrated at Site 227 consists of four lithologic units, ranging in age from Late Miocene to Quaternary. A total sediment thickness of 359 meters was continuously cored. Four different units are recognized as shown in Table 2.

#### Unit I

The top 70 cm are composed of a sand-sized yellowish-brown pteropod-foram ooze. In general, unit I consists of soft to semilithified light gray to dark greenish gray micarb-rich detrital clay nanno ooze and chalk (nannofossils 30%-60%, carbonate particles 10%-30%, detrital clay 20%-50%, foraminifera 3%-10%, dolomite 3%-10%). The unit is characterized by alteration of light gray with dark gray to black colors, often with very sharp

boundaries. The dark layers are enriched in organic material (~5%) and pyrite (~5%). In these layers nannofossils and foraminifera seem to be less recrystallized than in the light gray sediments. Bioturbation and intraclasts are common in the light gray layers. Pieces of lithified carbonate are found in the upper 30 meters of the sediments.

#### Unit II

Unit II consists of semilithified to lithified gray micarb-rich nanno detrital silty claystone (nannofossils 20%-50%, micarb 10%-20%, detrital material 30%-60%). As in unit I, there are alternating dark layers characterized by a relatively high organic carbon (3%-6%) and pyrite content (3%-7%). Clinoptilolite is found frequently in the sediments of unit II. The top section of this unit shows intensive burrowing.

TABLE 1  
Coring Summary, Site 227

Core	Date/Time Core on Deck (Time Zone 13)	Subbottom Depth (m)	Cored (m)	Recovered (m)
	18 Apr:			
1	2210	0-3	3.0	1.5
2	2335	18-27	9.0	0.2
	19 Apr:			
3	0125	27-36	9.0	1.5
4 <sup>a</sup>	0210	36-36	0.0	CC
5	0420	36-45	9.0	1.8
6	0540	45-54	9.0	2.9
7	0700	54-63	9.0	0.2
8	0815	63-72	9.0	0.5
9 <sup>a</sup>	0905	72-72	0.0	CC
10	1100	72-81	9.0	1.9
11 <sup>a</sup>	1140	81-81	0.0	CC
12	1335	81-90	9.0	2.3
13	1440	90-99	9.0	3.0
14	1550	99-108	9.0	0.9
15	1640	108-113	5.0	0.8
16	1745	113-122	9.0	2.4
17 <sup>b</sup>	1915	122-131	9.0	2.6
18	2000	131-140	9.0	3.4
19	2100	140-149	9.0	4.0
20	2200	149-158	9.0	6.5
21 <sup>a</sup>	2250	158-158	0.0	5.5
	20 Apr:			
22	0010	158-167	9.0	5.1
23	0125	167-176	9.0	1.3
24	0230	176-185	9.0	7.9
25	0350	185-194	9.0	2.0
26	0510	194-203	9.0	1.7
27	0645	203-212	9.0	1.5
28	0815	212-221	9.0	3.2
29	0905	221-226	5.0	7.0
30	1115	226-235	9.0	1.8
31	1225	235-244	9.0	0.7
32	1410	244-253	9.0	6.7
33	1545	253-262	9.0	6.0
34	1715	262-271	9.0	5.0
35	1910	271-280	9.0	7.0
36	2120	280-289	9.0	2.2
37	2320	289-292	3.0	1.9
	21 Apr:			
38	0235	292-297	5.0	0.3
39	0520	297-305	8.0	0.4
40	0645	305-314	9.0	2.8
41	0825	314-323	9.0	0.8
42	0950	323-332	9.0	4.5
43	1110	332-341	9.0	6.7
44	1335	341-350	9.0	2.1
45	1500	350-359	9.0	3.0
	Totals		344.0	123.5

<sup>a</sup>Von Herzen temperature probe run.

<sup>b</sup>Spotted mud while coring.

TABLE 2  
Lithologic Units, Site 227

Lithologic Units	Thick- ness (m)	Sub- bottom Depth (m)	Cores
I Gray MICARB-RICH DETRITAL CLAY NANNO OOZE and CHALK	131	0-131	1-17
II Gray MICARB-RICH NANNO DETRITAL SILTY CLAYSTONE	63	131-194	18-25
III Dark Gray DOLOMITIC SILTY CLAYSTONE	32	194-226	26-29
IV EVAPORITES	≥ 133	226-	30-45

### Unit III

This unit is a dark gray to black semilithified to lithified dolomitic silty claystone (composition: clay 30%-60%, dolomite 20%-70%, pyrite 5%-10%). Analcite is a common constituent of the clays. The matrix is made up of microcrystalline analcite 0.01-0.1 mm in diameter. In thin sections these claystones reveal a slight lamination caused by the alternation of pyrite- and dolomite-rich zones.

### Unit IV

Anhydrite and halite with interbeds of very hard black shale characterize the evaporite facies of unit IV.

Anhydrite occurs in two different types. The upper part of the section is a fine wavy laminated anhydrite. The laminae of alternating white and grayish color are about 3 mm thick with a general dip of 40°-60°. In the lower part of the core the anhydrite is massive and nodular. The nodules (1-3 cm thick) of white anhydrite are separated by thin greenish-gray seams composed of dolomitic claystone. Bedding is still present. The first occurrence of halite was found in Core 30 at a depth of about 230 meters. The contact between anhydrite and halite is very sharp. Due to solution by water during coring, the halite cores are thinned. The less soluble material (mostly anhydrite and clay) within the halite therefore forms very distinct 0.5 to 1-cm-thick layers showing a general dip of 40°-60°. Alternation of pure white with dirty gray halite in intervals of approximately 3-7 cm are typical of the whole halite sequence.

The evaporite facies is interrupted by several black shale layers. These very finely laminated, hard shales are mostly fragmented by coring. They are composed of montmorillonite, organic matter, and pyrite. Thin-section studies reveal that in some of the layers cristobalite is a major constituent of the clays.

A detailed description of this unit and a discussion of its origin are given by Stoffers and Kühn (this volume).

Due to limited space, the tables of grain size, carbon-carbonate, and X-ray mineralogy data are presented with the data of other sites in Appendices I, II, and III, respectively, at the end of the volume.

## BIOSTRATIGRAPHY

### Foraminifera

Planktonic foraminiferal faunas are essentially similar in composition to those found at Site 225. Cores 1 and 2, of Pleistocene age according to nannofossil data, contain assemblages referred to the *Globigerinoides sacculifer* Biofacies (cf. Foraminifera section, Site 225). Much of the

interval occupied by the *G. ruber* Biofacies at Site 225 appears to be missing here; populations in Core 3 belong to the *Globigerinita glutinata* Biofacies, and Cores 5 through 7 fluctuate between these latter two assemblages. The highest occurrence of *Globigerinoides obliquus* is in Sample 3-1, 50-52 cm; that of the Pliocene benthic fauna, in sample 5-1, 139-141 cm.

Cores 8 through 16 are dominated by the *G. glutinata* Biofacies, although planktonic species are all but absent in Cores 13 and 14 (except for 13, CC, which contains abundant *Turborotalita quinqueloba*). Similar assemblages are found in Cores 17 and 18, but *G. obliquus* and *Streptochilus* cf. *tokelauae* are abundant in several samples in the latter core. Planktonics are generally rare in Cores 19 through 22, where the faunas consist largely of *T. quinqueloba*; they are virtually absent below Sample 22, CC. A sample from 36, CC, however, contains a well-preserved fauna of abundant planktonic and benthic species; whether it represents contamination from higher horizons is not clear. Otherwise, the lowest occurrence of benthic foraminifera is in Sample 25, CC; the very poor preservation here and at lower horizons suggests that their absence is due, at least in part, to recrystallization.

#### Nannofossils

Site 227 was drilled in sediments ranging in age from Late Pleistocene to Late Miocene. All of the transoceanic nannofossil zones are present with the exception of the *Discoaster brouweri* Zone of Late Pliocene, the absence of which suggests an unconformity. Nannofossils are virtually absent within the anhydrite and halite section of the Late Miocene.

The Pleistocene occurs in Cores 1 and 2. Sample 1-1, 43-44 cm contains nannofossils belonging to the *Gephyrocapsa oceanica* Zone (Boudreaux and Hay, 1969) of Late Pleistocene. The core catcher sample of Core 2, taken at 27 meters, contains elements of the *Pseudoemiliania lacunosa* Zone of Early Pleistocene.

The Late Pliocene *Discoaster brouweri* Zone is absent in this hole, and a hiatus of approximately 300,000 years is represented by the missing section. Sample 3-1, 13-14 cm contains abundant *Discoaster pentaradiatus* of the Late Pliocene. The *Discoaster surculus* Zone appears in Samples 3-1, 60-61 cm and 4, CC and represents the lower portion of the lower Pliocene. Abundant specimens of *Sphenolithus abies* are present in Cores 5, 6, and 7 and are representative of the lowermost Upper Pliocene. The Early Pliocene *Reticulofenestra pseudoumbilica* Zone is present in Sample 8, CC and extends to 13, CC. The level of extinction of *Ceratolithus rugosus* appears in Sample 3-1, 13-14 cm. The *Discoaster asymmetricus* Zone extends from Core 14 down through Core 29. *Ceratolithus tricorniculatus* appears in Cores 13, 14, 18, 19, 22, 23, 24, and 25.

Cores 26 through 28 are virtually barren of nannofossils due to high salinity contents. Samples 29-1, 99-100 cm and 29-3, 74-75 cm contain common *Reticulofenestra pseudoumbilica* and *Sphenolithus abies* with only rare fragments of discoasters. Core 30 contains anhydrite and nannofossils are completely absent in these sediments.

The Late Miocene is recognized in Sample 31-1, 130-131 cm by the presence of *Discoaster quinqueramus*. Abundant

sphenoliths are also present at this level. Cores 32 through 45 contain anhydrite and halite, and nannofossils belonging to the *Discoaster quinqueramus* Zone are present only in Sample 35, CC. The Late Miocene *Discoaster quinqueramus* Zone is the last reliable age obtained from nannofossils within the evaporite section, and an absolute age of 5.0 million years is assigned to sediments within this zone.

#### Radiolaria

Radiolaria are absent from most of the cores recovered at Site 227. There are, however, poorly preserved specimens in the core catchers of Cores 24 and 25. These forms have recrystallized to analcite, making specific recognition and age determinations impossible. The preservation and general faunal character is similar to that found in Cores 19 and 20 of Site 225, and a correlation between Site 225, Cores 19 and 20 and Site 227, Cores 24 and 25 seems likely (cf. Nannofossil sections for Sites 225 and 227).

Working with piston cores from the hot brine area, Goll (1969) reported a "brief invasion" of radiolarians between 12,000 and 9000 years ago. He attributed this occurrence to changes in the concentration of dissolved silica (and hence with volcanic activity) in the central region of the Red Sea, rather than to changes in temperature and salinity. Herman (1965) noted small, sporadic occurrences of Radiolaria in Quaternary piston cores from the southern Red Sea.

There are at least two possible explanations for these intermittent occurrences: (1) Radiolaria have been present in the surface waters of the Red Sea throughout postevaporite time, albeit in varying abundance depending upon temperature, salinity, and dissolved silica concentration in the surface waters. Conditions favorable to preservation may also vary with temperature, salinity, and dissolved silica concentration and with the rate of burial. (2) Radiolaria "invade" the Red Sea from time to time when surface water conditions are favorable.

If the former is true, then the nonradiolarian sequences represent conditions of relatively high temperature and salinity in the bottom waters in which amorphous silica is completely dissolved. There was, however, a brief interval in the lowermost Pliocene, which can be recognized at both Sites 225 and 227, when there were slightly lower temperatures and salinity conditions and an otherwise favorable geochemical climate allowing amorphous silica to be preserved or, in this case, to go to zeolite, but retain some structure. There might also have been a concomitant radiolarian bloom and hence a sufficient number of tests to allow marginal preservation of a few.

If the latter is true, then the radiolarian horizons at Sites 225 and 227 may represent the first postevaporite conditions favorable to a siliceous fauna, and the first "invasion."

Goll (1969) also noted an association between radiolarians and sphalerite in the brine area. Sphalerite was found in Sample 13, CC, but is apparently not associated with Radiolaria.

At Site 225 a few, moderately well preserved diatoms (which can be more tolerant to hypersaline conditions) were found in Core 25. No such occurrence was noted at Site 227.

## Palynology

Samples (32-3, 52-57 cm; 33-2, 102-107 cm; 34-2, 120-125 cm; 35-2, 38-43 cm; 40-2, 0-5 cm; 41-1, 85-90 cm; 42-2, 0-6 cm; 43-2, 20-25 cm and 45-2, 28-32 cm) from within the evaporite sequence were examined for spores and pollen by Dr. David Wall of the Woods Hole Oceanographic Institution, but none were found.

## Biostratigraphic Summary

Rare and poorly preserved (recrystallized) radiolarians are present only in Samples 24, CC and 25, CC, a level which appears to correlate with a similar occurrence in Cores 19 and 20 at Site 225. The brief appearance of Radiolaria may be due either to a temporary invasion of the Red Sea by these forms or to temporary changes in the geochemical environment which favored their preservation.

Planktonic foraminifera are common throughout most of the cored interval, but populations are again relatively nondiverse. Faunas dominated by *Globigerinoides quadrilobatus sacculifer*, common in the Pleistocene at Site 225, appear here only in Cores 1 and 2; most of the remainder of the planktonic assemblages observed are assigned to the *Globigerinita glutinata* Biofacies (cf. Foraminifera section, Site 225). These forms were observed as low as Sample 22, CC, with a single occurrence within the evaporite sequence in Core 36. Neritic to upper bathyal benthic species are present as low as Core 25, but are also present in Core 36.

The time-stratigraphic framework, as at other Red Sea sites, is provided by abundant and diverse nannofossil floras. Late and Early Pleistocene assemblages are present in Cores 1 and 2, respectively. Late Pliocene floras in Core 3 represent the *Discoaster pentaradiatus* Zone, indicating the absence of part of the Late Pliocene, and perhaps of the Early Pleistocene as well. The highest occurrence of Early Pliocene assemblages is in Section 8, CC; Lower Pliocene sediments persist as low as Core 29, although nannofossils are rare or absent in Cores 26 through 29.

The uppermost occurrence of the Late Miocene *Discoaster quinquerramus* Zone was recognized in shale interbeds within the evaporite sequence, in Sample 31-1, 130-131 cm. This flora is present as low as Core 35, and represents the earliest age recognized at this site.

## Sedimentation Rates

Patterns of sedimentation at this site (Figure 4) contrast distinctly with those observed at Site 225. The highest rate observed here (85-130 m/m.y.) is in the Upper Miocene and Lower Pliocene sediments above the evaporites (94-236 m). Late Pliocene sedimentation (28-60 m) was at about the same rate (90-105 m/m.y.). The change in sedimentation rate appears to have occurred within the *Reticulofenestra pseudoumbilica* Zone; whether the transition is marked by an unconformity or by a relatively short period of decreased sedimentation rate cannot be determined from the available evidence. The absence of the *Discoaster brouweri* Zone in the Late Pliocene, however, suggests that an unconformity is present between Cores 2 and 3. Inadequate paleontologic data preclude a rate determination for Quaternary sediments.

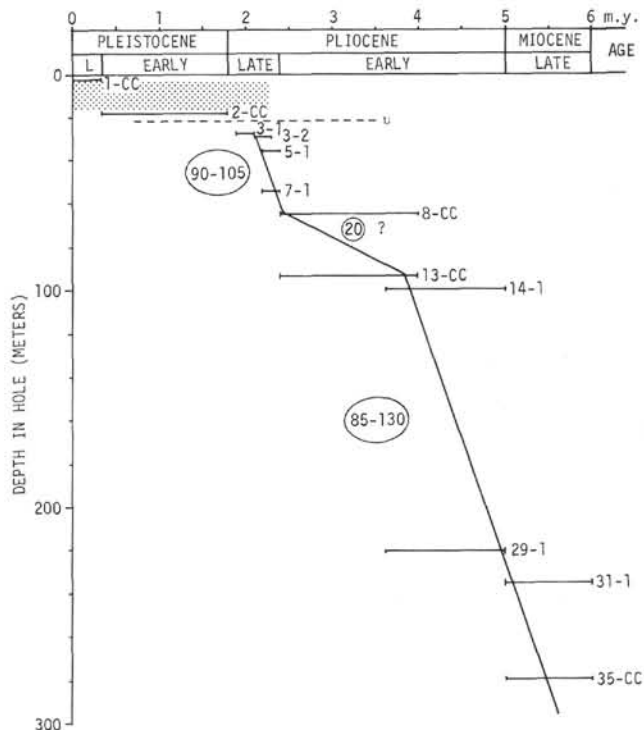


Figure 4. Sedimentation rates at Site 227. Plotted bars are those sufficient to control slopes of lines.

## GEOCHEMISTRY

### Solids

The spectrographic analyses (see Table 3 of Manheim and Siems, Chapter 29) confirm petrographic indications that Site 227 sediments are richer in clays, silicate minerals, and iron-containing components than those of Site 225. Iron concentrations in the marls were frequently higher than 5%, reaching 15% Fe. Titanium and chromium concentrations often reach 7000 ppm and 200 ppm, respectively. These values suggest that basaltic or gabbroic weathering products may be supplying an appreciable part of the noncarbonate fraction of the sediments. A heavy mineral separate revealed 7%, 5%, and 5% Ti, Mg, and Ca, respectively, even though dominated by pyrite.

Most striking was the continued evidence, similar to Site 225, of high vanadium and molybdenum concentrations in the dark muds and shales in the sediments from 28 meters down to the evaporitic rocks. In addition, these shales contained copper concentrations as high as 700 ppm, and the deepest shale recovered, from about 250 meters in the evaporitic sequence, contained 2000 ppm Zn. These indications strongly suggest that the sediment sequences surrounding the hot brine deeps can serve as sources of metals for the metal-rich deposits in the deeps. Only lead is rarely found in the sediments, and lead is also present in relatively minor amounts in most of the Atlantis II and Discovery deep cores reported to date.

The composition of sulfide minerals (Manheim and Siems, Chapter 29) found in the foraminiferal samples (sieved at 74 mm) show that the lighter, whitish pyrites consistently contained high arsenic (suggesting arsenopyrite) and nickel, whereas the brassy pyrites were low in

TABLE 3  
Interstitial Water Properties

Core, Section, Interval (cm)	Subbottom Depth (m)	H <sub>2</sub> O Recovered (ml)	Pore Water pH	Lab. Temp. (°C)	Salinity (Corr) (‰)	Alkalinity (meq/kg)	Sp. G <sup>a</sup>
Surface Seawater			8.29	25.8	39.3	—	—
3-1, 18-27	27	10	7.47	26.0	46.4	1.6	—
5-2, 0-4	38	16	7.17	25.6	46.8	1.4	1.031
6-2, 0-10	47	8	7.20	25.7	53.4	1.5	—
10-2, 140-150	74	10	7.10	26.0	55.2	2.2	—
12-2, 0-10	83	20	(7.00)	26.2	78.6	1.5	—
14-1, 109-114	100	12	7.30	26.2	101.7	.97	—
16-1, 130-140	114	5	7.05	26.0	125.0	1.5	—
18-3, 140-150	137	6	6.73	26.1	165.9	1.8	—
20-3, 0-10	154	7	—	26.2	187	1.3	—
23-1, 0-5	158	5	6.46	26.0	214	2.2	—
25-2, 0-10	187	2	—	—	237 <sup>b</sup>	—	—
27-1, 0-8	203	3.5	—	26.0	240 <sup>b</sup>	—	—
30-1, 135-140	223	1.5	—	—	(226) <sup>b</sup>	—	—
36-2, 46-53	282	1.5	~6.5 <sup>c</sup>	26.0	250.5 <sup>b</sup>	—	1.198
44-CC	350	0.75	6.2 <sup>c</sup>	26.2	256 <sup>b</sup>	—	—

Note: Water depth = 1795 meters. Analysts: F. Manheim and D. Marsee. Salinity by index of refraction is uncorrected for composition and does not necessarily correspond to total salt content. Depth assigned from top of cored interval according to position on recovery. Parentheses refer to uncertain value.

<sup>a</sup>Determined by micropycnometer.

<sup>b</sup>Determined by weight dilution with distilled water, followed by refractive index measurement ( $\Delta N$ ).

<sup>c</sup>pH paper measurement, rather than electrode measurement, because of shortage of pore water.

trace metals. In addition to pyrite, sphalerite (ZnS) was noted in Cores 3 and 13 and HCl-bromoform separations were performed. Prominent accessory metals were cadmium, copper, and arsenic. Germanium was also detected in the sphalerite from Core 13.

In the carbonate fractions of the rocks, high magnesium concentrations predominate. However, in the core catcher of Core 1 (3 m) calcium carbonate having a radial, fibrous habit and forming vein-like encrustations was found to contain relatively high strontium. This may be authigenic aragonite. High magnesium concentrations are also noted in rocks associated with the evaporites below 230 meters; these are partly associated with dolomite.

Finally, the dark shales associated with the evaporitic rocks showed, as did similar rocks at Site 225, extraordinarily high boron concentrations (300-700 ppm B). Interestingly, the boron content of evaporated interstitial water from Core 44 (about 350 m) also contained anomalous boron concentrations. High boron concentrations are common from "salt clays" in other areas, but boron-rich brines are common only in continental evaporites receiving leaching products from young volcanics (e.g., Death Valley, Mono Lake, Green River Formation) or later stage evaporites (e.g., Stassfurt salts of Germany).

### Interstitial Waters

As shown in Table 3 and Figure 5, interstitial waters again yielded the pattern of initially slow increases in salinity with depth, followed by more rapid increases to near saturation as evaporites were reached. pH values also decreased, as did samples from Site 225, from values

starting below 8.0 and fall to near pH 6 in the strongest brines, whereas alkalinities remained at about seawater levels (2 meq/kg or below). Interestingly, however, the lowest obtained water, from shale between anhydrite and rock salt beds, contained substantial magnesium and boron. This was discovered by spectrographic analyses of dried salt. One may note that appreciable quantities of magnesium and boron are characteristic of brines which have been influenced by late stage evaporites (i.e., those precipitated from "mother liquor" residues after calcium sulfate and sodium chloride saturation levels are reached). Another source for boron is evaporated residues of leachates of young volcanic rocks and pyroclastic debris. The fact that the "shale" at 350 meters depth (Core 44) contained chiefly cristobalite, rather than clay minerals (Stoffers and Ross, this volume), may be linked with intensive weathering (subsea, subaerial?) of pyroclastics. The shore-based studies of interstitial waters (see Manheim et al., Chapter 35) confirmed the presence of high boron and magnesium concentration in the deep brine, as well as marked enrichment in calcium. Moreover, analysis of halite showed boron enrichments as well (Manheim and Siems, Chapter 29).

The site in general gave the pore water program a good workout, beginning with sediment yielding large quantities of fluids, and ending with brick-hard shales, from which one could obtain a milliliter of fluid only with good luck and a maximum of pressure from the squeezer (highest pressure 11,000 psi). In spite of the high pressures, however, it seems unlikely that appreciable adsorbed water (which is poor in salts) was squeezed out as an artifact, since the pore fluids approached saturation with NaCl and

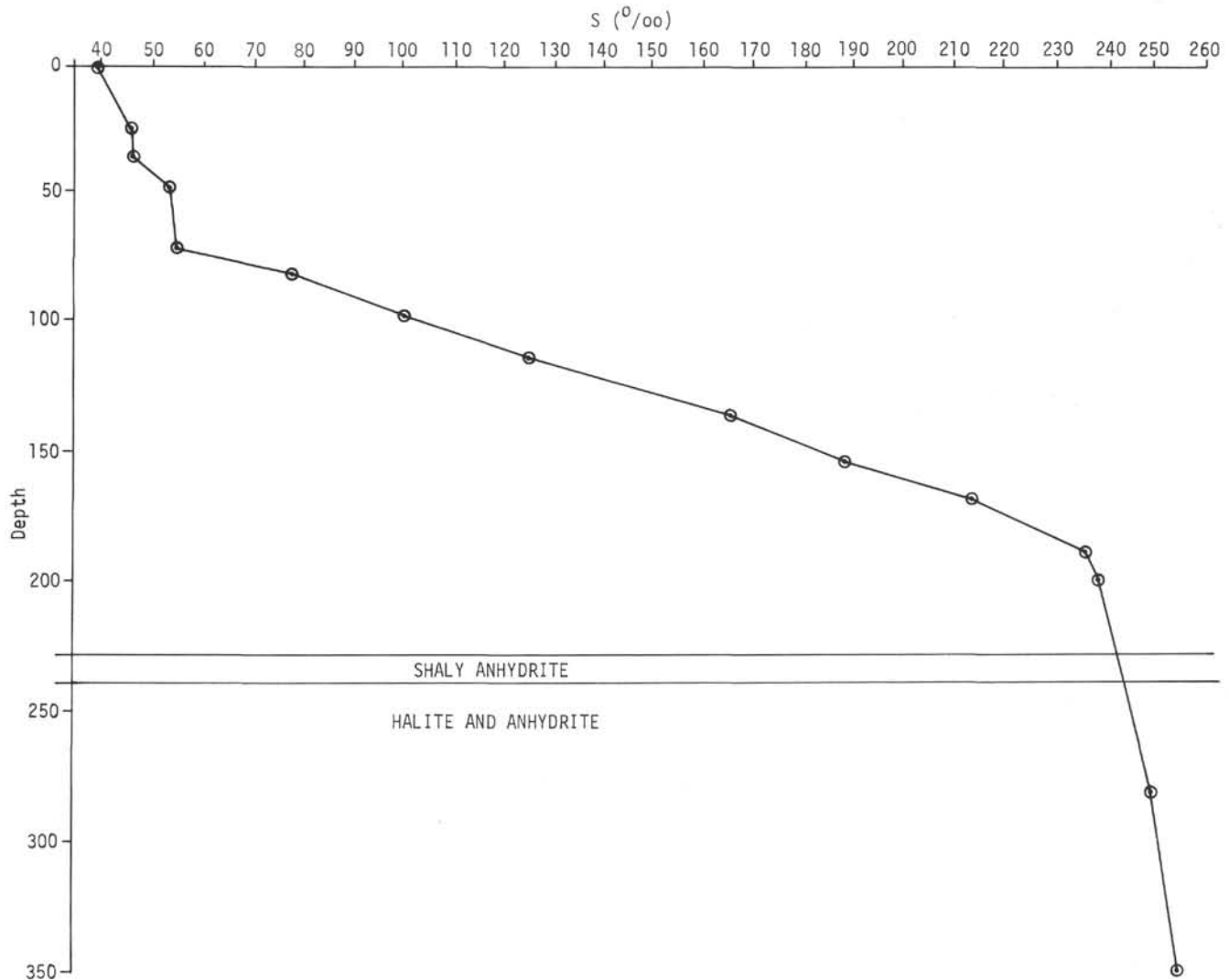


Figure 5. Interstitial salinity (g/kg) as determined by index of refraction onboard ship. Note that the "salinities" are calibrated on a seawater basis and are not to be equated with a true total dissolved solids or seawater definition (see *Manheim et al., chapter 35*).

showed a highly consistent pattern in spite of varying lithology. However, in spite of care in selecting internal parts of cores, one cannot completely exclude slight contamination with drilling fluid.

#### Water Content

Water content data are enigmatic. Although sediments (Table 4, Figure 6) became noticeably more consolidated with depth, this is little reflected in water content (nor in GRAPE density), which shows only a marginal decrease until the evaporitic strata are encountered at around 230 meters depth. As mentioned for Site 225, the zigzags appear to be real, though in the upper 80 meters of the section disturbance was so great that errors and artifacts are unavoidable.

Increase in rigidity with depth may possibly be explained by cementation with silica and carbonate in a way that strongly affects shear strength, but decreases porosity to a lesser extent. A second factor might be increasing shaliness with depth.

An interesting aspect is that although the shales became hard and brittle with depth, they still yielded water on squeezing. In contrast, highly montmorillonitic clays from the Atlantic and Gulf coasts yield water with more difficulty even when less consolidated. The interconnected nature of pore structure is also reflected in their conductivity. The phenomena may be related to the appreciable presence of nonlayer-lattice silicate minerals (e.g., cristobalite) in the "clayey" or "shaley" rocks.

Salt contains virtually no mobile water, whereas anhydrite contains water chiefly in proportion to its shaliness. The relative solubility of these minerals accounts for this behavior, solids being easily redissolved and reprecipitated to plug interconnected pores. One can observe in polished sections of anhydrite large transparent masses of monocrystalline anhydrite filling large voids in a sugary, finer-crystalline mass. Wetting polished faces produces pitting and etching of fine-grained crystals around the rims of large crystals. Presumably, shale layers within the impermeable evaporite deposits should retain their

TABLE 4  
Water Content (Weight %) From  
Syringe Samples Plus Other  
Samplings

Core, Section, Interval, (cm)	Subbottom Depth (m)	H <sub>2</sub> O (%)
3-1, 16	2	35.6
3-1, 148	3	21.1
5-1, 115	37	21.9
5-2, 50	38	28.7
6-1, 68	46	22.5
6-1, 78	46	29.0
6-2, 88	48	17.8
8-1, 120	65	20.6
10-2, 145	76	21.2
12-1, 140	82	23.2
12-2, 91	84	18.7
13-1, 25	91	24.2
14-1, 78	101	21.7
15-1, 101	109	25.6
16-1, 104	114	15.1
16-2, 30	115	18.0
17-1, 110	123	19.2
17-2, 143	125	23.2
18-1, 130	132	20.3
18-2, 128	134	19.4
18-3, 40	135	17.5
19-1, 95	141	23.3
19-3, 45	143	21.4
19-3, 15	143	18.4
20-2, 80	150	25.3
20-3, 100	153	14.8
20-4, 80	155	18.2
20-5, 85	156	16.4
22-2, 90	160	25.1
22-3,	162	21.1
22-4, 68	172	19.9
24-6, 51	185	17.8
25-2, 39	187	18.7
26-2, 115	197	17.3
27-1, 40	203	10.0
28-1, 135	213	17.8
28-2, 46	214	17.8
28-3, 35	215	19.1
30-1, 130	228	1.0 <sup>a</sup>
32-3	248	0.2 <sup>b</sup>
32-5, 83	252	0.2 <sup>b</sup>
36-2, 46-53	282	2.43
36-2, 106	283	22.4
44-CC	350	14.0 <sup>c</sup>

<sup>a</sup>Shaly anhydrite.

<sup>b</sup>Rock salt.

<sup>c</sup>"Analcimolite" (shale whose chief silicate mineral is analcime), later found to be predominately cristobalite.

porosity indefinitely, for there is little exit path for the water.

#### Diffusimetry-Resistivity Measurements on Cores

Table 5 contains the resistivity and formation factor results for this site. For a detailed description of the techniques employed, see Chapter 2.

#### Isotope Studies

Delevaux and Doe (this volume) have measured uranium, thorium, and lead contents and lead isotopic compositions of a single sediment sample from this site. The lead isotopic composition and lead concentration of Sample 20-4, pelagic sediment are virtually identical to those of the most radiogenic pelagic sediments from the Red Sea as reported by Chow (1968) and from oceanic manganese nodules as reported by Reynolds and Dasch (1971).

Deuterium/hydrogen ratios of interstitial waters are described by Friedman and Hardcastle (this volume). Shanks et al. (this volume) describe sulfur isotope measurements on anhydrites and shales.

### PHYSICAL PROPERTIES

#### Water Content, Porosity, and Density

At this site, the strong contrast between the Pleistocene and Pliocene detrital sediments and the Miocene evaporites is reached at a depth of 226 meters. The contrast is not well seen in the Site Summary because of the poor GRAPE porosity and density plots for the evaporites. The top 226 meters of sediment consist of 194 meters of carbonate ooze underlain by 32 meters of claystone. The ooze shows a gentle decrease of porosity with depth (about 50%-40%) and a corresponding gentle increase of density with depth (about 1.83 g/cm<sup>3</sup> at 30 m to about 1.94 g/cm<sup>3</sup> at 230 m). The trend is sometimes just discernible at the core level (e.g., Core 20).

Laboratory measurements of densities of the evaporites are given in Wheildon et al. (this volume) and give a mean of 2.90 ± 0.02 g/cm<sup>3</sup> (*N* = 3) for anhydrite and 2.14 ± 0.01 g/cm<sup>3</sup> (*N* = 8) for halite.

The GRAPE plots at the core level unfortunately show many breaks. For the GRAPE densities:

Core 6—sharp minima at 0.8 meters and 1.7 meters which are, respectively, correlated with dark material and less consolidated material.

Cores 16-19—frequent oscillations due to voids and the broken nature of the cores.

Core 20—increase with depth discernible from 1.85 to 1.95 g/cm<sup>3</sup> and a minima at 6.5 meters correlated with dark material.

Cores 24-27—minima due to fragmentation and voids.

Core 29—a small maximum at 4.2 meters (reaching 2.1 g/cm<sup>3</sup>) correlating with a patch of consolidated material.

#### Compressional Wave Velocity

The compressional wave velocities (see Site Summary) also show a gentle increase with depth through the 194 meters of carbonate nanno oozes with a more sharp

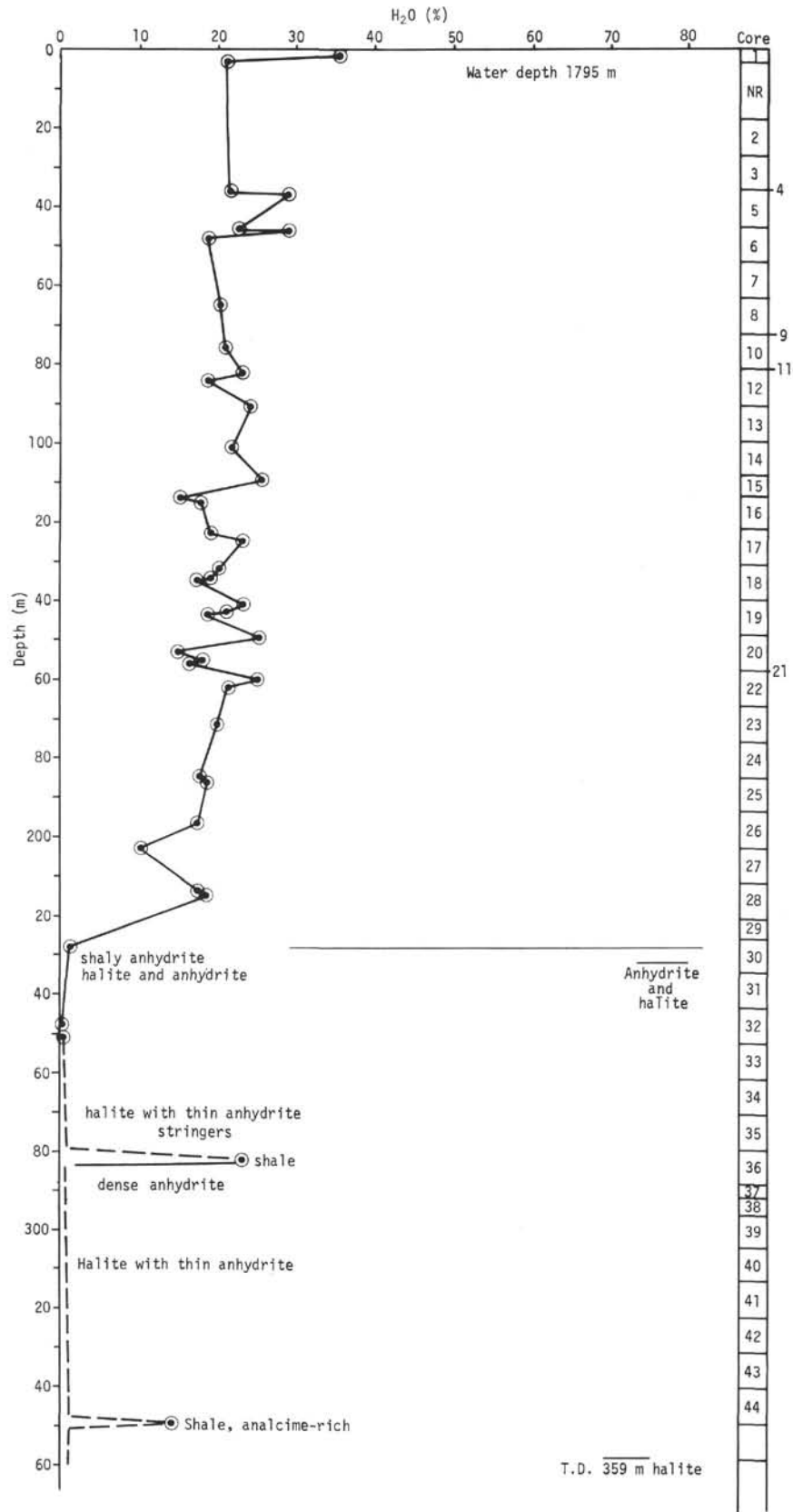


Figure 6. Water content values of sediments at Site 227.

TABLE 5  
Resistivity Measurements, Site 227

Core, Section Interval (cm)	Subbottom Depth (m)	$R_s$ (app)	T (°C)	$R_w$ (app)	T (°C)	$R_{pw}$	T (°C)	S (‰)	$R_s$	C	F
3-1, 115	28	0.101	22.5	0.0306	25.9	0.146	26	47.2	0.63	6.3	4.0
3-1, 140	29	0.105	23	0.0306	25.9	0.146	26	47.2	0.66	6.3	4.2
6-2, 0-10	47	0.0954	24	—	—	0.130	24	53.4	0.60	6.3	4.5
10-2, 140-150	75	0.0823	24.8	—	—	0.125	24.6	55.2	0.52	6.3	4.2
12-2, 0-10	83	0.0982	24.8	0.0341	24.5	0.094	25	78.6	0.57	5.8	6.1
14-1, 109-114	101	0.136	24.7	0.0342	24.0	0.076	24	101.7	0.80	5.9	10.5
16-1, 130-140	114	0.0670	23.8	0.0330	24.0	0.061	25	125	0.41	6.1	6.7
18-3, 140-150	135	0.0571	24.6	0.0290	25.0	0.0503	24.4	165.9	0.39	6.8	7.8
20-3, 0-10	153	0.0576	25	0.0300	25	0.0466	25	187	0.37	6.5	8.0
23-1, 0-5	168	0.0503	25	0.0361	25	0.0424	25	214	0.27	5.4	6.4
25-2, 0-10	187	0.219	25	0.0360	25	0.0402	25	237	1.19	5.4	30 <sup>a</sup>
27-1, 0-8	203	0.156	25	0.0371	25	0.0407	24.8	240	0.82	5.3	20 <sup>b</sup>
36-2, 46-53	283	0.0625	25	0.0508	25	0.0400	—	250.5	0.24	3.9	(6.1) <sup>c</sup>

Note: All measurements in ohm-m. Reference fluid has  $S = 35.4$  ‰ ( $R_w = 0.196$  at 25°C).  $R_s$  is resistivity of sediment,  $R_{pw}$  is resistivity of pore water, and  $R_w$  is resistivity of reference water. C is cell constant and F is formation factor as defined by Manheim et al., Chapter 35.

<sup>a</sup>Dense chalk, dark.

<sup>b</sup>Hard, black claystone.

<sup>c</sup>Shale, some cracking between electrodes.

increase in the last 10 meters. The velocities increase from about 1.6 km/sec at 30 meters depth to 2.1 km/sec at 170 meters. Between 180 and 220 meters (claystones) velocities of 2.6-3.3 km/sec are reached.

The velocities in the evaporites are widely scattered (Site Summary). This is due to the presence of both anhydrite and halite which have velocities differing by about 0.6 km/sec. Further measurements of the velocities of these rocks (Wheildon et al., this volume) gave a mean of  $4.9 \pm 0.33$  km/sec ( $N = 3$ ) for anhydrite and a mean of  $4.2 \pm 0.37$  km/sec ( $N = 7$ ) for halite.

#### Specific Acoustic Impedance

Through the nanno oozes, the specific acoustic impedance increases from about  $3 \times 10^6$  Nsm<sup>-3</sup> at 30 meters depth to just over 4 Nsm<sup>-3</sup> at 190 meters depth emphasizing the gentle increase with depth of both the densities and sonic velocities (Site Summary). Because of the failure of the GRAPE densities for the evaporites, the impressive increase at 226 meters depth is not displayed in Figure 2. Values of 14 Nsm<sup>-3</sup> are reached for the anhydrites and 9 Nsm<sup>-3</sup> for the halites.

#### Thermal Conductivity

The thermal conductivities as a function of depth for the soft sediments are shown in Figure 4 of Girdler et al. (this volume). The values show a large scatter (much larger than for Sites 225 and 228) and give a mean of  $1.252 \pm 0.205$  Wm<sup>-1</sup> K<sup>-1</sup> ( $N = 12$ ).

Values for the thermal conductivities of anhydrite and rock salt from this site are given in Wheildon et al. (this volume). The means are  $5.15 \pm 0.346$  Wm<sup>-1</sup> K<sup>-1</sup> ( $N = 3$ ) for anhydrite and  $5.13 \pm 0.191$  ( $N = 7$ ) for halite. The value

for anhydrite is significantly higher than the value of  $4.51 \pm 0.084$  ( $N = 6$ ) obtained for Site 225.

#### HEAT FLOW MEASUREMENTS

Four downhole temperatures were obtained at 37, 73, 82, and 159 meters. Some difficulty was experienced with penetration of the probe. This was due to the hardness of the bottom. Considering the difficulties experienced at this site, it is perhaps surprising, when the temperatures are plotted against subbottom depths, that the temperatures lie so nicely on a straight line. In accord with the interpretation of the temperature-time plots (see Girdler et al., this volume), the maximum thermal gradient is favored, this being 117 K km<sup>-1</sup>.

The temperature gradient is estimated as  $117 \pm 8$  K km<sup>-1</sup>; this is slightly weighted in favor of the higher values. There are seven thermal conductivity measurements (Site Summary) over the 160-km depth range of the temperature measurements, and these give a mean of  $1.305 \pm 0.161$  Wm<sup>-1</sup> K<sup>-1</sup>. The heat flow is thus  $153 \pm 29$  mWm<sup>-2</sup>, the experimental error of just less than  $\pm 20\%$  is considered reasonable and acceptable.

#### CORRELATION OF REFLECTION PROFILES AND LITHOLOGIES

As at Site 225, only the strong S reflector was visible in the vicinity of Site 227. The reflector appeared rather diffuse and had an indistinct onset (Figure 7). At the site the top of the reflector was estimated to be 0.19 sec below the sea bed (Figure 7b). During coring, the top of a semilithified to lithified claystone was met at 194 meters,

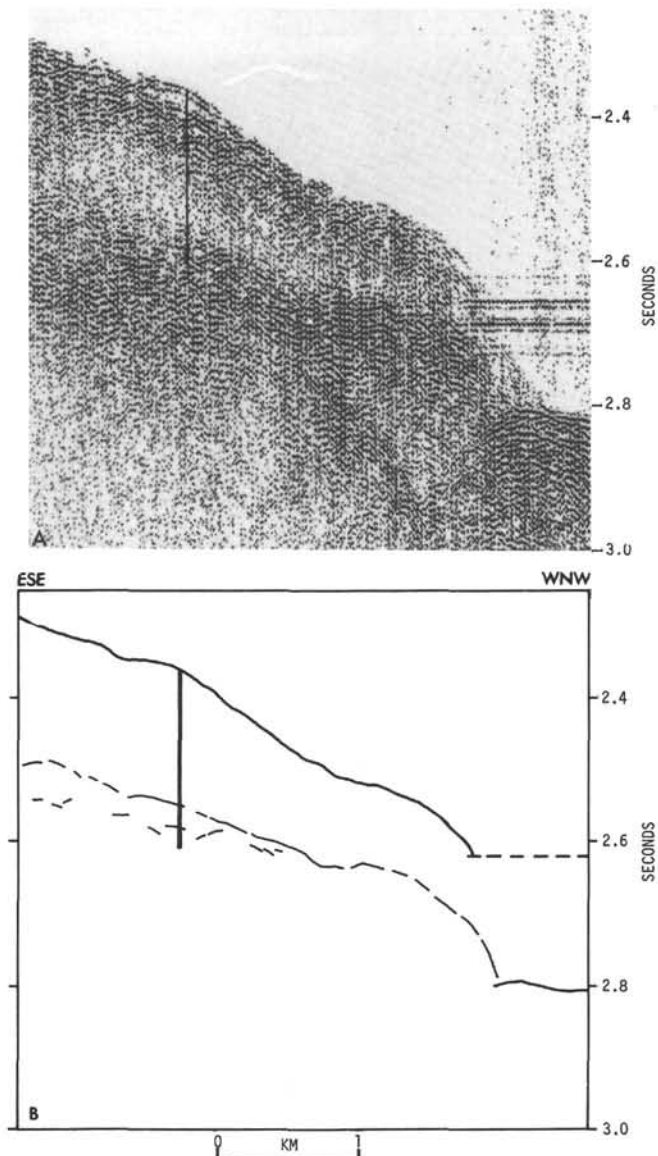


Figure 7. (a) Seismic reflection profile obtained on the approach to Site 227. Atlantis II Deep and the reflections from the hot brines can also be seen. The vertical line marks the position of the drilled hole. (b) Line drawing interpretation of Figure 7 used to determine the onset time of the S reflection. The lines beneath the onset of the reflection mark the first succeeding strong pulse, perhaps attributable to the top of the anhydrite. The vertical line has tenth second divisions.

whereas anhydrite marking the top of the evaporite sequence was met at 232 meters. If the S reflection is attributed to the top of the anhydrite, a mean velocity down to the reflector of 2.45 km/sec is indicated. Velocity measurements made onboard ship suggest the mean velocity is no more than 2.0 km/sec although some, but not all, of the discrepancy between these two figures could be attributed to the absence in the laboratory of the

\*"This chapter will now be published in Volume 24 of the Initial Reports series."

overburden and hydrostatic pressures experienced by the sediment in situ. It seems more likely that the onset of the S reflector is due in this case to hard bands of claystone first cored between 194 and 203 meters. The inferred mean velocity is then 2.04 to 2.14 km/sec which is in much better agreement with the shipboard measurements. The strength of the S reflection is again explainable by the high average compressional wave velocity of the anhydrite, which was 4.95 km/sec.

It should be noted that with such a shallow reflector the uncertainties in picking the onset of the reflection ( $\pm 0.01$  sec) can lead to quite large uncertainties in the calculated mean velocity ( $\pm 0.11$  km/sec).

## DISCUSSION AND CONCLUSIONS

Site 227 is located near the edge of the axial trough about 5 km east of Site 226. It was thought that since Site 227 was so close to the Atlantis II brine pool, we would have a good opportunity to ascertain if there had been any geochemical effects on the sediments from migrating fluids related to the hot brine area. Other objectives at this site were to see if enrichments similar to those found at Site 225 were present and to further document the age of reflector S and the recent history of the Red Sea. As with all our Red Sea sites, we essentially continuously cored the entire hole following the recommendations of the Safety Panel. We penetrated to a depth of 359 meters and recovered 123.5 meters of core.

## Lithology

Four distinct sedimentary units were penetrated:

Unit I: Gray micarb-rich detrital clay nanno ooze and chalk ranging in age from Early Pliocene to Late Pleistocene (total thickness 131 m). There is an unconformity at the Pliocene-Pleistocene boundary. Sedimentation rates before the unconformity were up to 130 m/m.y.

Unit II: Gray micarb-rich nanno detrital silty claystone of Early Pliocene age (total thickness 63 m). The sedimentation rate for this unit lay between 85 and 130 m/m.y.

Unit III: Dark gray dolomite silty claystone of Early Pliocene age (total thickness 32 m).

Unit IV: Lithified anhydrite and halite with interbeds of hard black shales (total thickness drilled 133 m). The core immediately above the evaporites (Core 29) contained Early Pliocene nannofossils, whereas Core 31, a shale interbed within the evaporite sequence, contains fossils of the Late Miocene *Discoaster quinquemurum* Zone. Thus, a Late Miocene to very early Pliocene age seems appropriate here for the top of the evaporite sequence.

Bedding planes within the evaporite section are rather steep with a general dip of between  $40^\circ$ - $60^\circ$ . This could be due to salt flowage, to collapse due to solution, or perhaps to deformation related to regional tectonism like sea-floor spreading.

The sedimentary sequence is similar to that found at Sites 225 and 228 and is correlative on the basis of microfauna (see Fleisher, this volume\*). The sediments themselves indicate Late Miocene evaporite deposition in a relatively shallow evaporite basin (a point further confirmed by geochemical studies discussed later). The

black shale layers contain relatively high amounts of organic material and pyrite, suggesting at least occasional reducing conditions. Units I, II, and III were deposited in more open ocean conditions, with occasional bottom reducing conditions indicated by dark layers containing relatively high organic carbon and pyrite contents.

Reflector S, first cored at Site 225, was also reached at Site 227. A seismic reflector was observed at a depth of 0.19 sec below the sea bed and the anhydrite was reached by the drill at 232 meters depth. Thus, a mean seismic velocity of 2.45 km/sec is indicated although shipboard velocity measurements average about 2.0 km/sec. Part of the discrepancy could be due to the absence in the laboratory of overburden and hydrostatic pressures experienced by the sediment in situ. Another possibility is that in this area the beginning of the S reflector is caused by some hard claystone (between 194 and 203 m).

### Paleontology

Planktonic foraminiferal assemblages are similar in composition to those of Site 225 and are not diverse enough for good correlation with other deep-sea sediments. Benthic foraminifera are not found below the base of sedimentary unit II.

Radiolarians are relatively rare except for some poorly preserved specimens in unit II. Their preservation and general faunal character are similar to those found at Site 225 which indicates a Lower Pliocene correlation. The limited appearance of Radiolaria may either represent a brief invasion (a similar one has been noted in Recent Red Sea sediments) or a favorable geochemical environment for their preservation.

As with the other Red Sea sites, a fairly diverse and abundant nannofossil assemblage was found. Essentially all of the post-Miocene transoceanic nannofossil zones are present with the exception of the Late Pliocene *Discoaster brouweri* zone. A Late Miocene Zone, *Discoaster quinqueramus*, was found in shale interbeds within the evaporite sequence and is the earliest zone found.

### Geochemistry

Sediments obtained at Site 227 are richer in silicate minerals, clays, and iron-containing components than sediments from Site 225. This suggests that volcanic weathering products are more common at this site. The reasons for this variation are not obvious since the sites are so close to each other.

Vanadium and molybdenum enrichments noted in the postevaporite dark muds and shales of Sites 225 and 228 were also observed at Site 227. There were also copper concentrations as high as 700 ppm in one of the shales, a zinc concentration of 2000 ppm and high boron concentrations (300-700 ppm) from a shale within the evaporite sequence.

Interstitial water salinities showed, as did those from other Red Sea sites, an increase in salinity with depth which eventually reached saturation with NaCl when the evaporites were reached.

### Discussion

The Discussion and Conclusions section for Site 225 has discussed the implications of the Red Sea drilling program on the interpretation of the recent history of the Red Sea. Briefly, it appears that the evolution of the Red Sea has occurred in two phases. The first phase probably occurred in pre-Miocene times. A second has formed the central axial valley in the last 3 m.y.

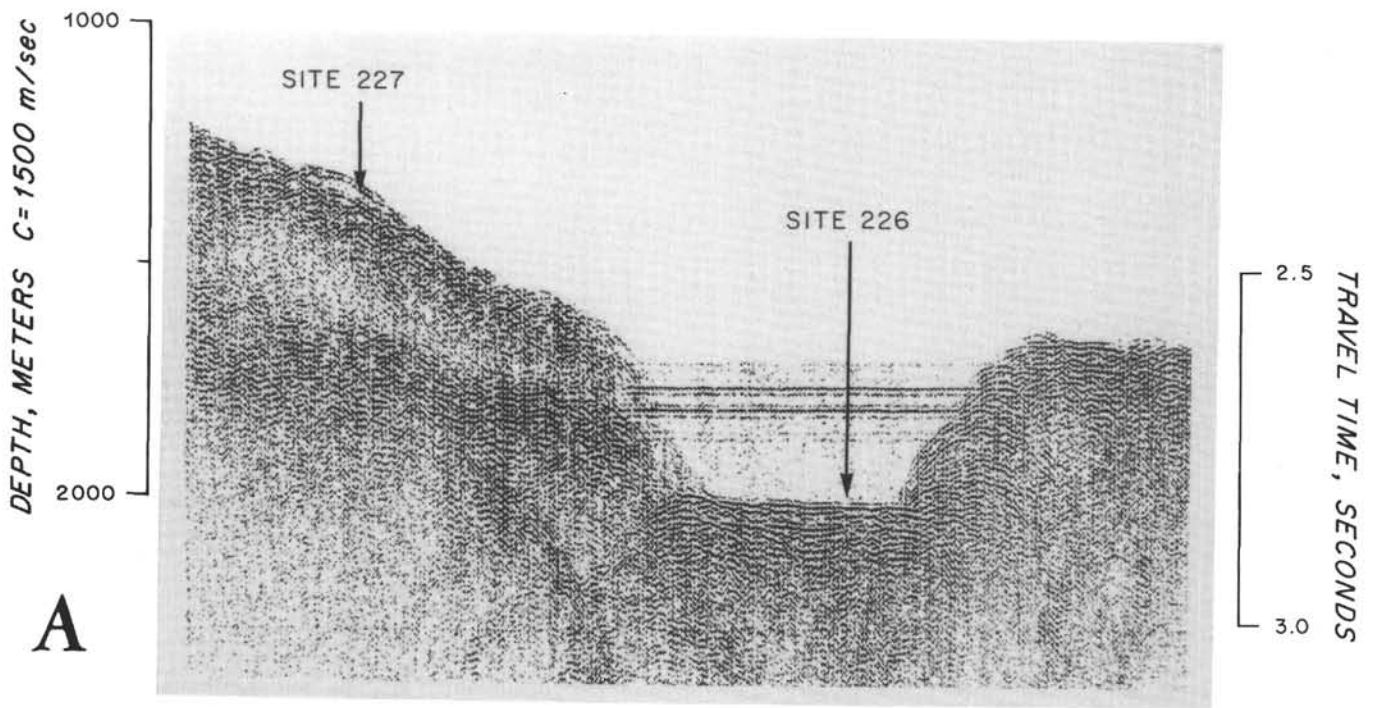
Two interesting problems related to this site concern the reconstruction of the sedimentary conditions during the period of evaporite deposition and the determination of the relationship, if any, between the heavy metal enrichments and the hot brine area. Stoffers and Kühn (this volume) argue very convincingly that the evaporites were deposited in a shallow water environment, perhaps similar to a present-day sabkha. Their main evidence is the nodular character of the anhydrites which is similar to supratidal anhydrite nodules in recent sabkhas. Their geochemical data also suggest a shallow water environment; especially impressive are their bromine values which show fluctuations within the evaporites that suggest occasional dilution of the saline waters by the influx of seawater.

Variations in pore water content (Manheim et al., Chapter 35) and hydrogen isotope data (Friedman and Hardcastle, this volume) also suggest a shallow water situation with occasional influxes of salt or fresh water. The deuterium values associated with the evaporites suggest fresh water contamination either from rainfall or river run-off (Friedman and Hardcastle, this volume).

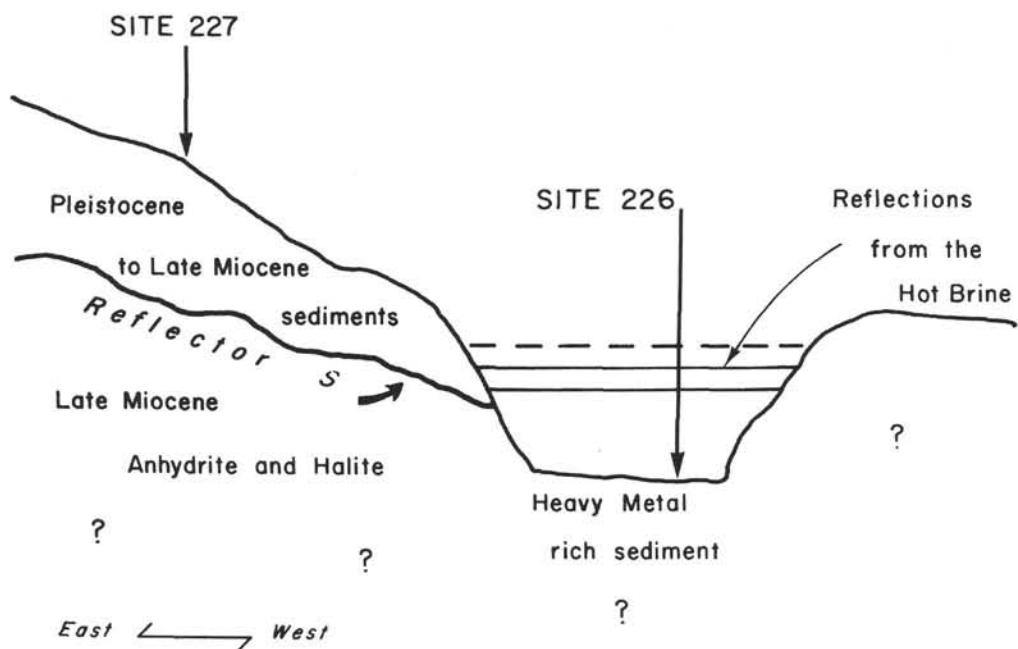
The enrichments of the shales and dark muds in elements such as vanadium, molybdenum, and copper suggest that these sediments could be a source for some of the metals found in the hot brine area. It was also interesting to note the coincidence in depth between the top of acoustic reflector S (Figure 8) and the brine seawater interface. This suggests that where the Miocene evaporites crop out in or near an enclosed basin, a brine pool is possible (Ross et al., 1973). Recent detailed studies of the Red Sea by Bäcker and Schoell (1972) have disclosed 13 new areas containing brines and/or metalliferous sediments. Unfortunately, no seismic reflection information was obtained to determine whether or not the brines occurred where the evaporites cropped out.

### REFERENCES

- Allan, T. D., 1966. A bathymetric chart of the Red Sea: *Int. Hyd. Rev.*, v. 43, p. 33-36.
- Amann, H., 1972. Marine raw material exploration with the 'Valdivia'; *Meerestechnik*, v. 3, p. 102-106.
- Bäcker, H. and Scholl, M., 1972. New deeps with brines and metalliferous sediments in the Red Sea: *Nat. Phys. Sci.*, v. 240, p. 153-158.
- Bischoff, J. L. and Manheim, F. T., 1969. Economic potential of the Red Sea heavy metal deposits. *In* Degens, E. T. and Ross, D. A. (Eds.). *Hot brines and recent heavy metal deposits in the Red Sea*: New York (Springer-Verlag), p. 535-541.
- Boudreaux, J. E. and Hay, W. W., 1969. Calcareous nannoplankton and biostratigraphy of the Late Pliocene-Pleistocene-Recent sediments in the Submarex cores: *Rev. Espan. Micropal.*, v. 1, p. 249-292.



**A**

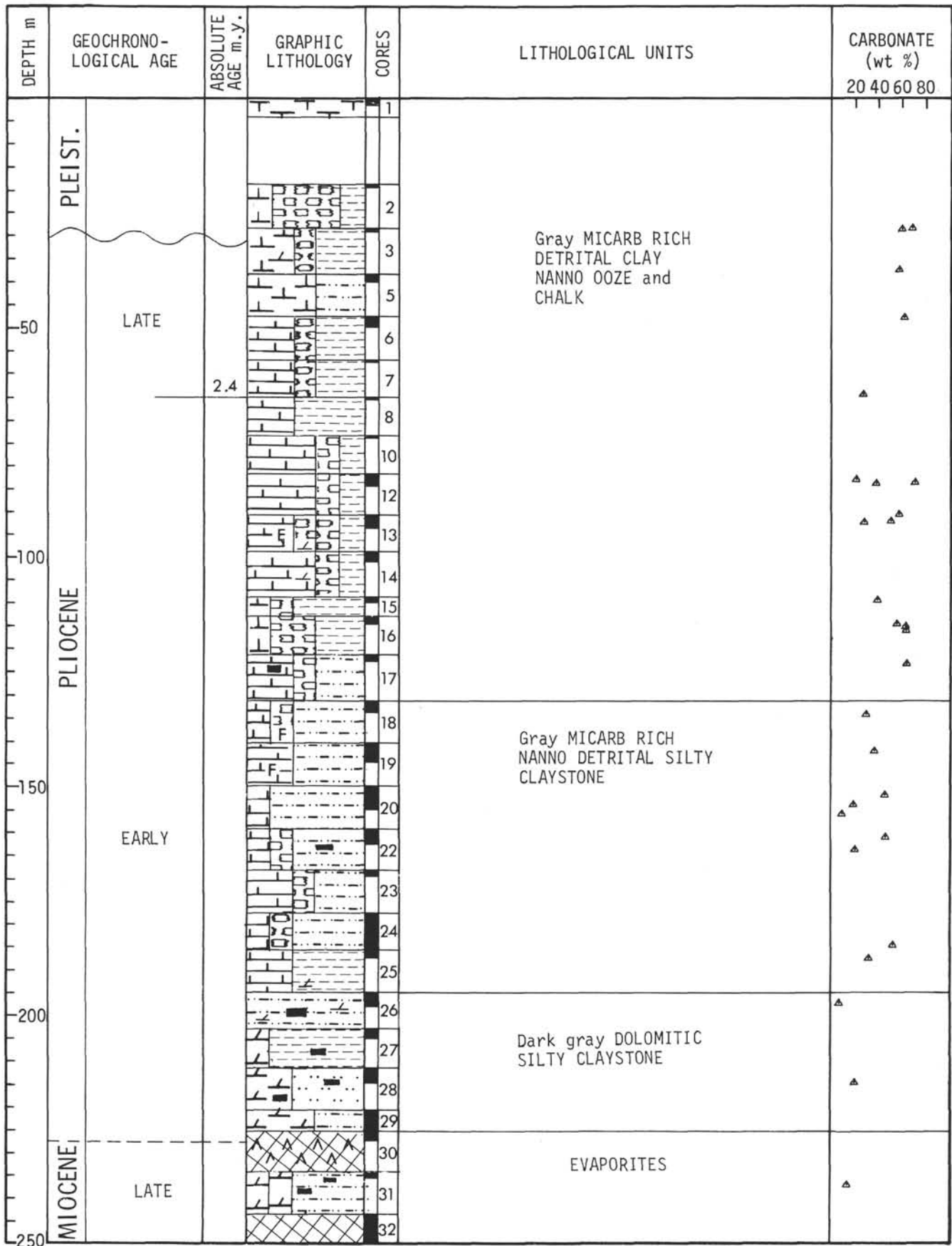


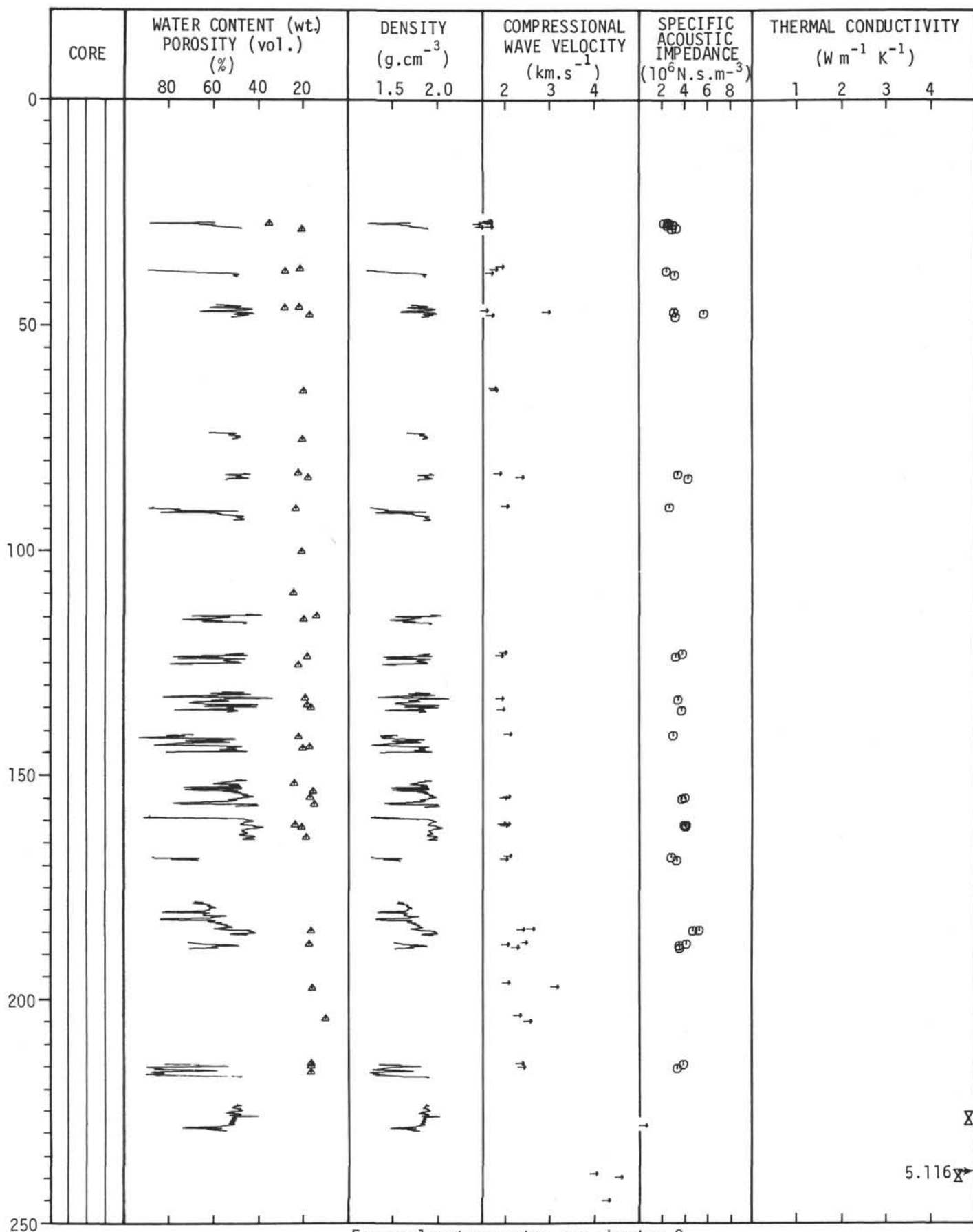
**B**

Figure 8. (a) Seismic profile record. (b) Interpretation of general stratigraphy near Sites 227 and 226. The travel time is the two-way travel time.

- Chou, T. J., 1968. Lead isotopes of the Red Sea region: *Earth Planet. Sci. Lett.*, v. 5, p. 143-147.
- Degens, E. T. and Ross, D. A. (Eds.), 1969. Hot brines and recent heavy metal deposits in the Red Sea: New York (Springer-Verlag).
- Erickson, A. J. and Simmons, G., 1969. Thermal measurements in the Red Sea hot brine pools. *In* Degens, E. T. and Ross, D. A. (Eds.), Hot brines and recent heavy metal deposits in the Red Sea: New York (Springer-Verlag), p. 114-121.
- Fairhead, J. D. and Girdler, R. W., 1960. The seismicity of the Red Sea, Gulf of Aden, and Afar Triangle: *Phil. Trans. Roy. Soc. London, Series A*, v. 267, p. 195.
- Girdler, R. W., 1960. A review of Red Sea heat flow: *Phil. Trans. Roy. Soc. London, Series A*, v. 267, p. 191.
- Goll, R., 1969. Radiolaria: The History of a Brief Invasion. *In* Degens, E. T. and Ross, D. A. (Eds.), Hot brines and recent heavy metal deposits in the Red Sea, New York (Springer-Verlag), p. 306-312.
- Herman, Y., 1965. Etudes des sédiments quaternaires de la Mer Rouge: Doctoral Thesis, University of Paris.
- Knott, S. T., Bunce, E. T., and Chase, R. L., 1966. Red Sea seismic reflection: The world rift system: *Geol. Surv. Canada Paper* 66-14, p. 5.
- Laughton, A. S., 1970. A new bathymetric chart of the Red Sea: *Phil. Trans. Roy. Soc. London, Series A*, v. 267, p. 21-22.
- Phillips, J. D. and Ross, D. A., 1970. Continuous seismic reflexion profiles in the Red Sea: *Phil. Trans. Roy. Soc. London, Series A*, v. 267, p. 143-152.
- Reynolds, P. H. and Dasch, E. J., 1971. Lead isotopes in marine manganese nodules and the ore-lead growth curve: *Geophys. Res.*, v. 76, p. 5124-5129.
- Ross, D. A., Hayes, E. E., and Allstrom, F. C., 1969. Bathymetry and continuous seismic profiles of the hot brine region of the Red Sea. *In* Degens, E. T. and Ross, D. A. (Eds.), Hot brines and recent heavy metal deposits in the Red Sea: New York (Springer-Verlag), p. 82-97.
- Ross, D. A., Whitmarsh, R. B., Ali, S. A., Boudreaux, J. E., Coleman, R., Fleisher, R. L., Girdler, R., Manheim, F., Matter, A., Nigrini, C., Stoffers, P., and Supko, P. R., 1973. Red Sea drillings: *Science*, v. 179, p. 377-380.
- Vine, F. J., 1966. Spreading of the ocean floor: new evidence: *Science*, v. 154, p. 1405.

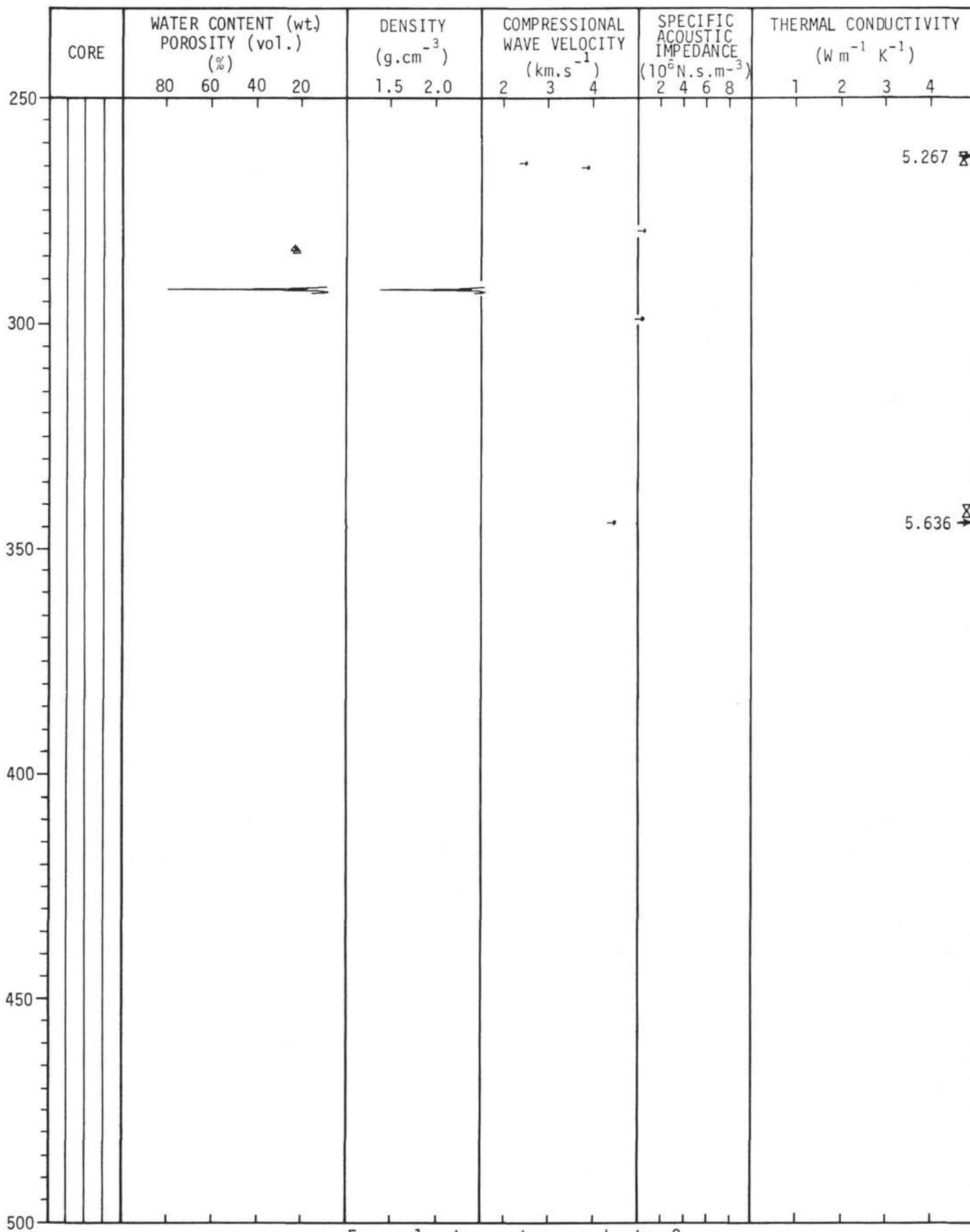
SITE 227



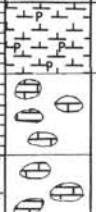


For explanatory notes see chapter 2.



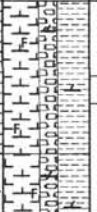


For explanatory notes see chapter 2.

Site 227		Hole		Core 1		Cored Interval: 0-3 m			
AGE	ZONE	FOSSIL CHARACTER			SECTION METERS	LITHOLOGY	DEFORMATION	LITHO. SAMPLE	LITHOLOGIC DESCRIPTION
		FORAMS	NANNOS	RADS					
LATE PLEISTOCENE	Gephyrocapsa oceanica	common, well preserved	abundant and well preserved	absent	0.5 1.0			1	Yellowish brown PTEROPOD - FORAM Ooze.  Dominantly sand size brown to cream CARBONATE GRAVEL. Gravel created by drilling. Particles are pieces of carbonate ooze that has been lithified in situ.  Color legend: 1 = yellowish brown 10YR 5/4
					Core Catcher				

Site 227		Hole		Core 2		Cored Interval: 18-27 m			
AGE	ZONE	FOSSIL CHARACTER			SECTION METERS	LITHOLOGY	DEFORMATION	LITHO. SAMPLE	LITHOLOGIC DESCRIPTION
		FORAMS	NANNOS	RADS					
EARLY PLEISTOCENE	Emilliantia lacunosa	common, well preserved	abundant and well preserved	absent	0.5 1.0	Void		122	Yellowish gray DETRITAL CLAY RICH MICARB CHALK better cemented at top, thin at bottom where it grades to being deformable with finger pressure.  Dominant lithology SS: Section 1-122 cm. Composition: Micarb 75% Detrital 20% Forams 5%  Color legend: 1 = yellowish gray 5Y 8/1
					Core Catcher			CC	

Explanatory notes in chapter 2

Site 227		Hole		Core 3		Cored Interval: 27-36 m			
AGE	ZONE	FOSSIL CHARACTER			SECTION METERS	LITHOLOGY	DEFORMATION	LITHO. SAMPLE	LITHOLOGIC DESCRIPTION
		FORAMS	NANNOS	RADS					
LATE PLEISTOCENE	Discoaster surculus Discoaster pentaradiatus	well preserved abundant and well preserved	absent		0.5 1.0			25 40 136 144 CC	Grayish MICARB RICH DETRITAL CLAY NANNO Ooze.  Stiff, massive bedding, lower part is mottled with dark gray (N3) pyrite-rich spots. Light bluish gray part is rich in FORAMS.  Dominant lithology SS: Section 1-136 cm. Composition: Nannos 40% Detrital clay 30% Micarb 15% Dolomite 10%  Color legend: 1 = yellowish gray 5Y 8/1 2 = lightbluish gray 5B 7/1 3 = greenish gray 5GY 6/1 4 = light gray N7 5 = light olive gray 5Y 6/1 6 = pinkish gray 5YR 8/1 7 = grayish black N2 8 = light bluish gray 5B 9/1
					Core Catcher			CC	Shore-based laboratory results Organic Carbon Carbonate Section 1-119 cm = .1% 68% Section 1-144 cm = .9% 59%  X-ray mineralogy: Section 1-120 cm Calcite 60% Dolomite 16% Quartz 5% K-feldspar 1% Plagioclase 3% Kaolinite 1% Mica 5% Chlorite 1% Palygorskite 8% Section 1-143 cm (MHO1) Calcite 55% Quartz 3% Plagioclase 4% Layered Silicates 30% Dolomite 8%

Explanatory notes in chapter 2

AGE	ZONE	FOSSIL CHARACTER			SECTION METERS	LITHOLOGY	DEFORMATION	LITHO. SAMPLE	LITHOLOGIC DESCRIPTION
		FORAMS	NANNOS	RADS					
LATE PLIOGENE	Discoaster surculus	abundant and well preserved							
		absent			0.5				Washed in material no real recovery. Grayish MICARB RICH DETRITAL CLAY NANNO OOZE.
					1				Dominant lithology SS: Section CC. Composition: Nannos 40% Detrital clay 35% Micarb 15% Dolomite 10%
					1.0				
					2				
					3				
					4				
					5				
					6				
					Core Catcher			CC	

Explanatory notes in chapter 2

AGE	ZONE	FOSSIL CHARACTER			SECTION METERS	LITHOLOGY	DEFORMATION	LITHO. SAMPLE	LITHOLOGIC DESCRIPTION
		FORAMS	NANNOS	RADS					
LATE PLIOGENE	Sphenolithus abies	few, well preserved	abundant and well preserved	absent					Grayish MICARB RICH DETRITAL SILT NANNO OOZE and CHALK.
		absent			0.5	Void			Homogeneous, stiff, no disturbance, semilithified chalk between 120-125 (Sec. 1) and 20-45 (Sec. 2).
					1				Dominant lithology SS: Section 2-120 cm. Composition: Nannos 55% Detrital silt 40% Dolomite 5%
					1.0				Color legend: 1 = greenish gray 5G 6/1 2 = grayish yellow green 5GY 7/2 3 = light olive gray 5Y 6/1
					2	Void			
					2				
					Core Catcher			CC	
									Shore-based laboratory results Organic Carbon Carbonate Section 1-115 cm = 1.4% 57% Section 2-120 cm = 40% X-ray mineralogy: Section 2-120 cm (WHOI) Calcite 44% Plagioclase 6% Quartz 3% Layered Silicates 43% Dolomite 4%

Site227		Hole		Core6		Cored Interval:45-54 m			
AGE	ZONE	FOSSIL CHARACTER			SECTION METERS	LITHOLOGY	DEFORMATION	LITHO. SAMPLE	LITHOLOGIC DESCRIPTION
		FORAMS	NANNOS	RADS					
LATE PLIOCENE	Sphenolithus abies	few to common, well preserved	abundant and well preserved	absent	1	[Lithology diagram]	O O O	45	Gray MICARB RICH DETRITAL CLAY NANNO CHALK intercalated with very dark green NANNO RICH DETRITAL CLAY MICARB CHALK.  Dominant lithology SS: Section 1-45 cm. MICARB RICH DETRITAL CLAY NANNO CHALK Composition: Nannos 50% Detrital clay 35% Micarb 15%  Minor lithology SS: Section 2-90 cm. NANNO RICH DETRITAL CLAY MICARB CHALK Composition: Micarb 45% Detrital clay 35% Nannos 20%  Color legend: 1 = light olive gray 5Y 6/2 2 = very dark gray 5Y 3/1 3 = olive gray 5Y 5/1  <u>Shore-based laboratory results</u> Organic Carbon Carbonate Section 2-108 cm = .1% 61% Section 1- 71 cm = 62%  X-ray mineralogy: Section 2-120 cm Calcite 57% Dolomite 12% Quartz 7% K-feldspar 2% Plagioclase 7% Kaolinite 1% Mica 7% Chlorite 2% Palygorskite 5%  Section 1-71 cm (WH01) Calcite 60% Layered Silicates 31% Plagioclase 5% Quartz 4%
					2			80	
					Core Catcher				

Site227		Hole		Core 7		Cored Interval:54-63 m			
AGE	ZONE	FOSSIL CHARACTER			SECTION METERS	LITHOLOGY	DEFORMATION	LITHO. SAMPLE	LITHOLOGIC DESCRIPTION
		FORAMS	NANNOS	RADS					
LATE PLIOCENE	Sphenolithus abies	common, fair preservation	abundant and moderately well preserved	absent	Core Catcher	[Lithology diagram]		CC 1	Gray MICARB RICH DETRITAL CLAY NANNO CHALK.  Dominant lithology SS: Section CC. Nannos 50% Detrital clay 30% Micarb 20%  Color legend: 1 = dark gray 5Y 4/1

Explanatory notes in chapter 2

Site227		Hole		Core 8		Cored Interval:63-72 m			
AGE	ZONE	FOSSIL CHARACTER			SECTION METERS	LITHOLOGY	DEFORMATION	LITHO. SAMPLE	LITHOLOGIC DESCRIPTION
		FORAMS	NANNOS	RADS					
EARLY PLIOCENE	Reticulofenestra pseudumbillica	few to absent, well preserved	abundant and moderately well preserved	absent	1	Void		120	Gray NANNO DETRITAL SILTY CLAY. Core catcher is DOLOMITE RICH.  Color legend: 1 = dark gray 5Y 4/1  <u>Shore-based laboratory results</u> Organic Carbon Carbonate Section 1-124 cm = .5% 27%
					Core Catcher			CC	

Site227		Hole		Core 9		Cored Interval:72-72 m (Heat flow)			
AGE	ZONE	FOSSIL CHARACTER			SECTION METERS	LITHOLOGY	DEFORMATION	LITHO. SAMPLE	LITHOLOGIC DESCRIPTION
		FORAMS	NANNOS	RADS					
EARLY PLIOCENE	Reticulofenestra pseudumbillica	abundant and well preserved	absent		Core Catcher	[Lithology diagram]		CC 1	Gray MICARB RICH DETRITAL CLAY NANNO CHALK.  Dominant lithology SS: Section CC. Composition: Nannos 45% Detrital clay 35% Micarb 15% Dolomite 5%  Color legend: 1 = olive gray 5Y 5/1

Site227		Hole		Core10		Cored Interval:72-81 m			
AGE	ZONE	FOSSIL CHARACTER			SECTION METERS	LITHOLOGY	DEFORMATION	LITHO. SAMPLE	LITHOLOGIC DESCRIPTION
		FORAMS	NANNOS	RADS					
EARLY PLIOCENE	Reticulofenestra pseudumbillica	rare to common, fair to good preservation	abundant and well preserved	absent	1	Void		50	Gray MICARB DETRITAL CLAY RICH NANNO CHALK. Cores badly disturbed by drilling.  Dominant lithology SS: Section 1-50 cm. Composition: Nannos 65% Micarb 15% Detrital clay 15% Dolomite 5%  Color legend: 1 = dark greenish gray 5G 4/1
					Core Catcher			CC	

Explanatory notes in chapter 2

Site 227		Hole		Core 11		Cored Interval: 81-81 m (Heat flow)			
AGE	ZONE	FOSSIL CHARACTER			SECTION METERS	LITHOLOGY	DEFORMATION	LITHO. SAMPLE	LITHOLOGIC DESCRIPTION
		FORAMS	NANNOS	RADS					
EARLY PLIOCENE	Reticulofenestra pseudumbillica	abundant and well preserved	absent				Core Catcher	CC 1	Gray MICARB RICH DETRITAL CLAY NANNO CHALK.  Dominant lithology SS: Section CC. Composition: Nannos           40% Detrital clay   40% Micarb           15% Dolomite         5%  Color legend: 1 = dark greenish gray   5G 4/1

Site 227		Hole		Core 12		Cored Interval: 81-90 m			
AGE	ZONE	FOSSIL CHARACTER			SECTION METERS	LITHOLOGY	DEFORMATION	LITHO. SAMPLE	LITHOLOGIC DESCRIPTION
		FORAMS	NANNOS	RADS					
EARLY PLIOCENE	Reticulofenestra pseudumbillica	abundant and well preserved	absent				Core Catcher	90 1 2 2 1 2 3 3 4 to 5 CC	Greenish gray DETRITAL CLAY MICARB RICH NANNO CHALK intercalated with greenish black MICARB NANNO RICH DETRITAL CLAYSTONE.  All layers except greenish black ones are moderately bioturbated. Lower part of the core is rich in Pyrite.  Dominant lithology SS: Section 1-90 cm. DETRITAL CLAY MICARB RICH NANNO CHALK Composition: Nannos           60% Micarb           20% Detrital clay   20% Forams           Trace  Minor lithology SS: Section 2-110 cm. MICARB NANNO RICH DETRITAL CLAYSTONE Composition: Detrital clay   70% Nannos           15% Micarb           15% Forams           Trace Dolomite         Trace  Color legend: 1 = greenish black       5G 2/1 2 = greenish gray       5G 6/1 3 = light olive gray     5G 6/1 4 = light bluish gray   5B 7/1 5 = medium bluish gray 5B 5/1  Shore-based laboratory results Organic Carbon   Carbonate Section 2- 22 cm = .2%   21% Section 2- 76 cm = .1%   70% Section 2-100 cm = .2%   38%

Explanatory notes in chapter 2

Site 227		Hole		Core 13		Cored Interval: 90-99 m			
AGE	ZONE	FOSSIL CHARACTER			SECTION METERS	LITHOLOGY	DEFORMATION	LITHO. SAMPLE	LITHOLOGIC DESCRIPTION
		FORAMS	NANNOS	RADS					
EARLY PLIOCENE	Reticulofenestra pseudumbillica	well preserved, common	absent				Core Catcher	1 2 1 2 1 2	Gray DETRITAL SILTY CLAY NANNO CHALK intercalated with gray DETRITAL CLAY RICH MICARB NANNO CHALK.  Homogeneous, semilithified, moderately bioturbated.  Color legend: 1 = dark greenish gray   5G 4/1 2 = greenish gray       5G 6/1  Shore-based laboratory results Organic Carbon   Carbonate Section 1-27 cm = 1.6%   57% Section 2-32 cm = 2.6%   50% Section 2-50 cm = .2%   28%  Grain size: Section 1-25 cm Sand           2% Silt           34% Clay           64%  X-ray mineralogy: Section 2-50 cm Calcite       33% Dolomite     3% Quartz       14% K-feldspar   3% Plagioclase 18% Kaolinite   1% Mica         11% Chlorite     3% Montmorillonite 7% Palygorskite 4% Clinoptilolite 2% Section 1-22 cm (WHOI) Calcite       63% Layered Silicates 30% Feldspar      6% Quartz       4%

Site 227		Hole		Core 14		Cored Interval: 99-108 m			
AGE	ZONE	FOSSIL CHARACTER			SECTION METERS	LITHOLOGY	DEFORMATION	LITHO. SAMPLE	LITHOLOGIC DESCRIPTION
		FORAMS	NANNOS	RADS					
EARLY PLIOCENE	Ceratoolithus rugosus - C. tricinctulatus	planktonics absent	abundant and well preserved	absent			Core Catcher	90 1	Gray DETRITAL CLAY MICARB RICH - NANNO CHALK.  Homogeneous, semilithified.  Dominant lithology SS: Section 1-90 cm. Composition: Nannos           70% Micarb           15% Detrital clay   15% Dolomite         Trace Pyrite           Trace  Color legend: 1 = greenish gray       5G 6/1

Explanatory notes in chapter 2

Site 227		Hole		Core 15		Cored Interval: 108-113 m				
AGE	ZONE	FOSSIL CHARACTER				SECTION METERS	LITHOLOGY	DEFORMATION	LITHO. SAMPLE	LITHOLOGIC DESCRIPTION
		FORAMS	NANNOS	RADS	OTHERS					
EARLY PLIOCENE	Cerastolithus rugosus	rare to few, well preserved	absent	absent	absent	0.5	Void			Gray FORAM MICARB - NANNO RICH DETRITAL CLAYSTONE.  Homogeneous, semlithified, partly disturbed by drilling, mottled from 110-115 cm.  Dominant lithology SS: Section 1-101 cm. Composition: Detrital clay 60% Nannos 25% Micarb 15% Forams Trace Pyrite Trace Dolomite Trace  Color legend: 1 = dark greenish gray 56 4/1 <u>Shore-based laboratory results</u> Organic Carbon Carbonate Section 1-93 cm - 1.1% 39%  X-ray mineralogy: Section 1-98 cm (WHOI) Calcite 44% Layered Silicates 40% Quartz 3% Plagioclase 3%
		absent	absent	absent	absent	1.0	Core Catcher	101	1	

Explanatory notes in chapter 1

Site 227		Hole		Core 16		Cored Interval: 113-122 m				
AGE	ZONE	FOSSIL CHARACTER				SECTION METERS	LITHOLOGY	DEFORMATION	LITHO. SAMPLE	LITHOLOGIC DESCRIPTION
		FORAMS	NANNOS	RADS	OTHERS					
EARLY PLIOCENE	Cerastolithus rugosus	absent	absent	absent	absent	0.5	Void			Gray NANNO RICH DETRITAL SILTY CLAY MICARB CHALK.  Relatively less nannos are found in the very dark gray sediments.  Dominant lithology SS: Section 2-63 cm. Composition: Nannos 50% Detrital 35% Micarb 15% Dolomite Trace  Color legend: 1 = olive gray 5Y 5/2 2 = dark gray 5Y 4/1 3 = very dark gray 5Y 3/1 4 = gray 5Y 6/1 5 = light gray 5Y 7/1  <u>Shore-based laboratory results</u> Organic Carbon Carbonate Section 1-109 cm = .1% 55% Section 2- 22 cm = 1.4% 63% Section 2-110 cm = .1% 63%  Grain size: Sections 1-105 cm, 2-22 cm Sand 2% 3% Silt 59% 34% Clay 38% 63%  X-ray mineralogy: Section 2-100 cm Calcite 62% Dolomite 11% Quartz 4% Plagioclase 8% Kaolinite 1% Mica 7% Chlorite 1% Montmorillonite 1% Palygorskite 4% Section 2-19 cm (WHOI) Calcite 60% Layered Silicates 35% Quartz 5%
		rare, fair penetration	rare and moderately well preserved	absent	absent	1.0	Void	95	1	

Explanatory notes in chapter 2

Site 227 Hole Core17 Cored Interval:122-131 m

AGE	ZONE	FOSSIL CHARACTER			SECTION	METERS	LITHOLOGY	DEFORMATION	LITHO. SAMPLE	LITHOLOGIC DESCRIPTION	
		FORAMS	NANNOS	RADS							OTHERS
EARLY PLIOCENE	Ceratolithus rugosus	few to absent, well preserved	abundant and well preserved	absent	1	0.5	Void		70	1	Gray MICARB RICH DETRITAL SILTY CLAY NANNO CHALK.
					2	1.0	transition		115	2	Dominant lithology SS: Section 1-115 cm. Composition: Nannos 45% Detrital 40% Micarb 15% Pyrite Trace
					Core Catcher				CC		Color legend: 1 = olive gray 5Y 4/1 2 = greenish gray 5GY 6/1 3 = dark greenish gray 5GY 4/1
											Shore-based laboratory results Section 1-85 cm Organic Carbon Carbonate = 1.0% 64% Section 1-40-43 cm = 67%
											X-ray mineralogy: Section 1-83 cm (WHOI) Calcite 60% Quartz 4% Layered Silicates 30% Clinoptilolite 2% Plagioclase 4%

Explanatory notes in chapter 2

Site 227 Hole Core18 Cored Interval:131-140 m

AGE	ZONE	FOSSIL CHARACTER			SECTION	METERS	LITHOLOGY	DEFORMATION	LITHO. SAMPLE	LITHOLOGIC DESCRIPTION
		FORAMS	NANNOS	RADS						
EARLY PLIOCENE	Ceratolithus rugosus	well preserved, common	abundant and well preserved	absent	1	0.5	Void			Gray MICARB NANNO RICH DETRITAL SILTY CLAYSTONE.
					2	1.0	transition		118	1
					Core Catcher					Color legend: 1 = dark gray 5Y 4/1 2 = gray 5Y 4/1 3 = very dark gray 5Y 3/1
										Shore-based laboratory results Section 2-122 cm Organic Carbon Carbonate = .5% 30% Section 3-53-55 cm = 48% Section 4-36-38 cm = 32%
										X-ray mineralogy: Section 2-120 cm Sand Trace Silt 43% Clay 57%
										X-ray mineralogy: Section 2-120 cm Calcite 32% Dolomite 10% Quartz 13% K-feldspar 5% Plagioclase 16% Mica 18% Chlorite 5% Montmorillonite 2%

Explanatory notes in chapter 2

Site227		Hole		Core19		Cored Interval:140-149 m										
AGE	ZONE	FOSSIL CHARACTER				SECTION METERS	LITHOLOGY	DEFORMATION	LITHO. SAMPLE	LITHOLOGIC DESCRIPTION						
		FORAMS	NANNOS	RAUS	OTHERS											
EARLY PLIOCENE	Ceratoithus rugosus	common to absent, well preserved				1	Void	140	1 to 2	140	Gray NANO DETRITAL SILTY CLAYSTONE, top is MICARB RICH. Semilithified, abundant burrows (1 mm to 1 cm $\phi$ ). Dominant lithology SS: Section 2-90 cm. Composition: Detrital 60% Nannos 30% Micarb 10% Pyrite Trace Dark layers are poorer in Forams. Nannos are better preserved. Pyrite slightly more abundant. Color legend: 1 = gray 5Y 5/1 2 = dark gray 5Y 4/1  Shore-based laboratory results Organic Carbon Carbonate Section 2-16 cm = .2% 37% Grain size: Section 2-14 cm Sand 1% Silt 48% Clay 51% X-ray mineralogy: Section 1-60 cm Calcite 42% Dolomite 6% Quartz 11% K-feldspar 5% Plagioclase 13% Kaolinite 2% Mica 11% Chlorite 3% Montmorillonite 2% Palygorskite 3% Pyrite 1% Amphibole 1%					
		abundant and well preserved										2	Core Catcher	90	1 to 2	90
		absent														
		Core Catcher										3	Core Catcher	1 to 2	90	90

Explanatory notes in chapter 2

Site227		Hole		Core20		Cored Interval:149-158 m									
AGE	ZONE	FOSSIL CHARACTER				SECTION METERS	LITHOLOGY	DEFORMATION	LITHO. SAMPLE	LITHOLOGIC DESCRIPTION					
		FORAMS	NANNOS	RAUS	OTHERS										
EARLY PLIOCENE	Ceratoithus rugosus	rare, well preserved				1	Void	115	1	115	Gray NANO RICH DETRITAL SILTY CLAYSTONE, top section is NANO DETRITAL SILTY CLAYSTONE. Up to 10% pyrite, forams and carbonaceous matter are found in the dark gray sediments. Dominant lithology SS: Section 3-45 cm. NANO RICH DETRITAL SILTY CLAYSTONE Composition: Detrital 70% Nannos 25% Pyrite 3% Forams 2% Minor lithology SS: Section 2-75 cm. NANO DETRITAL SILTY CLAYSTONE Composition: Detrital 55% Nannos 45% Color legend: 1 = dark gray 5Y 4/1 2 = gray 5Y 5/1 3 = black 5Y 2.5/1 4 = gray 2.5Y 5/1 5 = gray 2.5Y 6/1 6 = very dark gray 5Y 3/1				
		abundant and well preserved										2	75	2 to 1	75
		absent													
		Core Catcher										4	115	4-5	115
		Core Catcher													
Core Catcher				5	115	6	115								

Shore-based laboratory results  
Organic Carbon Carbonate  
Section 3-143 cm = .3% 19%  
Section 5- 36 cm = 6.0% 10%  
Grain size: Sections  
2-78 cm, 3-140 cm, 5-35 cm  
Sand 1% 2% 0%  
Silt 33% 47% 37%  
Clay 66% 51% 63%  
X-ray mineralogy: Section 3-140 cm  
Calcite 29%  
Dolomite 3%  
Quartz 17%  
K-feldspar 5%  
Plagioclase 20%  
Kaolinite 4%  
Mica 15%  
Chlorite 3%  
Montmorillonite 5%  
Section 2-80 cm (MHOI)  
Calcite 43%  
Quartz 10%  
Layered Silicates 35%  
Plagioclase 12%

Site227		Hole		Core21		Cored Interval:158-158 m (Heat Flow)				
AGE	ZONE	FOSSIL CHARACTER				SECTION METERS	LITHOLOGY	DEFORMATION	LITHO. SAMPLE	LITHOLOGIC DESCRIPTION
		FORAMS	NANNOS	RAUS	OTHERS					
						Core Catcher				Whole core was filled with washed in material.

Explanatory notes in chapter 2

Site 227 Hole Core 22 Cored Interval: 158-167 m

AGE	ZONE	FOSSIL CHARACTER			SECTION METERS	LITHOLOGY	DEFORMATION	LITHO. SAMPLE	LITHOLOGIC DESCRIPTION	
		FORAMS	NANNOS	RADS						OTHERS
EARLY PLIOCENE	Ceratolithus rugosus	rare to common, fair preservation abundant and well preserved	absent	absent	0.5	Void		1	Gray MICARB NANNO RICH DETRITAL CLAYEY SILTSTONE. With pyrite, forams and organic substance in dark gray sediments. Dominant lithology SS: Section 3-95 cm. Composition: Detrital 65% Nannos 20% Micarb 15% Pyrite Trace Minor lithology SS: Section 4-60 cm. Composition: Detrital 75% Nannos 25% Color legend: 1 = very dark gray 5Y 3/1 2 = gray 5Y 6/1 3 = gray 5Y 5/1 4 = dark gray 5Y 4/1	
					1.0					2 to 1
					2					2 to 1
					3					95
			4	60	2 graded to 1		3	Shore-based laboratory results Organic Carbon Carbonate Section 2-101 cm = 2.5% 46% Section 4- 69 cm = .3% 20% Grain size: Section 4-68 cm Sand 1% Silt 55% Clay 44% X-ray mineralogy: Section 4-70 cm Calcite 28% Dolomite 2% Quartz 20% K-feldspar 7% Plagioclase 20% Mica 13% Chlorite 4% Montmorillonite 5% Palygorskite 3% Section 2-99 cm (W/OI) Calcite 40% Quartz 5% Layered Silicates 35% Plagioclase 8% Pyrite 3% Clinoptilolite 6%		
			Core Catcher	1			4			

Explanatory notes in chapter 2

Site 227 Hole Core 23 Cored Interval: 167-176 m

AGE	ZONE	FOSSIL CHARACTER			SECTION METERS	LITHOLOGY	DEFORMATION	LITHO. SAMPLE	LITHOLOGIC DESCRIPTION
		FORAMS	NANNOS	RADS					
EARLY PLIOCENE	Ceratolithus rugosus - C. tricorniculatus	planktonics absent	abundant and moderately well preserved	absent	0.5	Void		1 to 2	Gray MICARB RICH NANNO DETRITAL SILTY CLAYSTONE. Color legend: 1 = light olive gray 5Y 6/1 2 = gray 5Y 5/1 3 = olive gray 5Y 4/1 4 = very dark gray 5Y 3/1 5 = black 5Y 2.5/1
				1				3 to 4	
					1.0			5	
					Core Catcher				

Explanatory notes in chapter 2





Site 227		Hole		Core 29		Cored Interval: 221-226 m			
AGE	ZONE	FOSSIL CHARACTER			SECTION METERS	LITHOLOGY	DEFORMATION	LITHO. SAMPLE	LITHOLOGIC DESCRIPTION
		FORAMS	NANNOS	RADS					
EARLY PLEISTOCENE	Ceratolithus rugosus - C. tricorniculatus	absent	few, well preserved	common and moderately well preserved	absent	0.5	[Lithology symbols]	130	<p>Gray black NANNO RICH DOLOMITIC DETRITAL SILTY CLAYSTONE. Lower section is a black SILTY CLAY RICH DOLOSTONE.</p> <p>Entire core is badly disturbed.</p> <p>Dominant lithology SS: Section 3-130 cm. NANNO RICH DOLOMITIC DETRITAL SILTY CLAYSTONE            Composition:            Dolomite 40%            Detrital 40%            Nannos 15%            Pyrite 5%</p> <p>Minor lithology SS: Section 5-135 cm. SILTY CLAY RICH DOLOSTONE            Composition:            Dolomite 90%            Detrital 10%</p> <p>Color legend:            1 = very dark gray 5Y 3/1            2 = black 5Y 2.5/1</p>
						1.0			
						2			
						3			
						4			
5	135	CC	Core Catcher						
<p>Shore-based laboratory results</p> <p>Section 5 = Silt Fraction Carbonate 90%</p> <p>X-ray mineralogy: Section 5 (WHOI)            Dolomite 80%            Plagioclase 4%            Quartz 2%            Layered Silicates 10%            Analcite 4%</p>									

Explanatory notes in chapter 2

Site 227		Hole		Core 30		Cored Interval: 226-235 m			
AGE	ZONE	FOSSIL CHARACTER			SECTION METERS	LITHOLOGY	DEFORMATION	LITHO. SAMPLE	LITHOLOGIC DESCRIPTION
		FORAMS	NANNOS	RADS					
LATE MIOCENE?		absent	absent	absent	absent	0.5	[Lithology symbols]	120	<p>ANHYDRITE and white HALITE.</p> <p>Anhydrite is thinly laminated (white and gray) in upper part, inclined bedding (20°).</p> <p>Shore-based laboratory results</p> <p>X-ray mineralogy: Section 1-135 cm (WHOI)            Dolomite 17%            Spälerite 1%            Quartz 7%            Plagioclase 10%            Layered Silicates 56%            Microcline 3%            Analcite 2%            Pyrite 3%</p>
						1.0			
						Core Catcher			
Site 227		Hole		Core 31		Cored Interval: 235-244 m			
AGE	ZONE	FOSSIL CHARACTER			SECTION METERS	LITHOLOGY	DEFORMATION	LITHO. SAMPLE	LITHOLOGIC DESCRIPTION
		FORAMS	NANNOS	RADS					
LATE MIOCENE	Discoaster quinqueramus	absent	abundant and well preserved	absent	absent	0.5	[Lithology symbols]	120	<p>Black DOLOMITE DETRITAL SILTY CLAYSTONE.</p> <p>Brecciated, lower part with fragments of anhydrite.</p> <p>Dominant lithology SS: Section 1-130 cm.            Composition:            Detrital 50%            Dolomite 35%            Nannos 10%            Pyrite 5%</p> <p>Color legend:            1 = black N1</p> <p>Shore-based laboratory results</p> <p>Organic Carbon Carbonate            Section 1-120 cm = 2.3% 14%            Section 1-140 cm = 50%</p> <p>X-ray mineralogy: Section 1-140 cm (WHOI)            Ca-Dolomite 43%            Quartz 8%            Pyrite 3%            Plagioclase 10%            Analcite 2%            Layered Silicates 30%            Calcite 4%</p>
						1.0			
						Core Catcher			

Explanatory notes in chapter 2

Site 227 Hole Core 32 Cored Interval: 244-253 m

AGE	ZONE	FOSSIL CHARACTER			SECTION METERS	LITHOLOGY	DEFORMATION	LITHO. SAMPLE	LITHOLOGIC DESCRIPTION
		FORAMS	NANNOS	PADS					
LATE MIOCENE		absent	absent	absent	0.5	[Cross-hatched pattern]		White HALITE.	
					1				
					1.0				
					2				
					3				
				4					
				5					
				Core Catcher					

Explanatory notes in chapter 2

Site 227 Hole Core 33 Cored Interval: 253-262 m

AGE	ZONE	FOSSIL CHARACTER			SECTION METERS	LITHOLOGY	DEFORMATION	LITHO. SAMPLE	LITHOLOGIC DESCRIPTION
		FORAMS	NANNOS	PADS					
LATE MIOCENE		absent	absent	absent	0.5	[Cross-hatched pattern]		White HALITE.	
					1				
					1.0				
					2				
					3				
				4					
				Core Catcher					

Explanatory notes in chapter 2

Site 227		Hole		Core 34		Cored Interval: 262-271 m			
AGE	ZONE	FOSSIL CHARACTER			SECTION METERS	LITHOLOGY	DEFORMATION	LITHO. SAMPLE	LITHOLOGIC DESCRIPTION
		FORAMS	NANNOS	RADS					
LATE MIOCENE		absent	absent	absent	0.5 1 1.0 2 3 4	Void			White HALITE with laminae, which consist mainly of weavy and often folded anhydrite.
					Core Catcher				

Explanatory notes in chapter 2

Site 227		Hole		Core 35		Cored Interval: 271-280 m			
AGE	ZONE	FOSSIL CHARACTER			SECTION METERS	LITHOLOGY	DEFORMATION	LITHO. SAMPLE	LITHOLOGIC DESCRIPTION
		FORAMS	NANNOS	RADS					
LATE MIOCENE		absent	common and well preserved	absent	0.5 1 1.0 2 3 4 5				White HALITE lower part of the core. ANHYDRITE in the salt. Some lamination with weavy and folded anhydrite. Inclined bedding up to 50°. Anhydrite in Core 5 is nodular. Nodules separated by thin greenish seams. These seams are composed of pyrite and probably dolomite.
					Core Catcher				Black transition zone.

Explanatory notes in chapter 2

Site 227 Hole Core 36 Cored Interval: 280-289 m

AGE	ZONE	FOSSIL CHARACTER				SECTION METERS	LITHOLOGY	DEFORMATION	LITHO. SAMPLE	LITHOLOGIC DESCRIPTION																								
		FORAMS	NANNOS	RADS	OTHERS																													
LATE MIOCENE	Discoaster quinqueramus	absent				0.5	Void			<p>ANHYDRITE with beds of CRISTOBALITIC BLACK SHALE.</p> <p>Anhydrite is laminated in the upper part nodular in the lower part of the core. Interlayered in high angle, convolute flow structure, some parts are badly disturbed by drilling.</p> <p>Lithology SS: Section 2-125 cm. Composition: Clay 80% Pyrite 10% Dolomite 10%</p> <p>Shore-based laboratory results</p> <table border="1"> <tr> <td></td> <td>Organic Carbon</td> <td>Carbonate</td> </tr> <tr> <td>Section 2-105 cm =</td> <td>1.4%</td> <td>3%</td> </tr> <tr> <td>Section 3- 3 cm =</td> <td>1.2%</td> <td>4%</td> </tr> </table> <p>X-ray mineralogy: Sections (MHOI) 2-140 cm, 3-3 cm</p> <table border="1"> <tr> <td>Disordered cristobalite</td> <td>80%</td> <td>77%</td> </tr> <tr> <td>Quartz</td> <td>10%</td> <td>11%</td> </tr> <tr> <td>Pyrite</td> <td>5%</td> <td>5%</td> </tr> <tr> <td>Dolomite</td> <td>5%</td> <td>6%</td> </tr> <tr> <td>Apatite</td> <td>0%</td> <td>2%</td> </tr> </table>		Organic Carbon	Carbonate	Section 2-105 cm =	1.4%	3%	Section 3- 3 cm =	1.2%	4%	Disordered cristobalite	80%	77%	Quartz	10%	11%	Pyrite	5%	5%	Dolomite	5%	6%	Apatite	0%	2%
			Organic Carbon	Carbonate																														
		Section 2-105 cm =	1.4%	3%																														
		Section 3- 3 cm =	1.2%	4%																														
Disordered cristobalite	80%	77%																																
Quartz	10%	11%																																
Pyrite	5%	5%																																
Dolomite	5%	6%																																
Apatite	0%	2%																																
		absent	absent	absent	1.0	Void																												
		common, well preserved			2	Void		125																										
					3	Void																												
					4	Void																												
								Core Catcher																										

Site 227 Hole Core 37 Cored Interval: 289-292 m

AGE	ZONE	FOSSIL CHARACTER				SECTION METERS	LITHOLOGY	DEFORMATION	LITHO. SAMPLE	LITHOLOGIC DESCRIPTION
		FORAMS	NANNOS	RADS	OTHERS					
LATE MIOCENE?		absent	absent	absent		Void			<p>ANHYDRITE.</p> <p>White in beds of 1-2 cm, separated by ~1-3 mm beds of pyrite and dolomite at high angles (70-80°).</p>	
					0.5					
					1.0					
					2					
								Core Catcher		

Explanatory notes in chapter 2

Site 227 Hole Core 38 Cored Interval: 292-297 m

AGE	ZONE	FOSSIL CHARACTER				SECTION METERS	LITHOLOGY	DEFORMATION	LITHO. SAMPLE	LITHOLOGIC DESCRIPTION
		FORAMS	NANNOS	RADS	OTHERS					
LATE MIOCENE?		absent	absent	absent		Void			<p>ANHYDRITE.</p> <p>Slightly nodular.</p>	
					0.5					
					1.0					
								Core Catcher		

Site 227 Hole Core 39 Cored Interval: 297-305 m

AGE	ZONE	FOSSIL CHARACTER				SECTION METERS	LITHOLOGY	DEFORMATION	LITHO. SAMPLE	LITHOLOGIC DESCRIPTION
		FORAMS	NANNOS	RADS	OTHERS					
LATE MIOCENE?		absent	absent	absent		Void			<p>ANHYDRITE with very thin greenish pyrite and dolomite rich layers.</p>	
					0.5					
					1.0					
								Core Catcher		

Site 227 Hole Core 40 Cored Interval: 305-314 m

AGE	ZONE	FOSSIL CHARACTER				SECTION METERS	LITHOLOGY	DEFORMATION	LITHO. SAMPLE	LITHOLOGIC DESCRIPTION																			
		FORAMS	NANNOS	RADS	OTHERS																								
LATE MIOCENE?		absent	absent	absent					<p>Black SHALE.</p> <p>Gravelly - sandy, broken up by drilling.</p> <p>Shore-based laboratory results</p> <table border="1"> <tr> <td>Section 2-30 cm =</td> <td>Carbonate</td> </tr> <tr> <td></td> <td>30%</td> </tr> </table> <p>X-ray mineralogy: Section 2-30 cm (MHOI)</p> <table border="1"> <tr> <td>Calcite</td> <td>22%</td> </tr> <tr> <td>Quartz</td> <td>5%</td> </tr> <tr> <td>Plagioclase</td> <td>7%</td> </tr> <tr> <td>Disordered cristobalite</td> <td>3%</td> </tr> <tr> <td>Layered Silicates</td> <td>50%</td> </tr> <tr> <td>Pyrite</td> <td>5%</td> </tr> <tr> <td>Analcite</td> <td>3%</td> </tr> <tr> <td>Clinoptilolite</td> <td>5%</td> </tr> </table>	Section 2-30 cm =	Carbonate		30%	Calcite	22%	Quartz	5%	Plagioclase	7%	Disordered cristobalite	3%	Layered Silicates	50%	Pyrite	5%	Analcite	3%	Clinoptilolite	5%
Section 2-30 cm =	Carbonate																												
	30%																												
Calcite	22%																												
Quartz	5%																												
Plagioclase	7%																												
Disordered cristobalite	3%																												
Layered Silicates	50%																												
Pyrite	5%																												
Analcite	3%																												
Clinoptilolite	5%																												
					0.5																								
					1.0																								
					2			Core Catcher																					

Explanatory notes in chapter 2

Site 227		Hole			Core 41		Cored Interval: 314-323 m		
AGE	ZONE	FOSSIL CHARACTER			SECTION METERS	LITHOLOGY	DEFORMATION	LITHO. SAMPLE	LITHOLOGIC DESCRIPTION
		FORAMS	MAMMOS	RADS					
?		absent	absent	absent	0.5 1 1.0	Void			White HALITE. ANHYDRITE in the lower part of the core.
					Core Catcher				

Site 227		Hole			Core 42		Cored Interval: 323-332 m		
AGE	ZONE	FOSSIL CHARACTER			SECTION METERS	LITHOLOGY	DEFORMATION	LITHO. SAMPLE	LITHOLOGIC DESCRIPTION
		FORAMS	MAMMOS	RADS					
?		absent	absent	absent	0.5 1 1.0 2 3				White HALITE.
					Core Catcher				

Explanatory notes in chapter 2

Site 227		Hole			Core 43		Cored Interval: 332-341 m		
AGE	ZONE	FOSSIL CHARACTER			SECTION METERS	LITHOLOGY	DEFORMATION	LITHO. SAMPLE	LITHOLOGIC DESCRIPTION
		FORAMS	MAMMOS	RADS					
?		absent	absent	absent	0.5 1 1.0 2 3 4 5	Void			White HALITE. Shale and anhydrite lamination.
					Core Catcher				

Explanatory notes in chapter 2

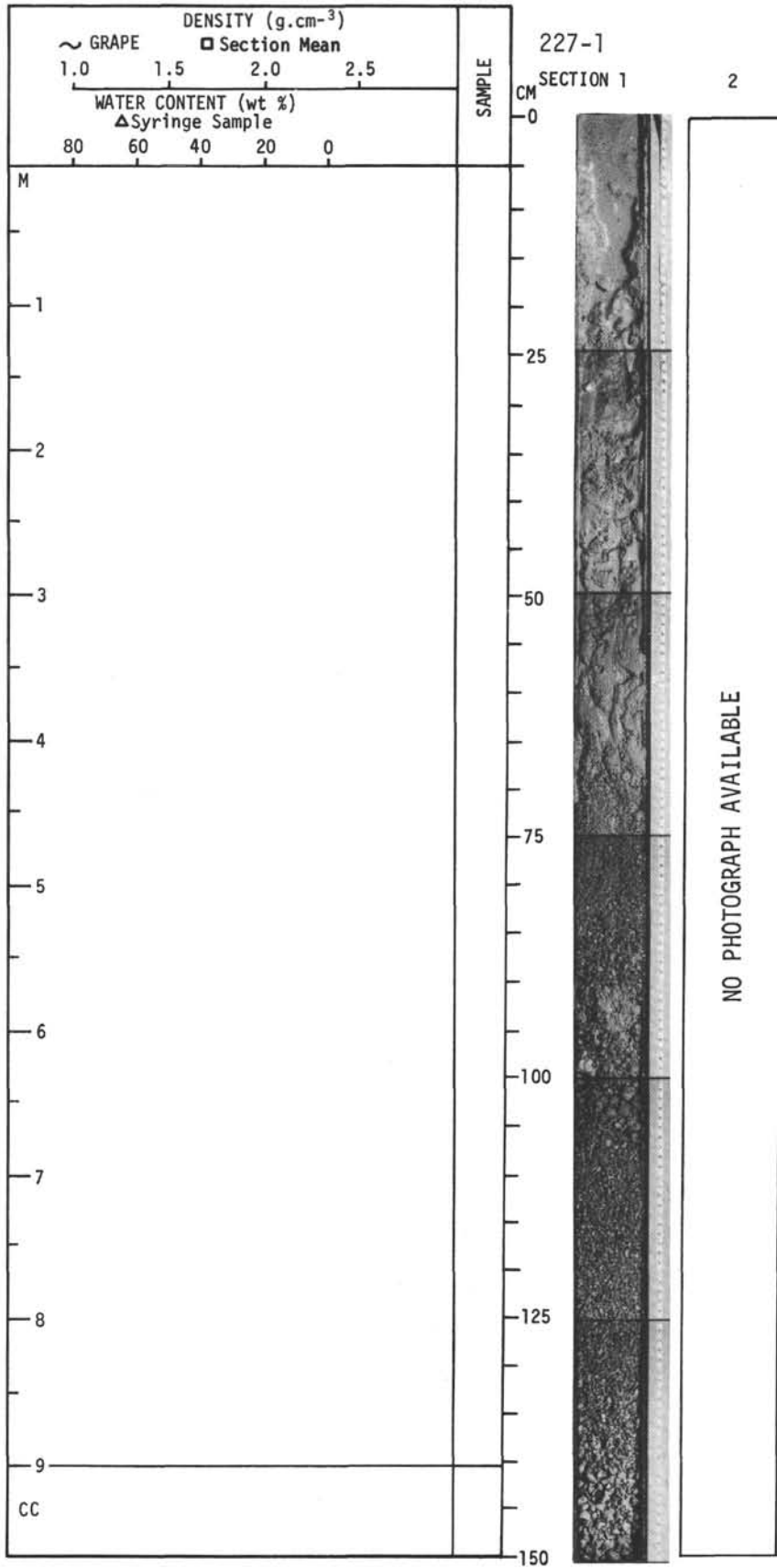
Site 227 Hole Core 44 Cored Interval:341-350 m

AGE	ZONE	FOSSIL CHARACTER				SECTION	METERS	LITHOLOGY	DEFORMATION	LITHO. SAMPLE	LITHOLOGIC DESCRIPTION
		FORAMS	NANNOS	RADS	OTHERS						
?		absent	absent	absent		0.5	Void			<p>ANHYDRITE.</p> <p>Laminated (whole anhydrite and greenish pyrite - dolomite laminae) at top and bottom. Middle part whole nodular anhydrite. Black SHALE in the core catcher.</p> <p><u>Shore-based laboratory results</u></p> <p>X-ray mineralogy: Section CC</p> <p>Quartz 9%</p> <p>Plagioclase 13%</p> <p>Layered Silicates 72%</p> <p>Pyrite 6%</p>	
						1.0	AAAAAAAA				
						2	AAAAAAAA				
						Core Catcher					

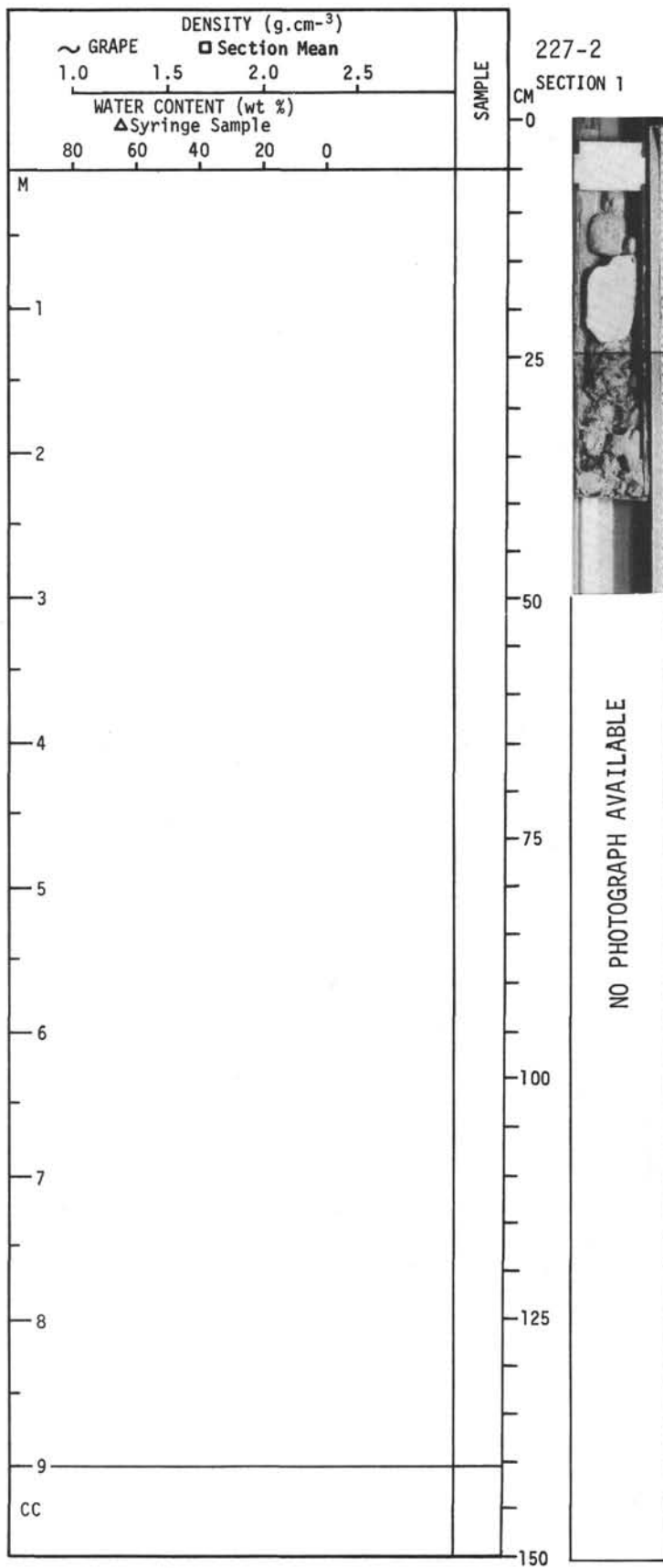
Site 227 Hole Core 45 Cored Interval:350-359 m

AGE	ZONE	FOSSIL CHARACTER				SECTION	METERS	LITHOLOGY	DEFORMATION	LITHO. SAMPLE	LITHOLOGIC DESCRIPTION
		FORAMS	NANNOS	RADS	OTHERS						
?		absent	absent			0.5				White HALITE.	
						1.0					
						2					
						Core Catcher					

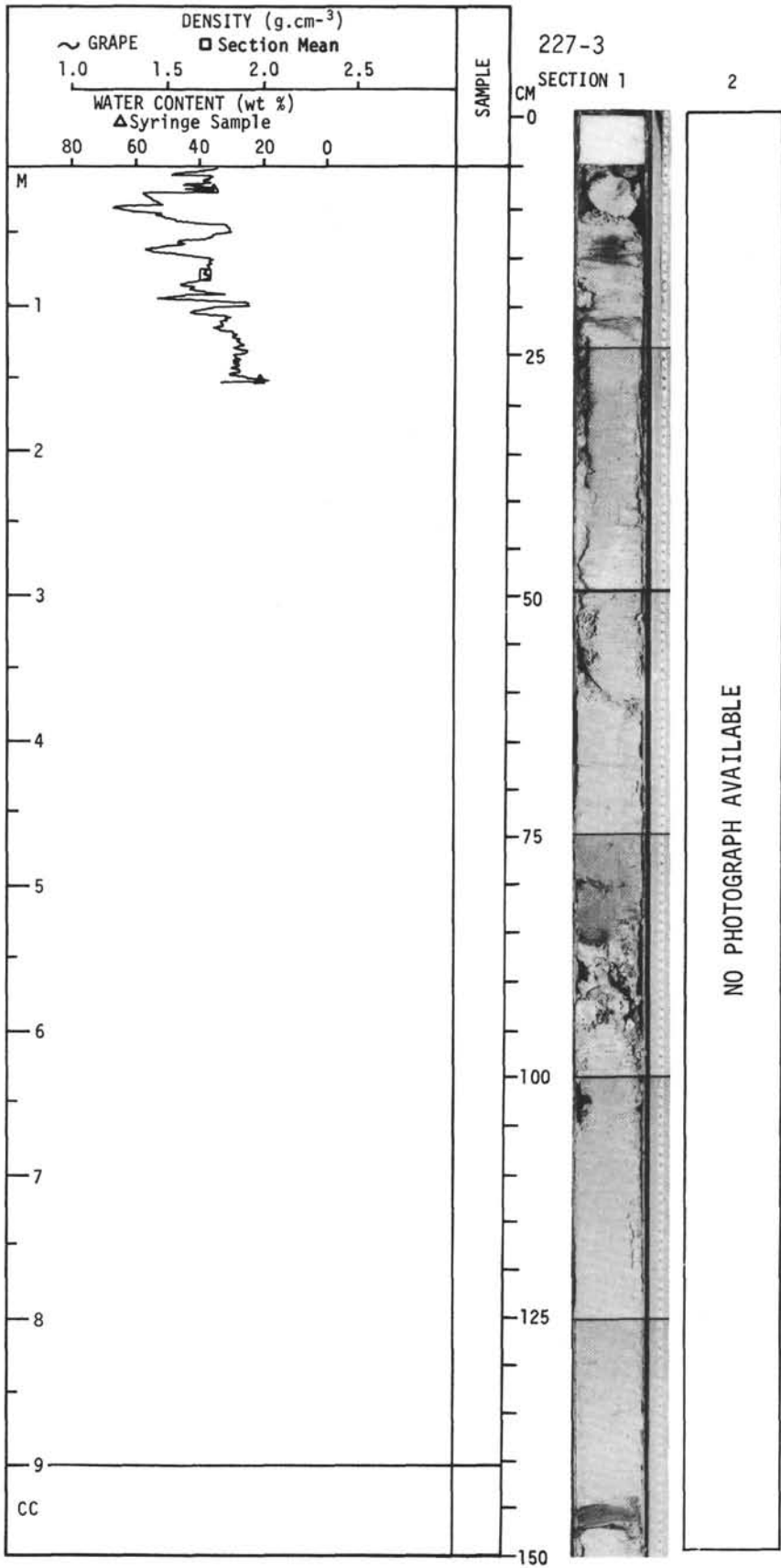
Explanatory notes in chapter 2



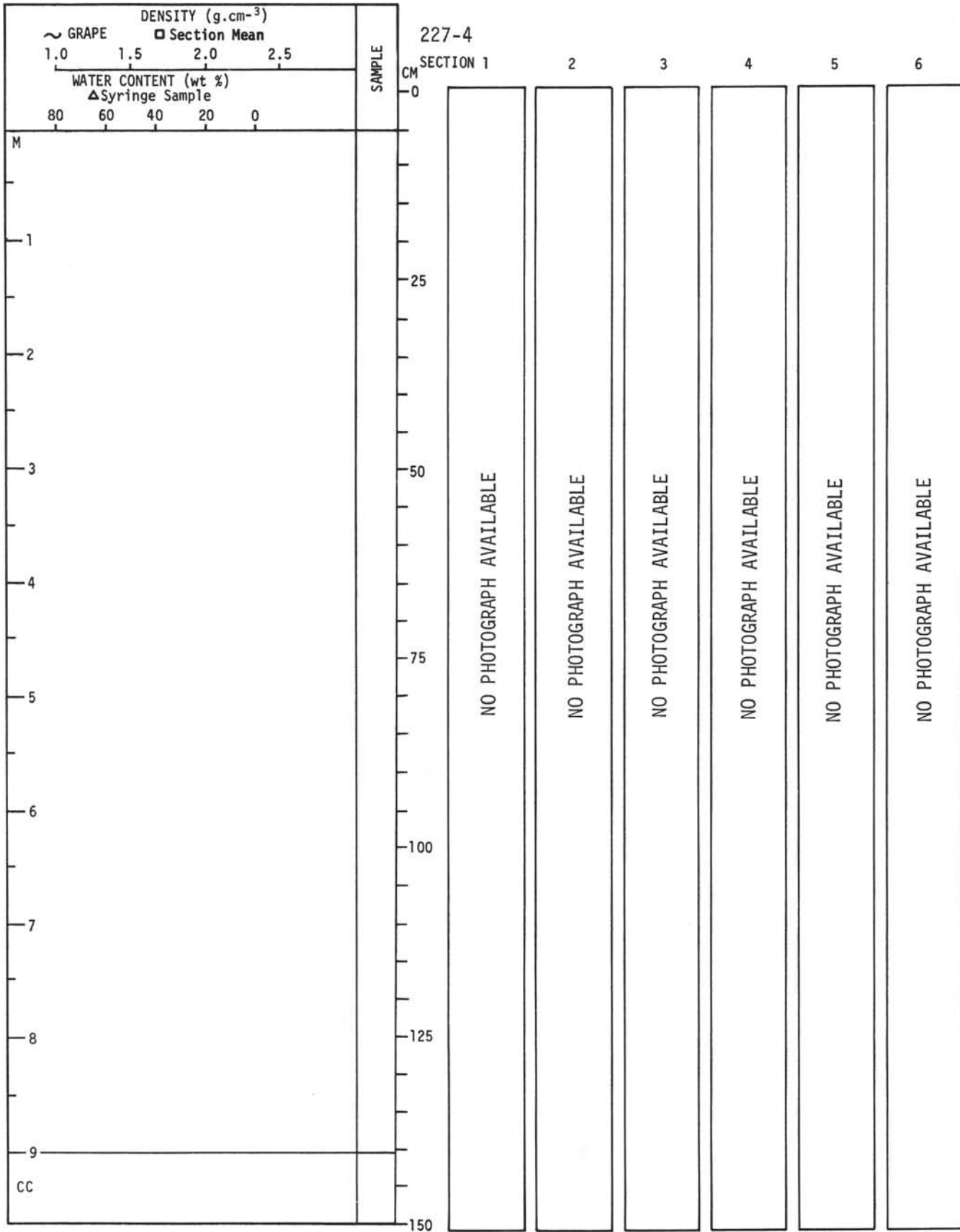
For Explanatory Notes, see Chapter 2



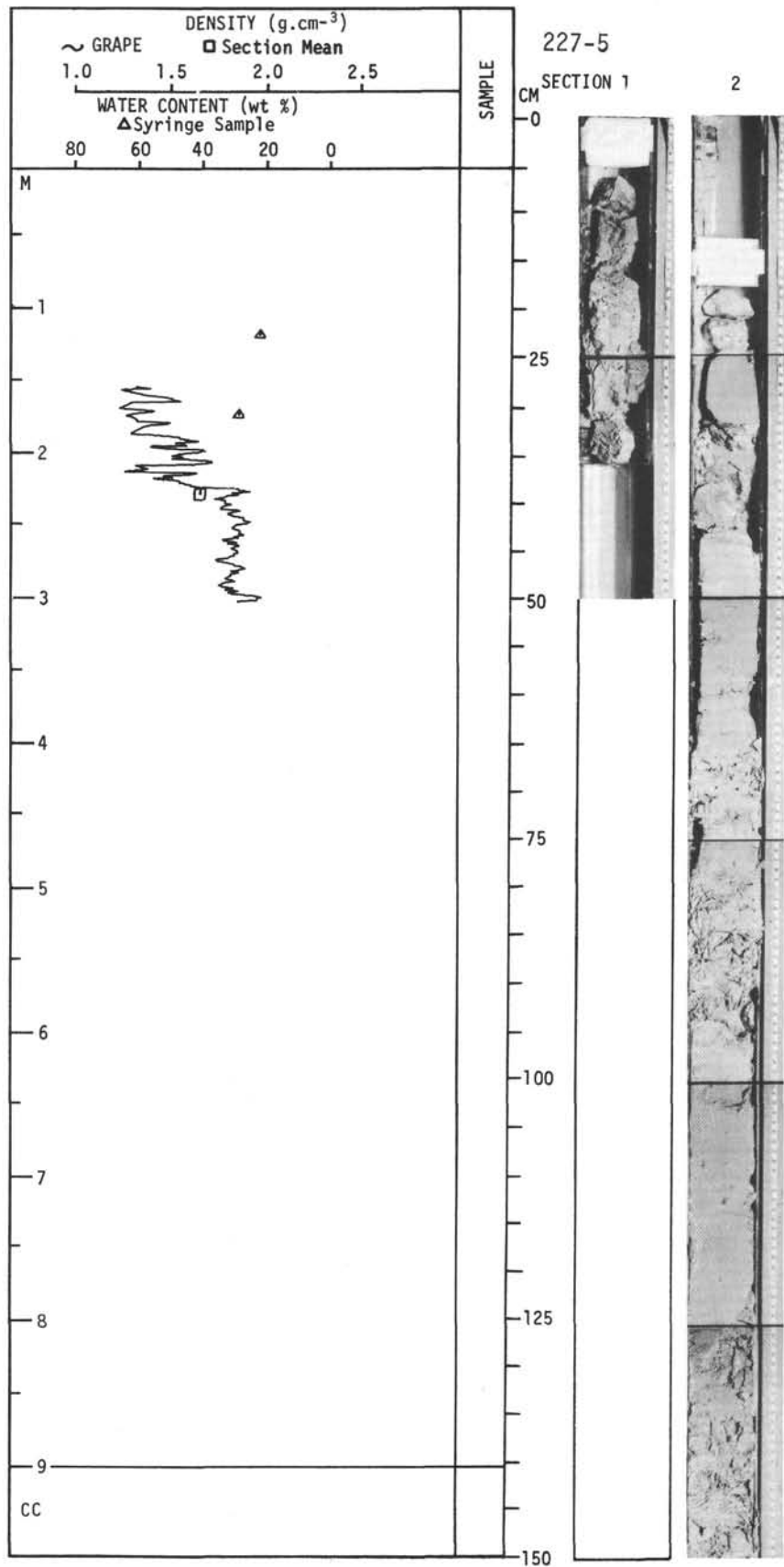
For Explanatory Notes, see Chapter 2



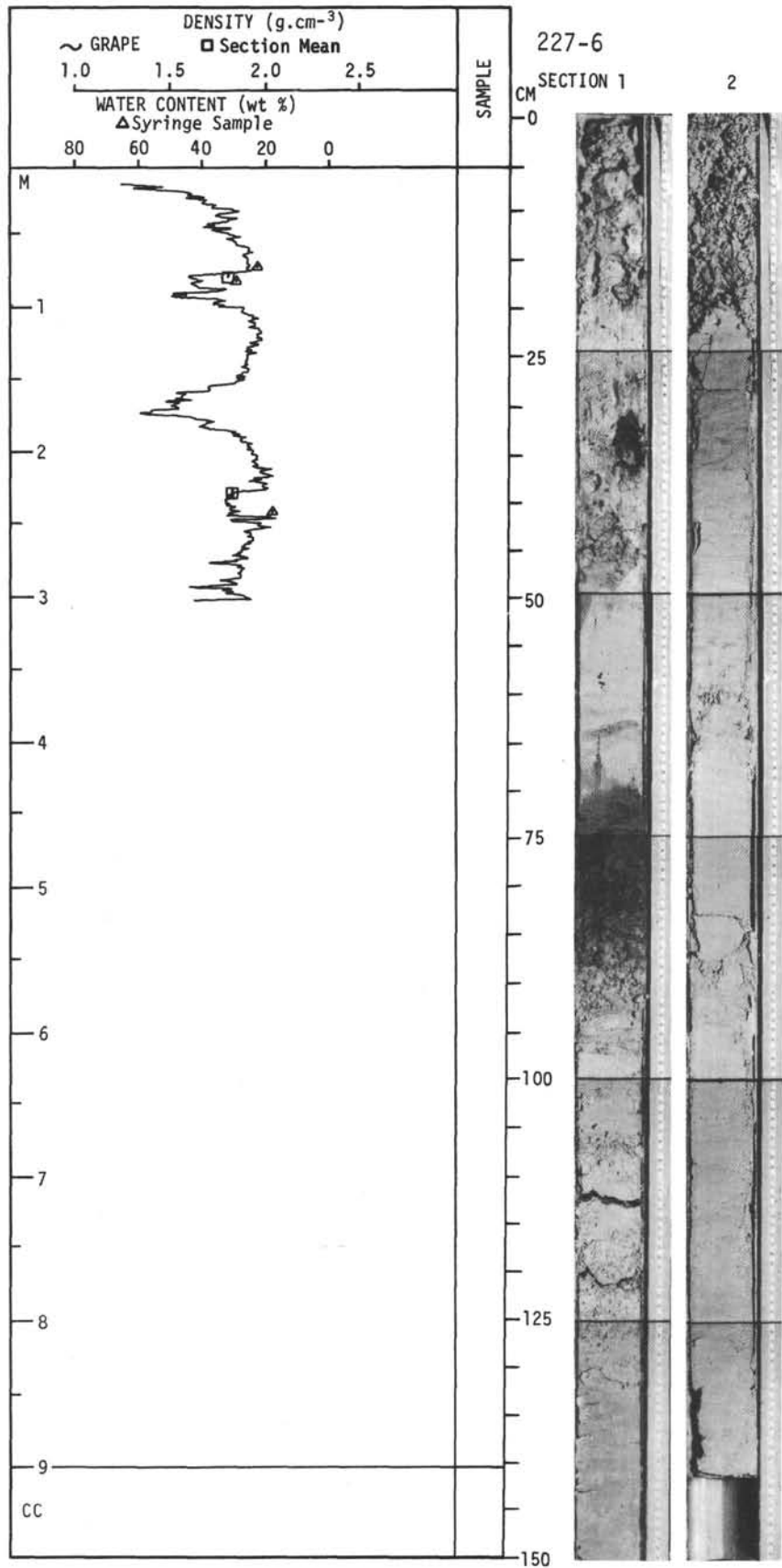
For Explanatory Notes, see Chapter 2



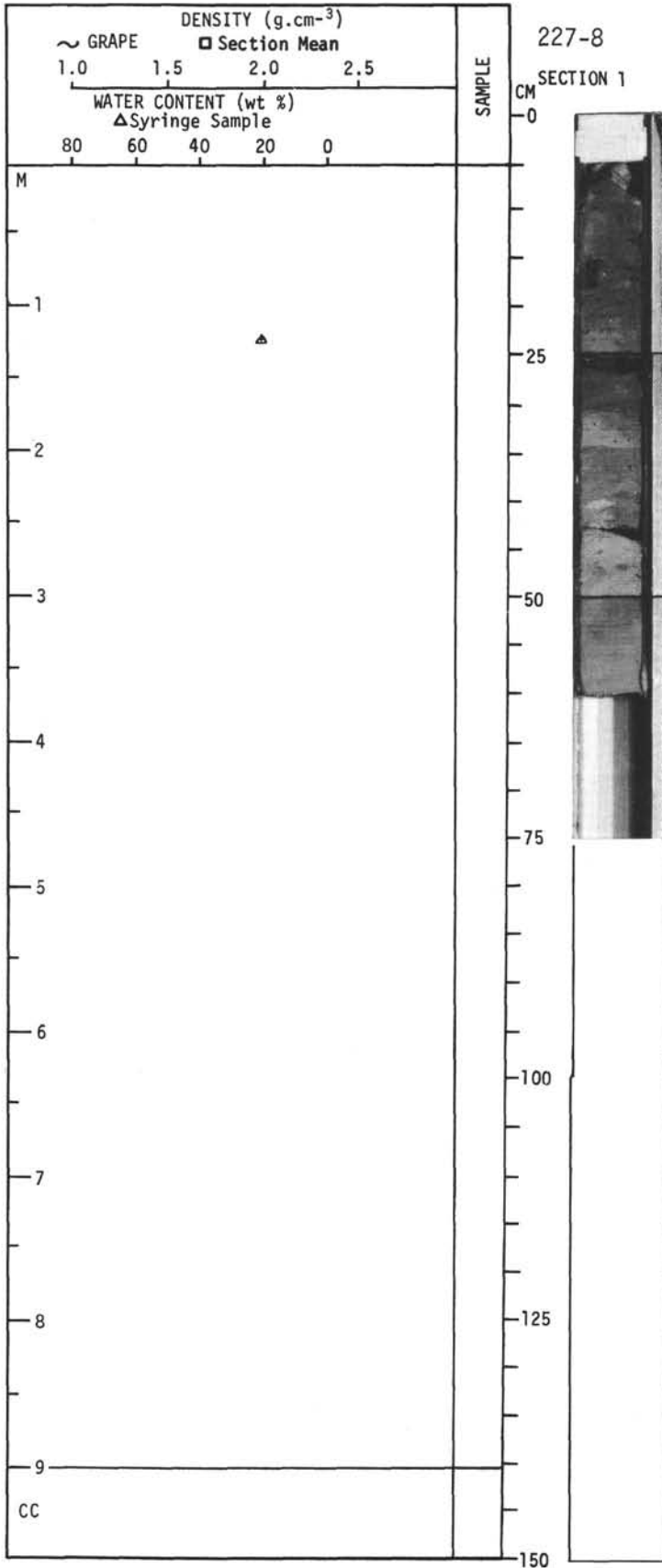
For Explanatory Notes, see Chapter 2



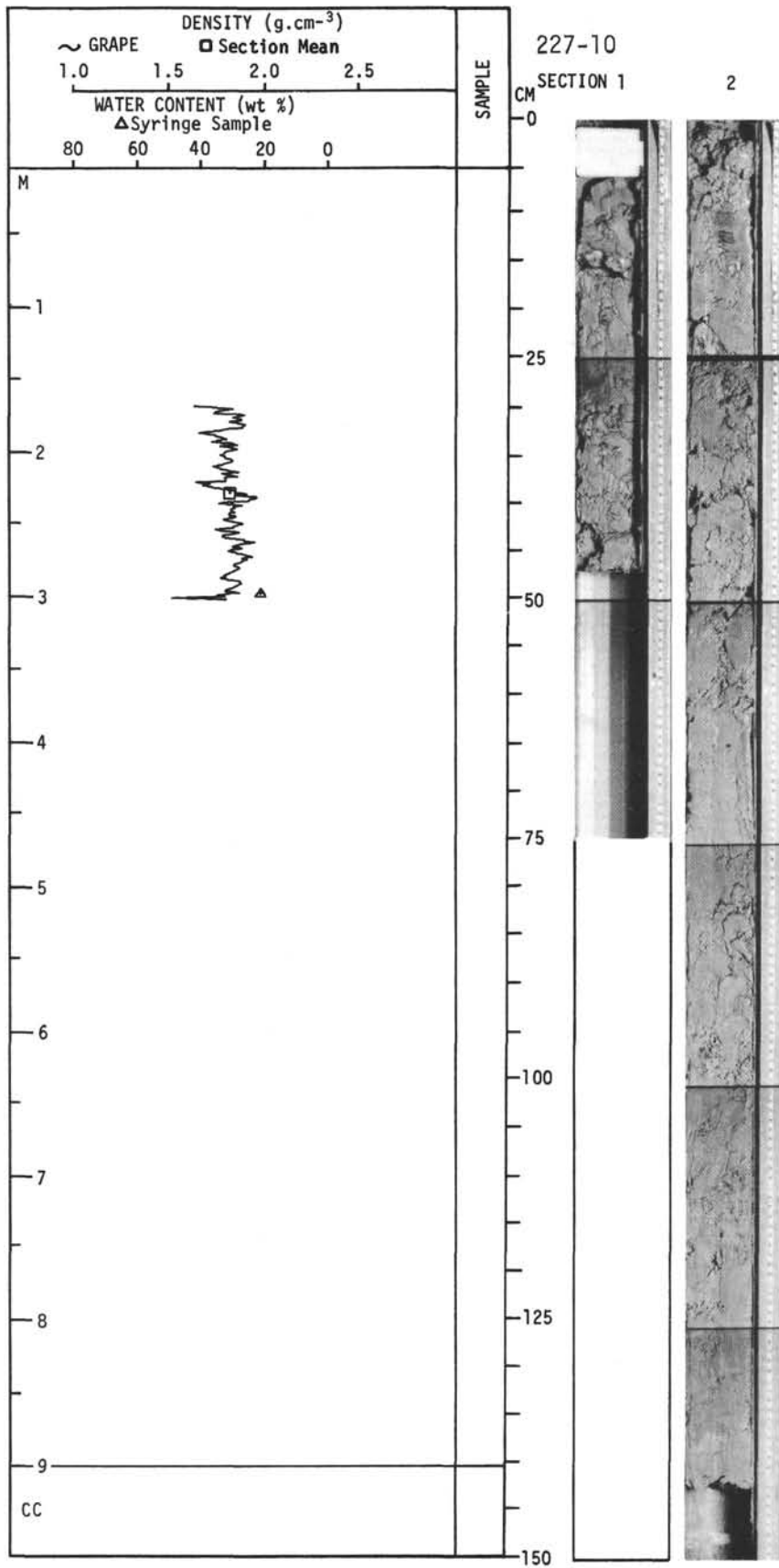
For Explanatory Notes, see Chapter 2



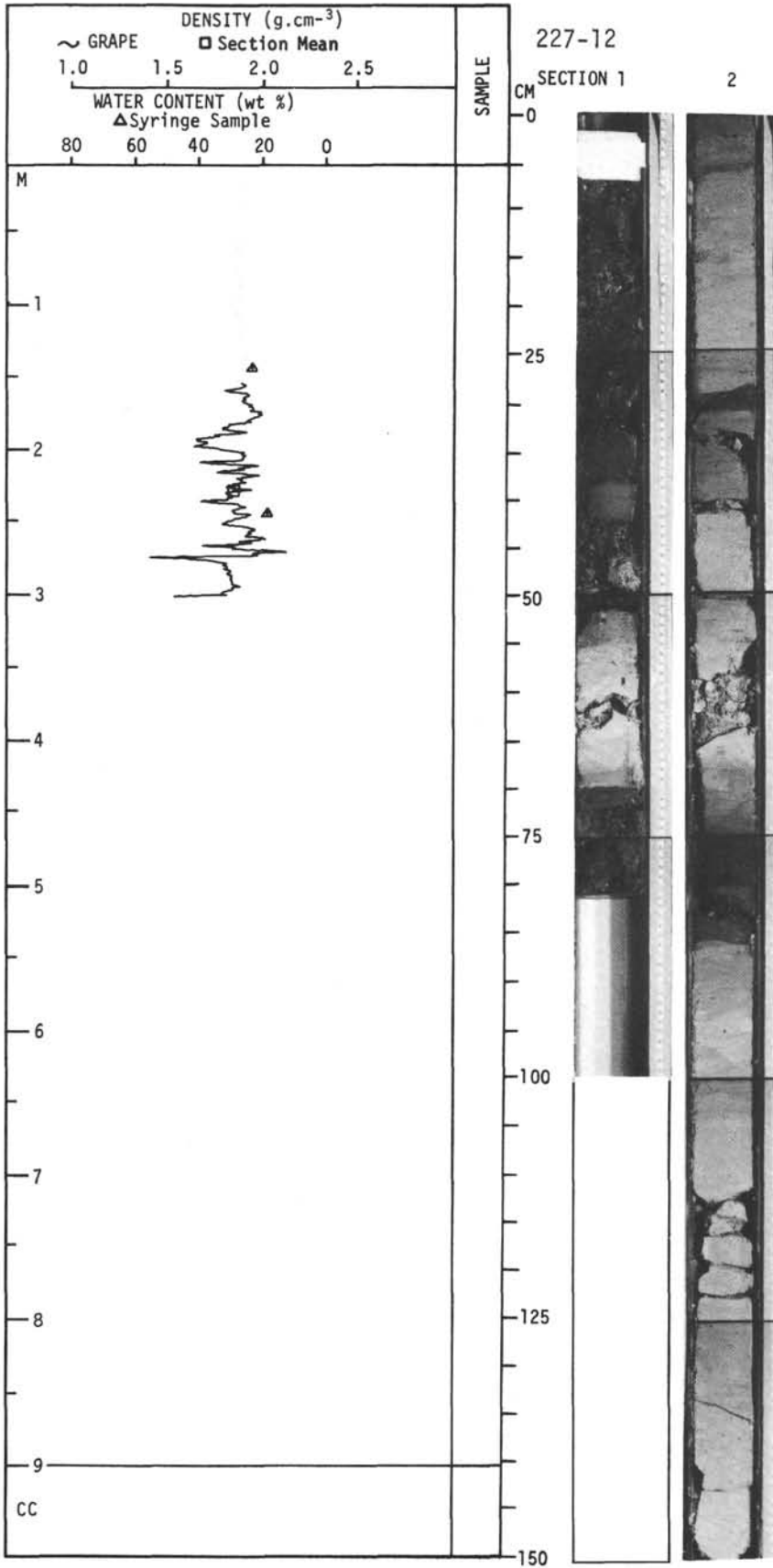
For Explanatory Notes, see Chapter 2



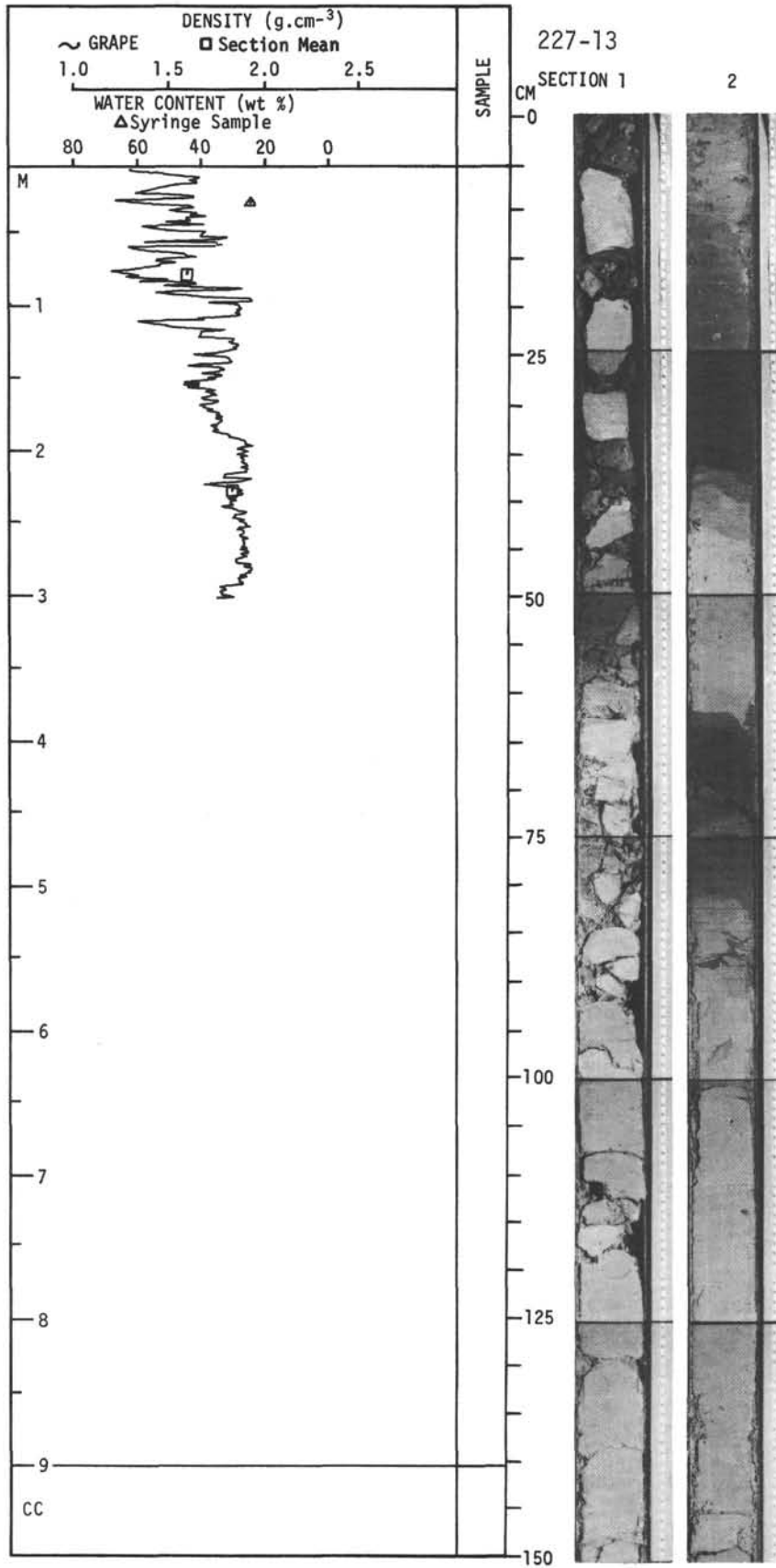
For Explanatory Notes, see Chapter 2



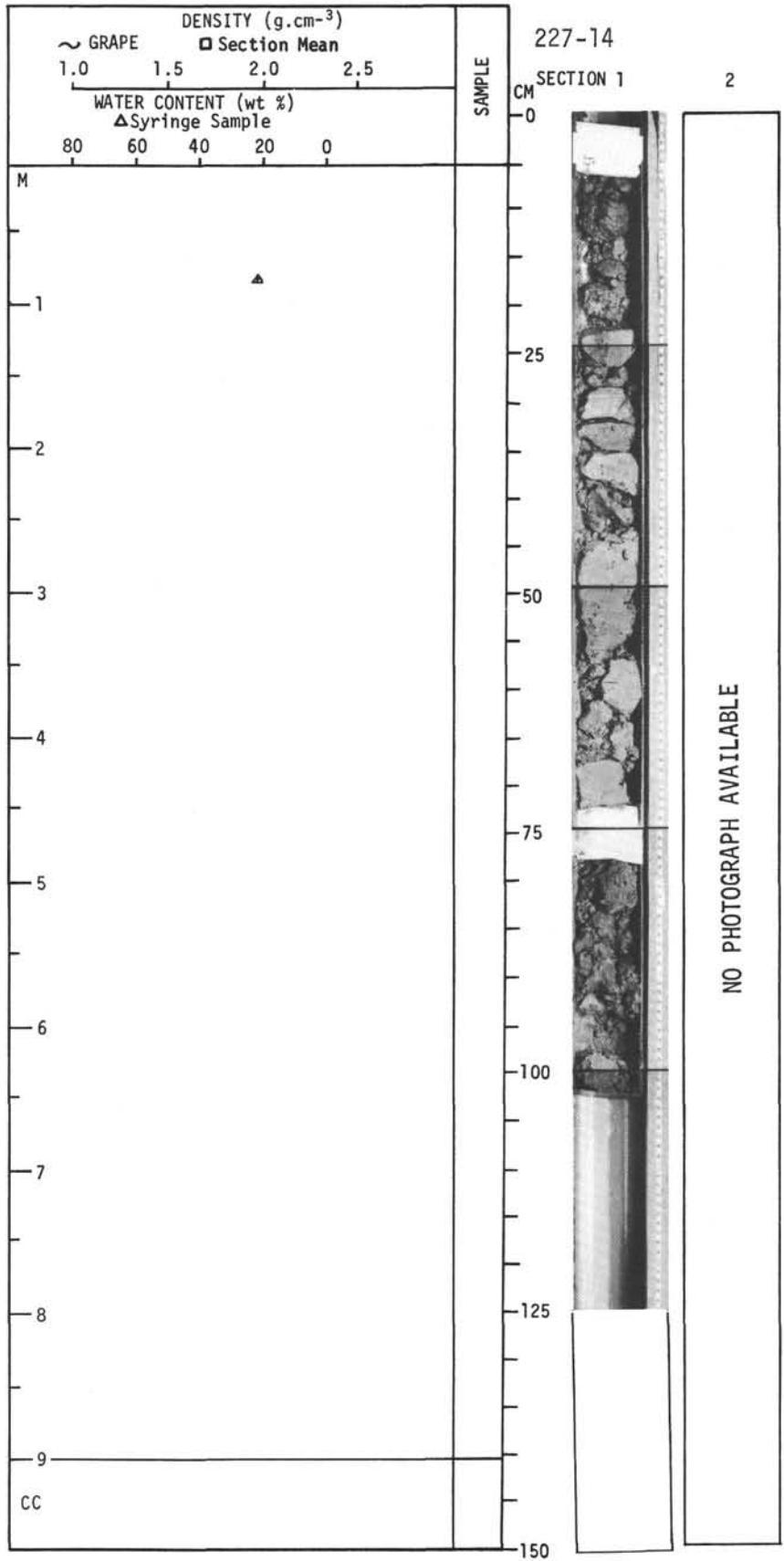
For Explanatory Notes, see Chapter 2



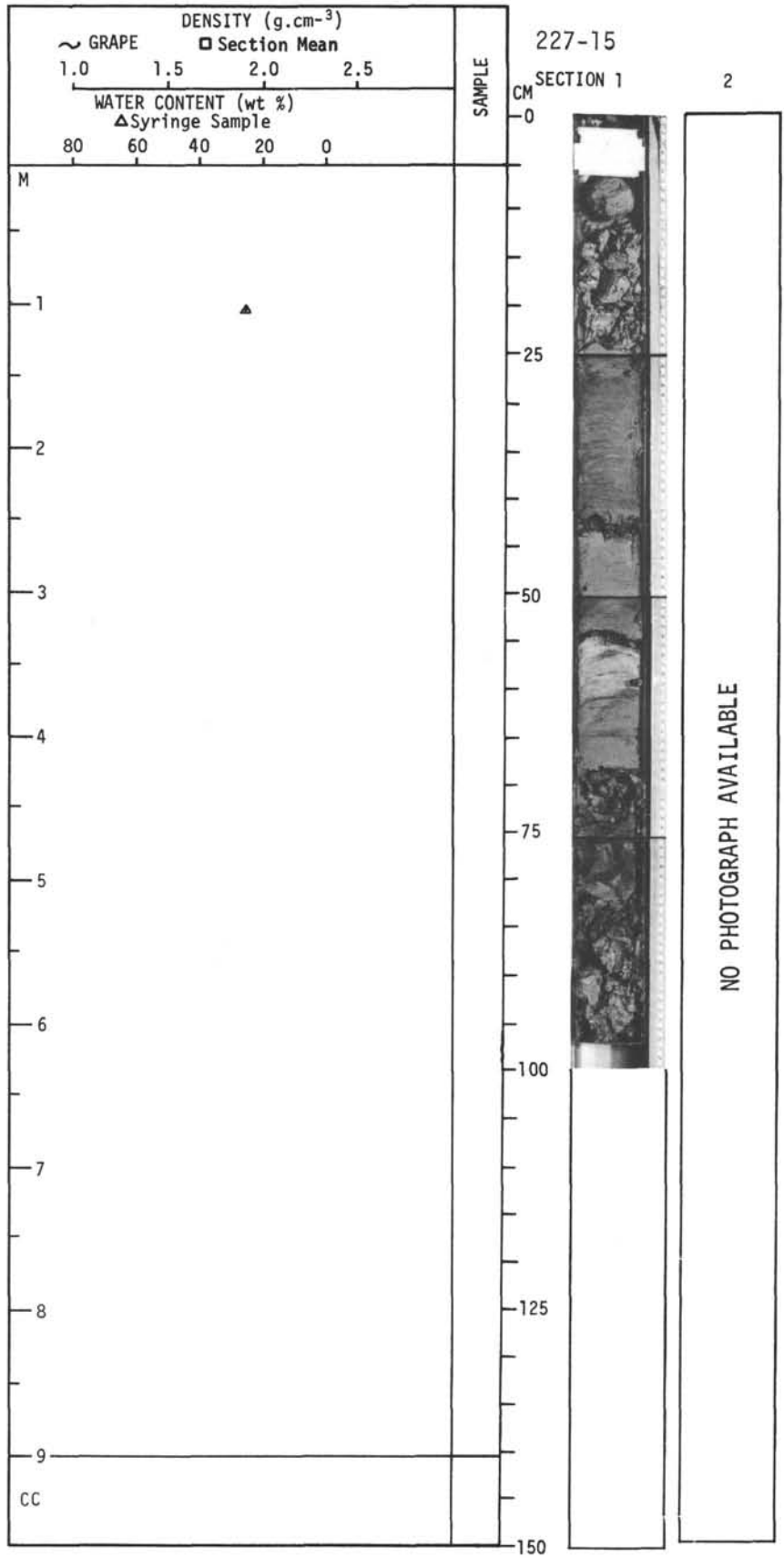
For Explanatory Notes, see Chapter 2



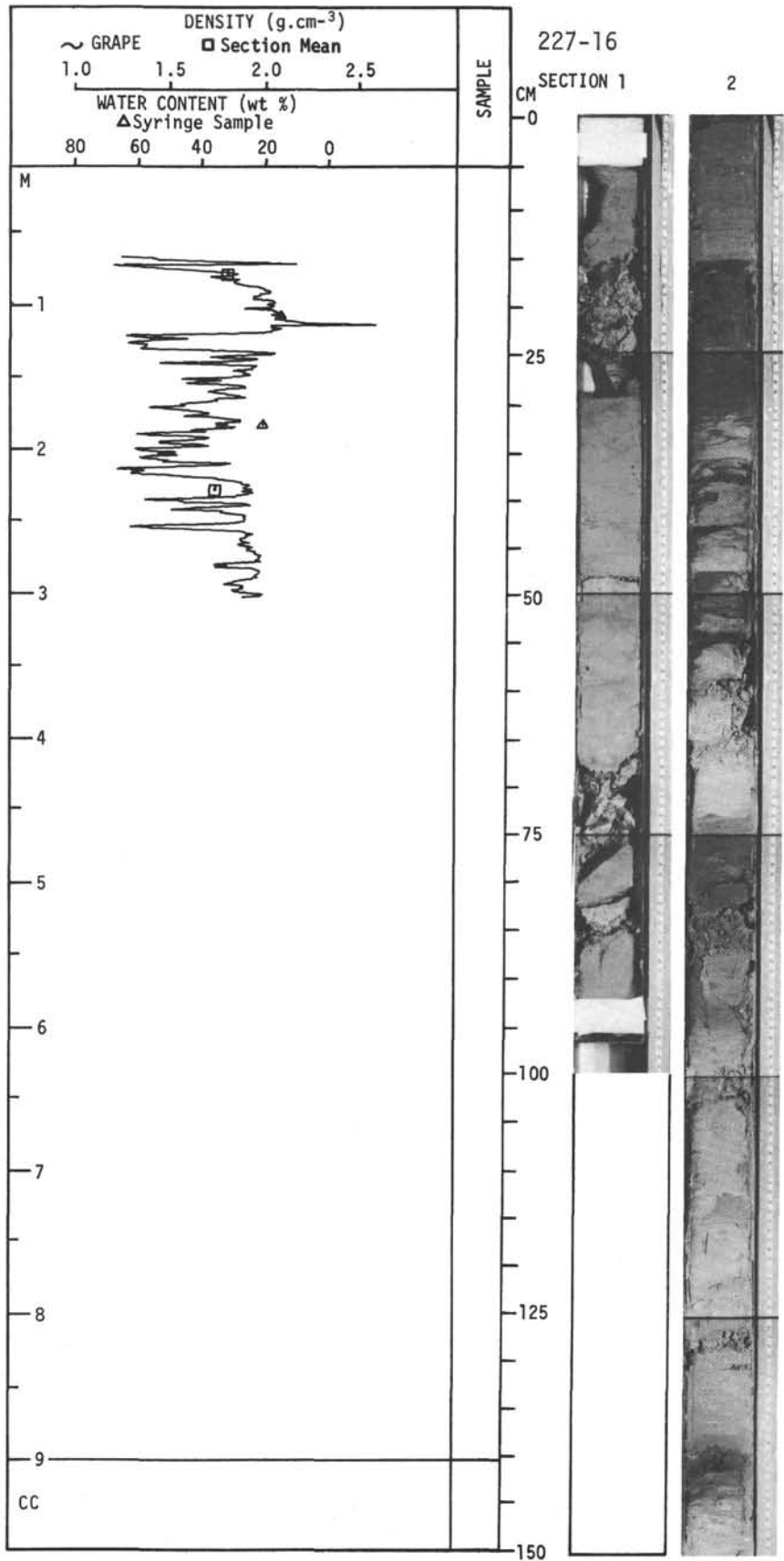
For Explanatory Notes, see Chapter 2



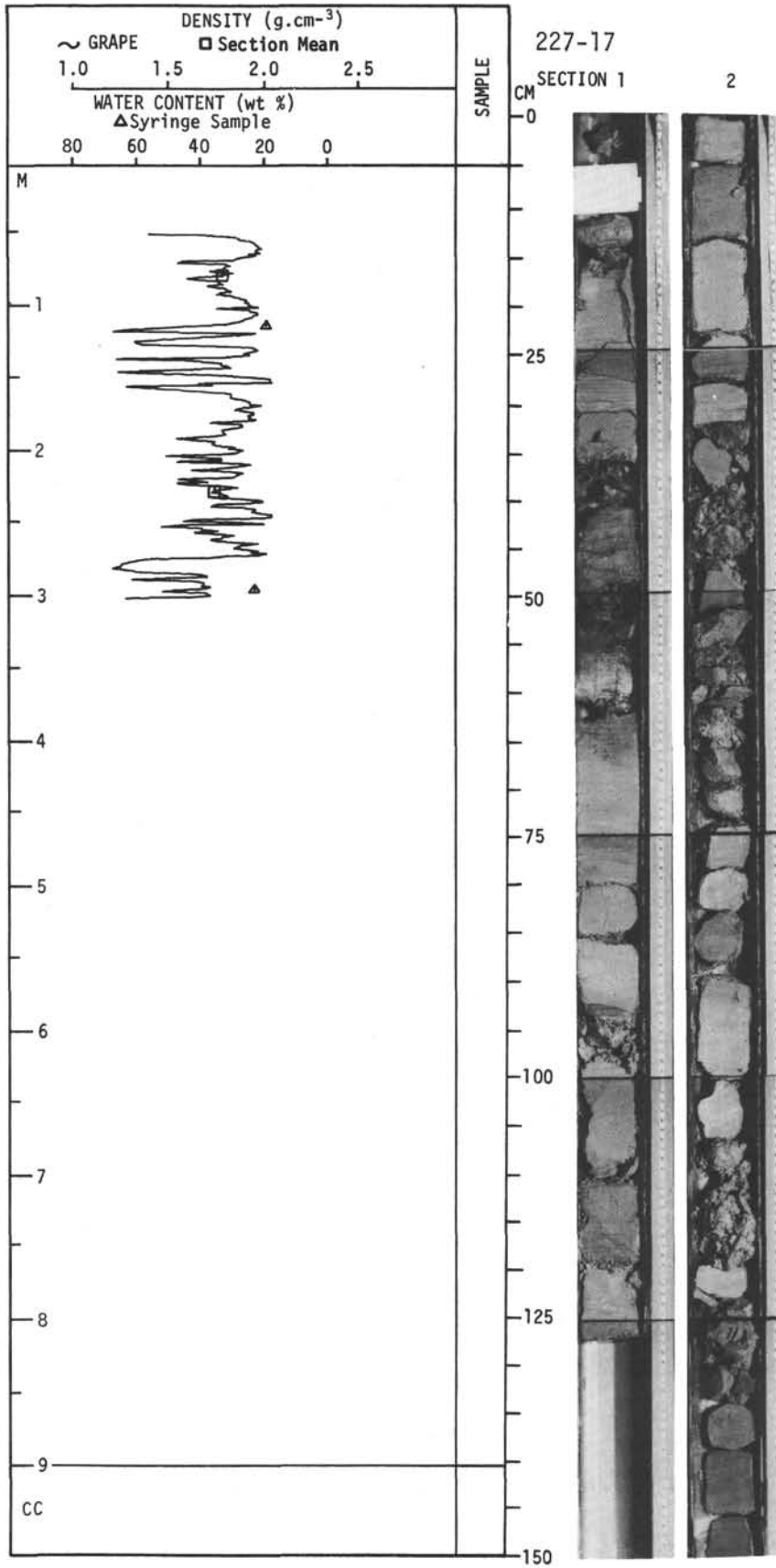
For Explanatory Notes, see Chapter 2



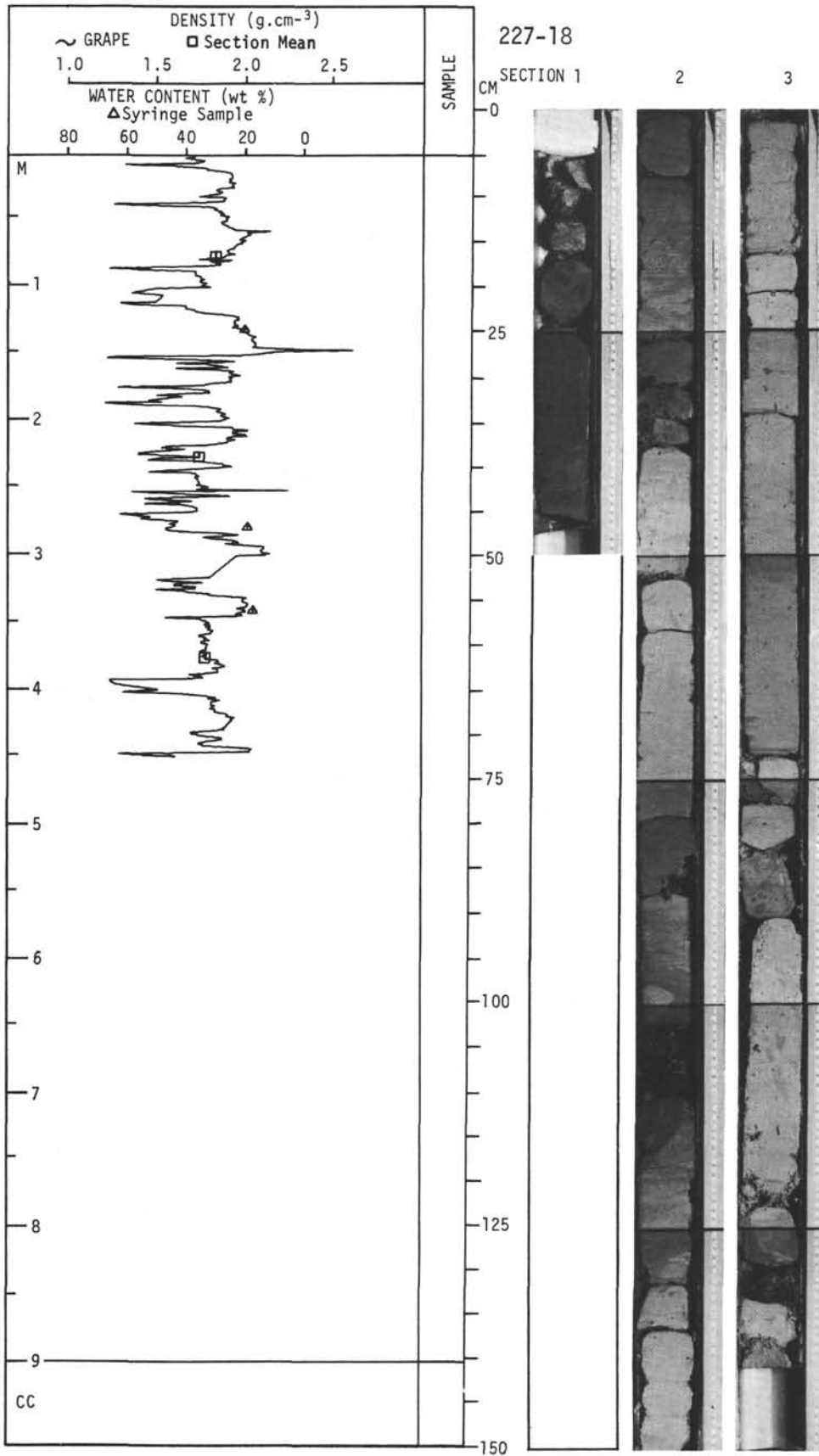
For Explanatory Notes, see Chapter 2



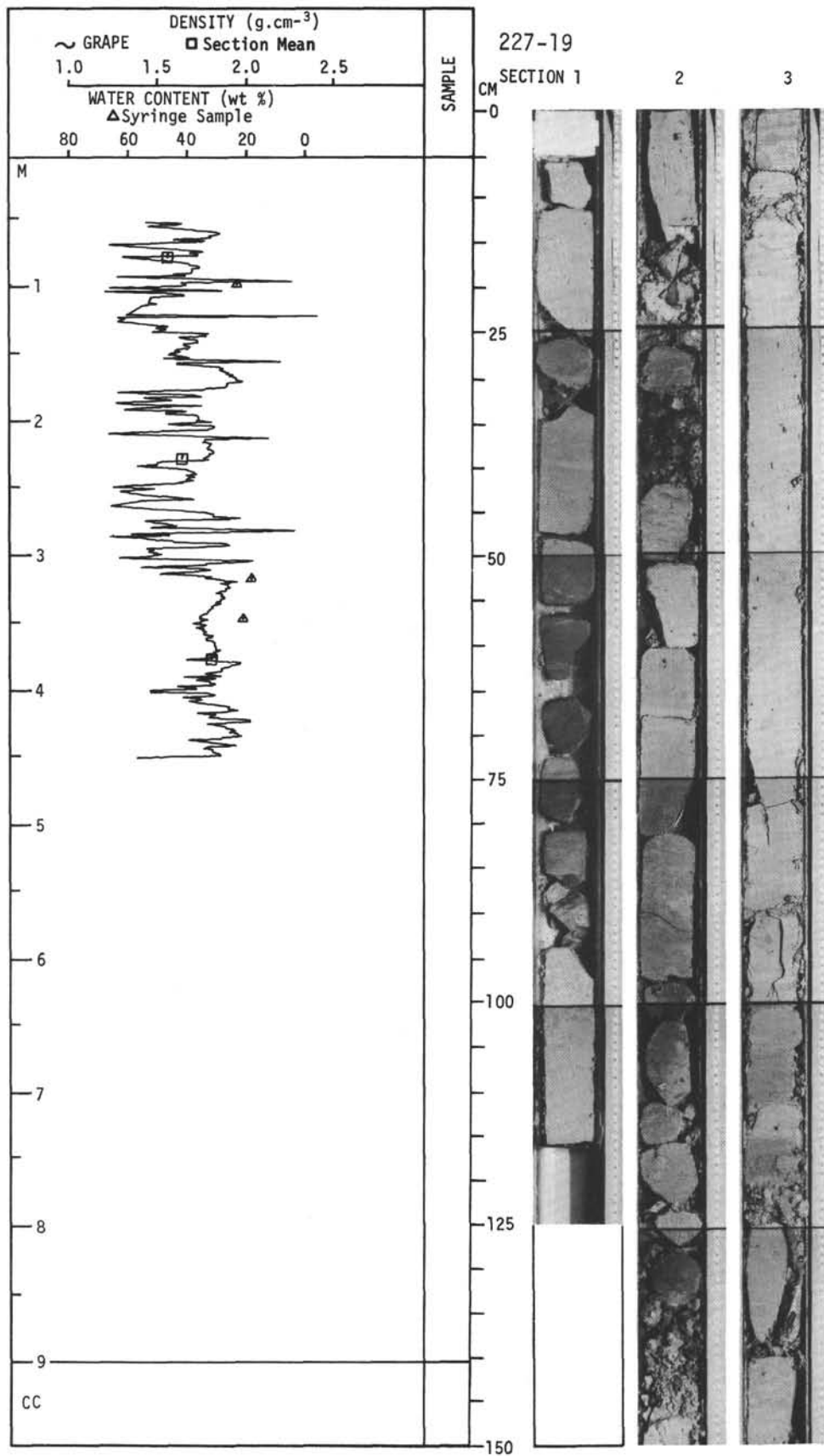
For Explanatory Notes, see Chapter 2



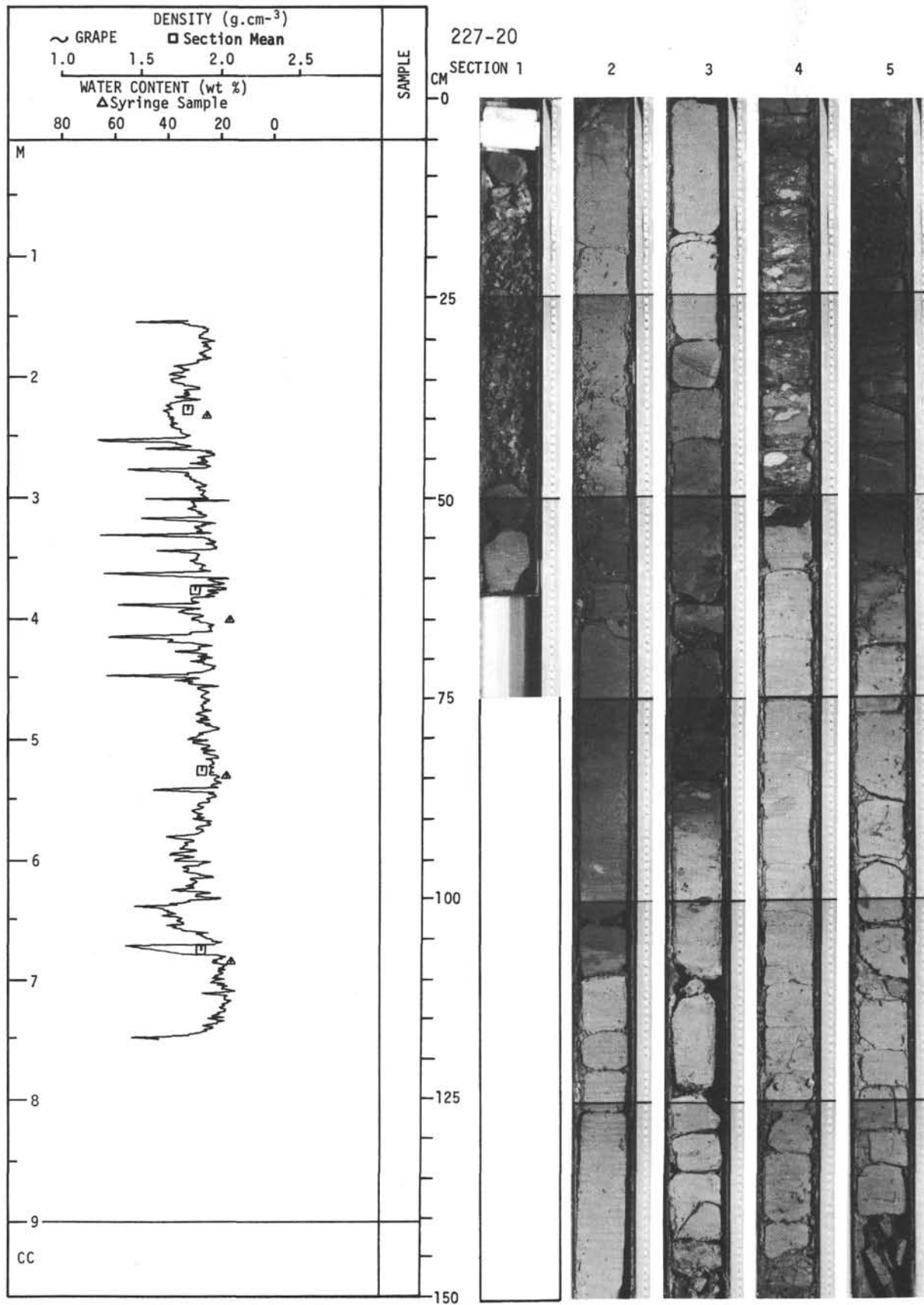
For Explanatory Notes, see Chapter 2



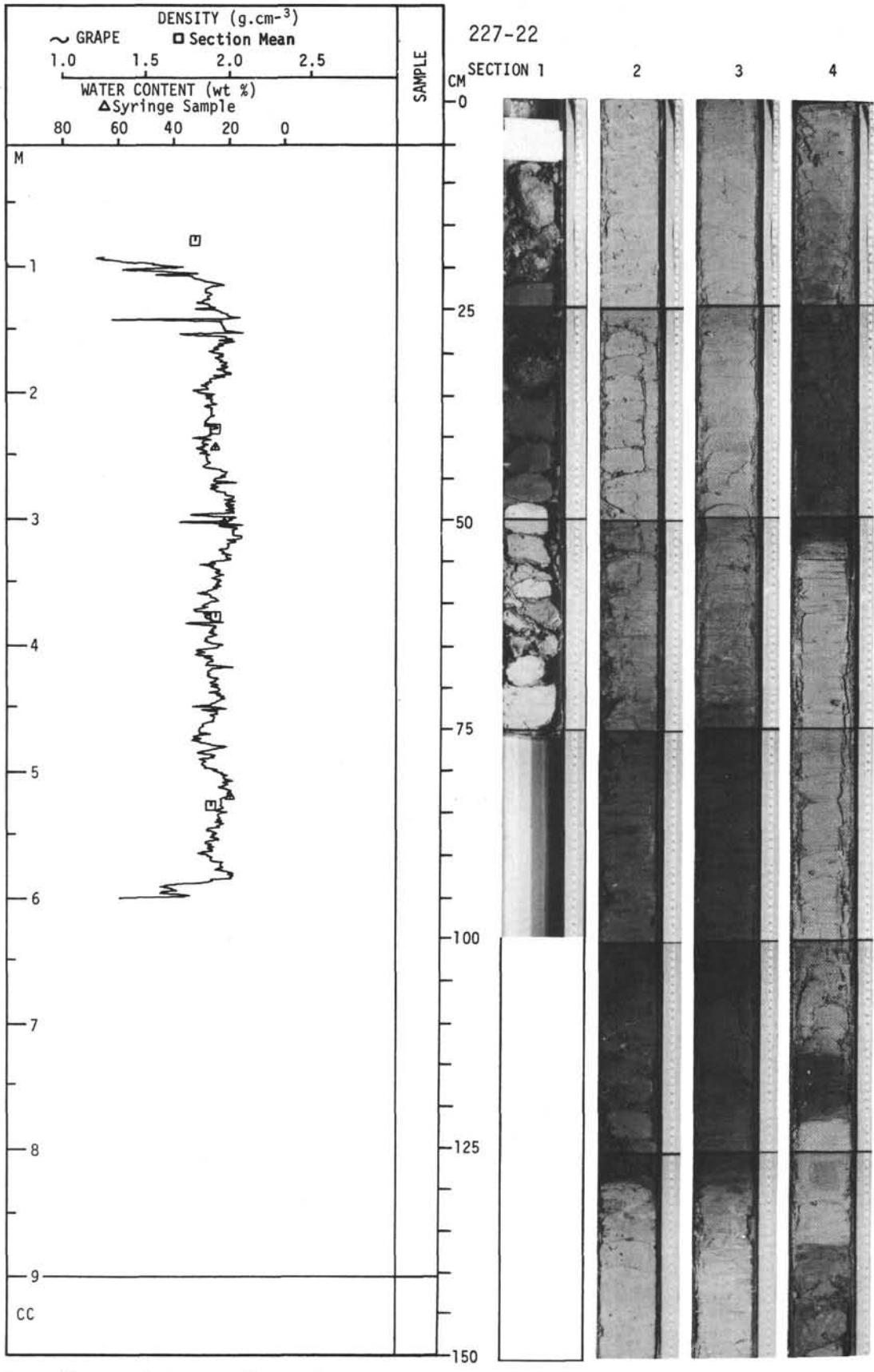
For Explanatory Notes, see Chapter 2



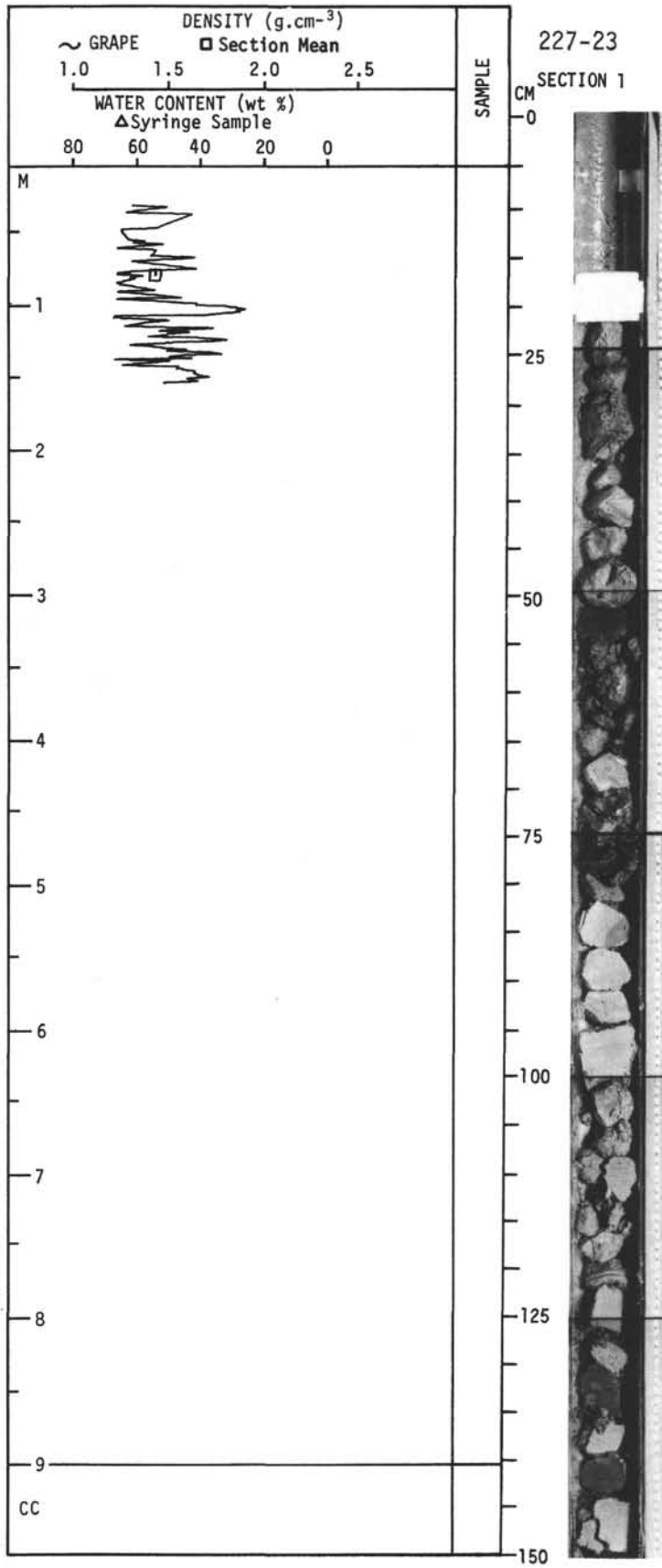
For Explanatory Notes, see Chapter 2



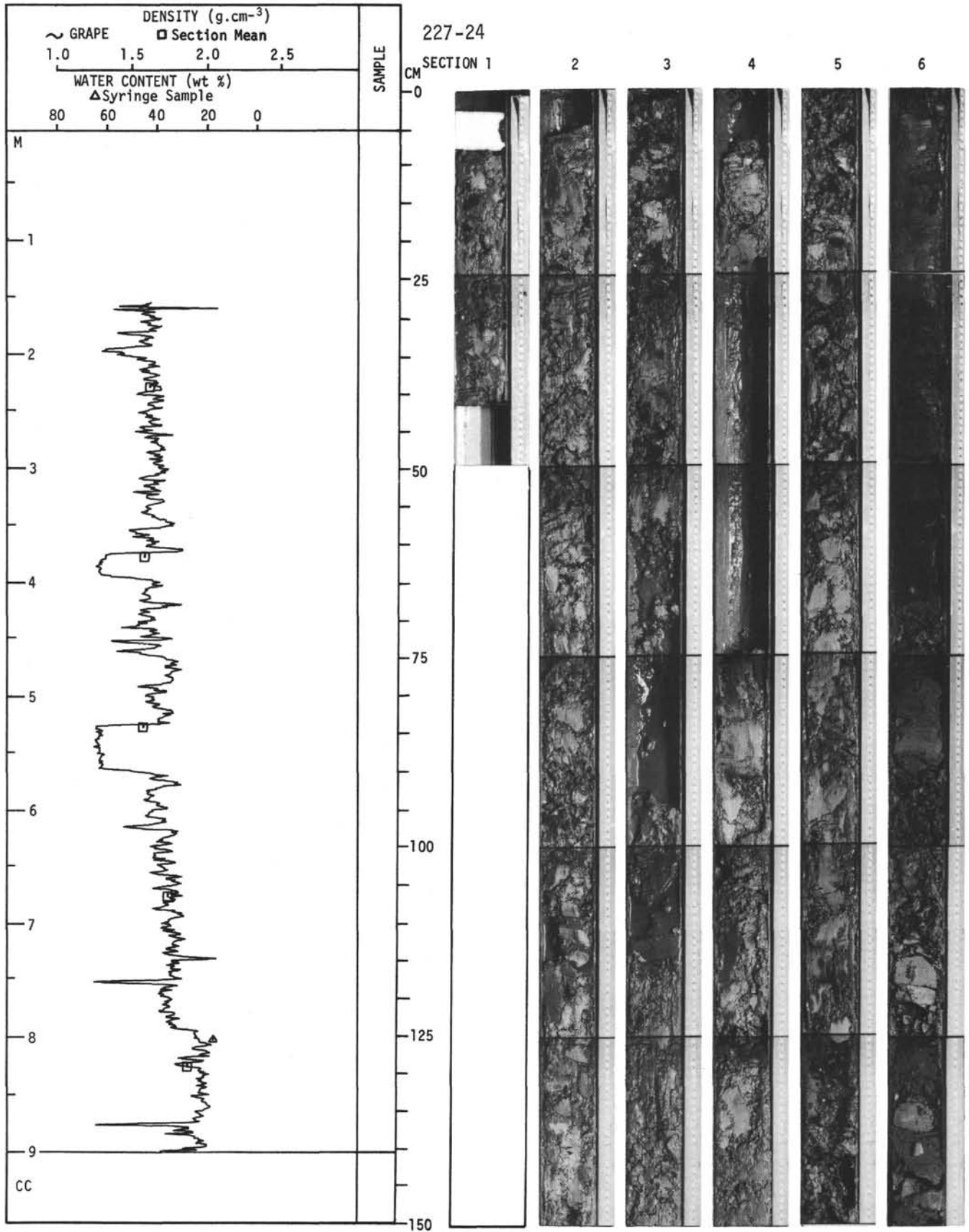
For Explanatory Notes, see Chapter 2



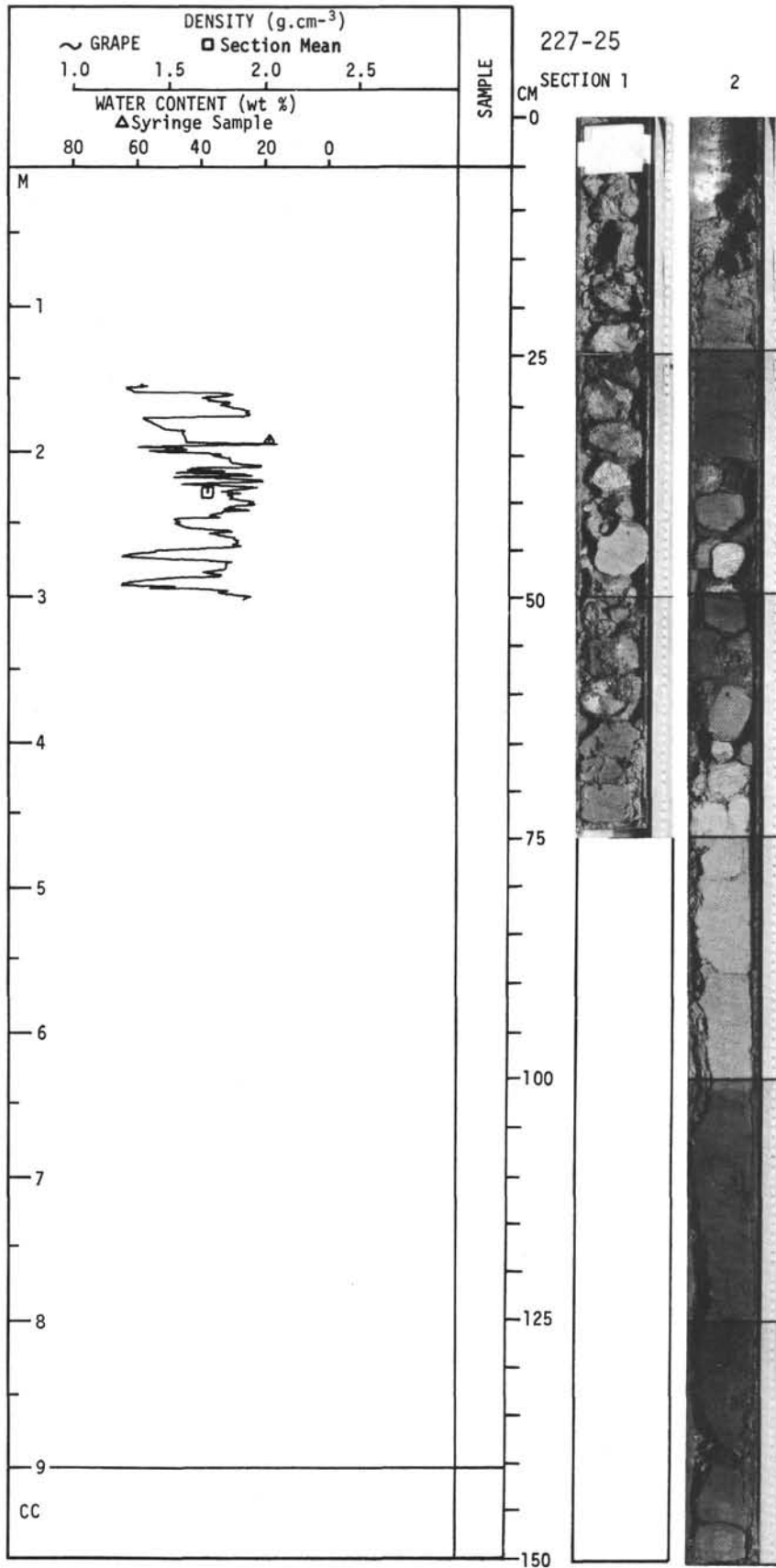
For Explanatory Notes, see Chapter 2



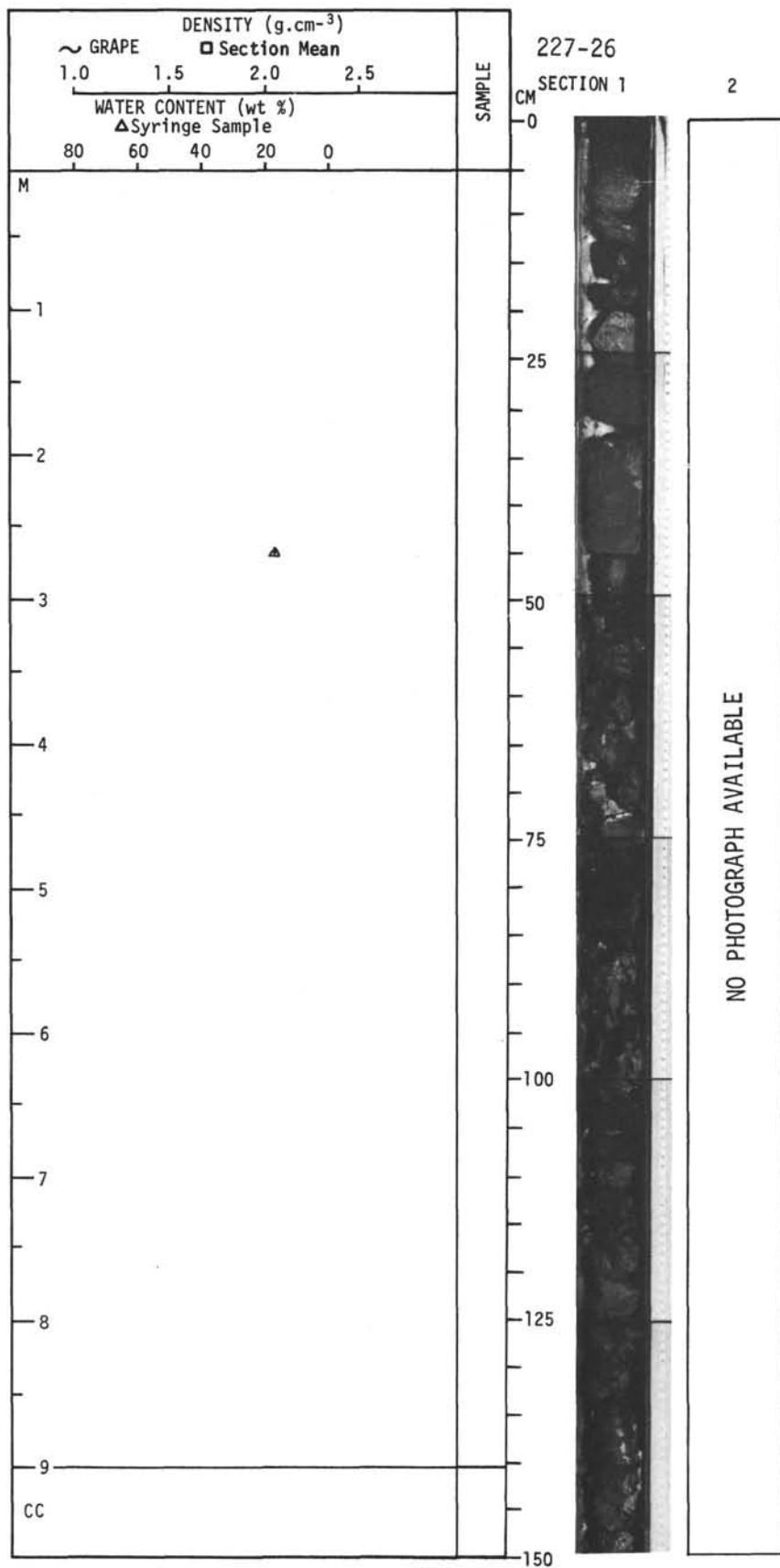
For Explanatory Notes, see Chapter 2



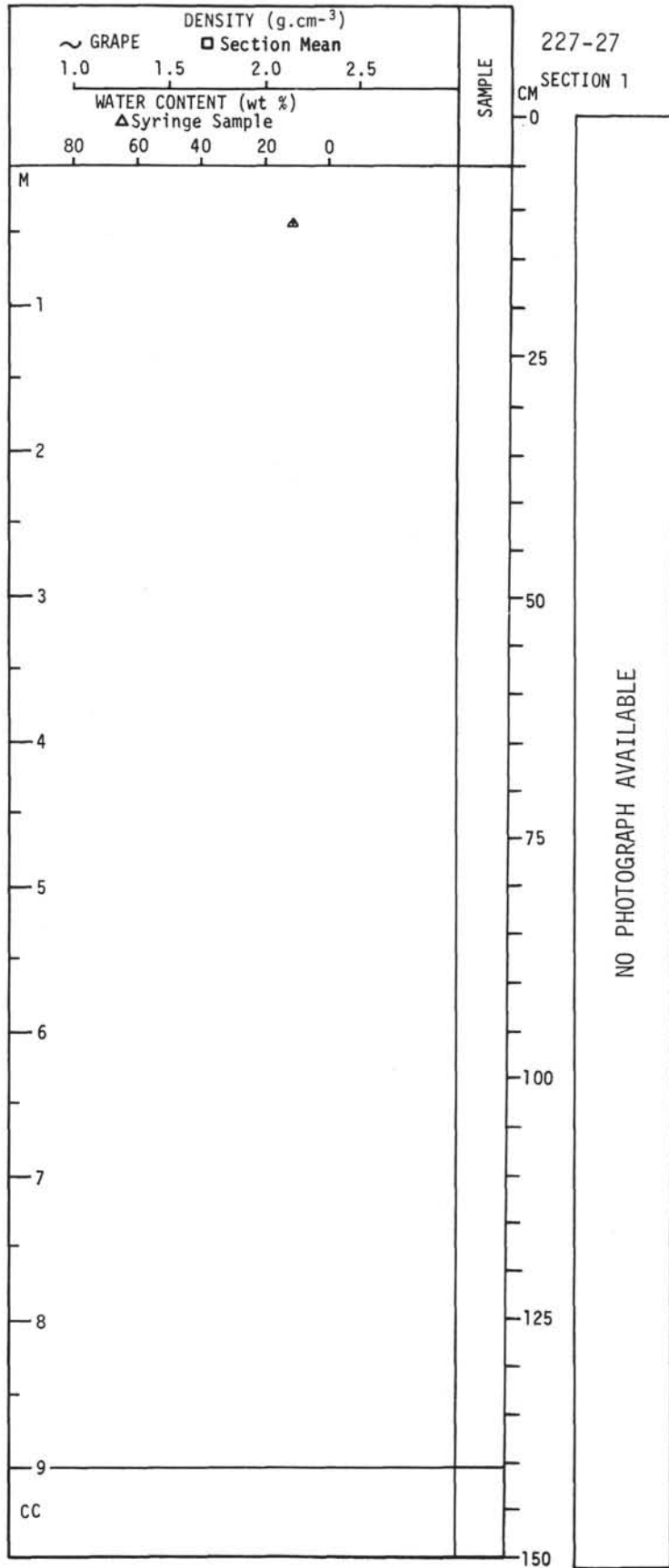
For Explanatory Notes, see Chapter 2



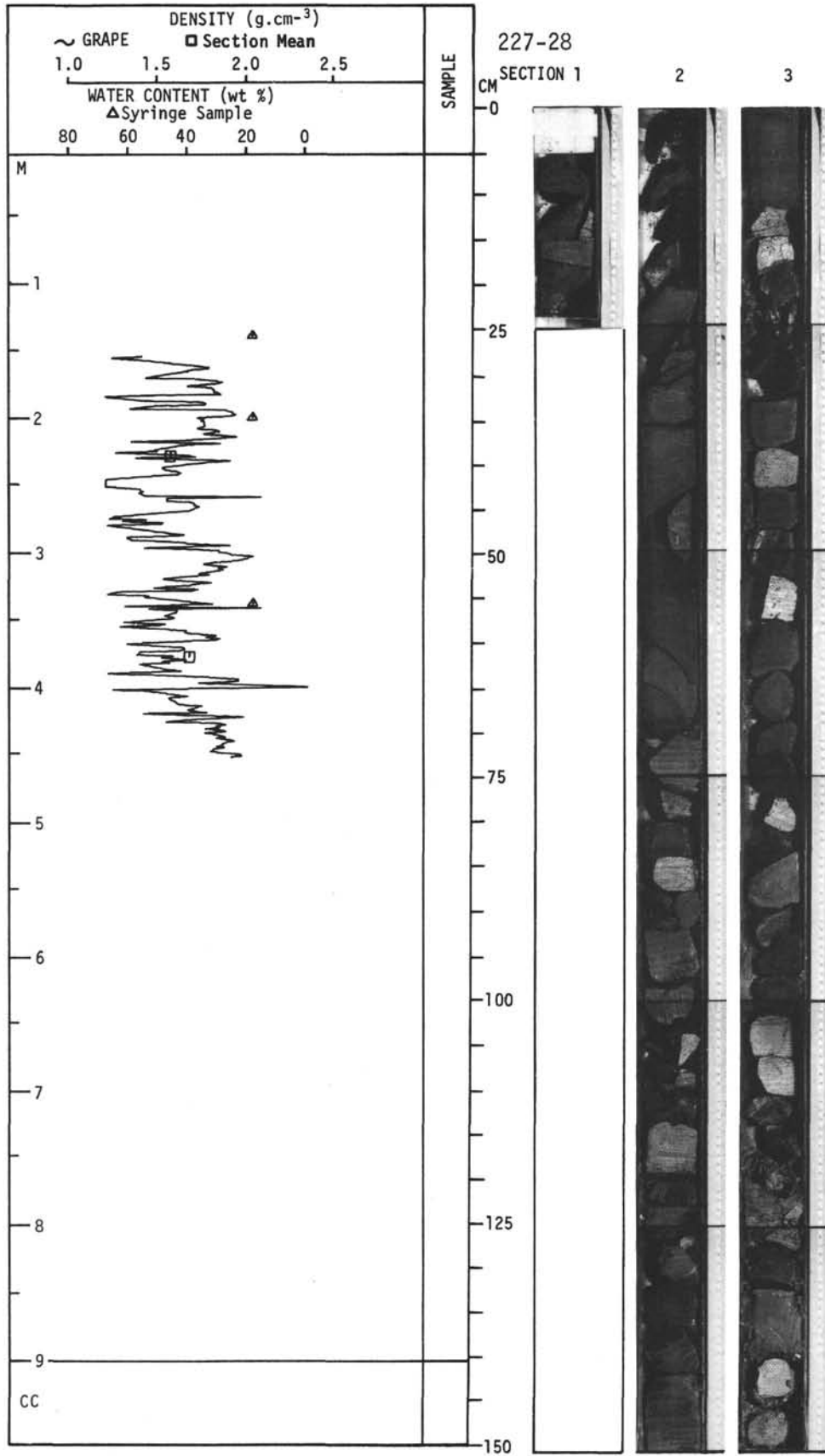
For Explanatory Notes, see Chapter 2



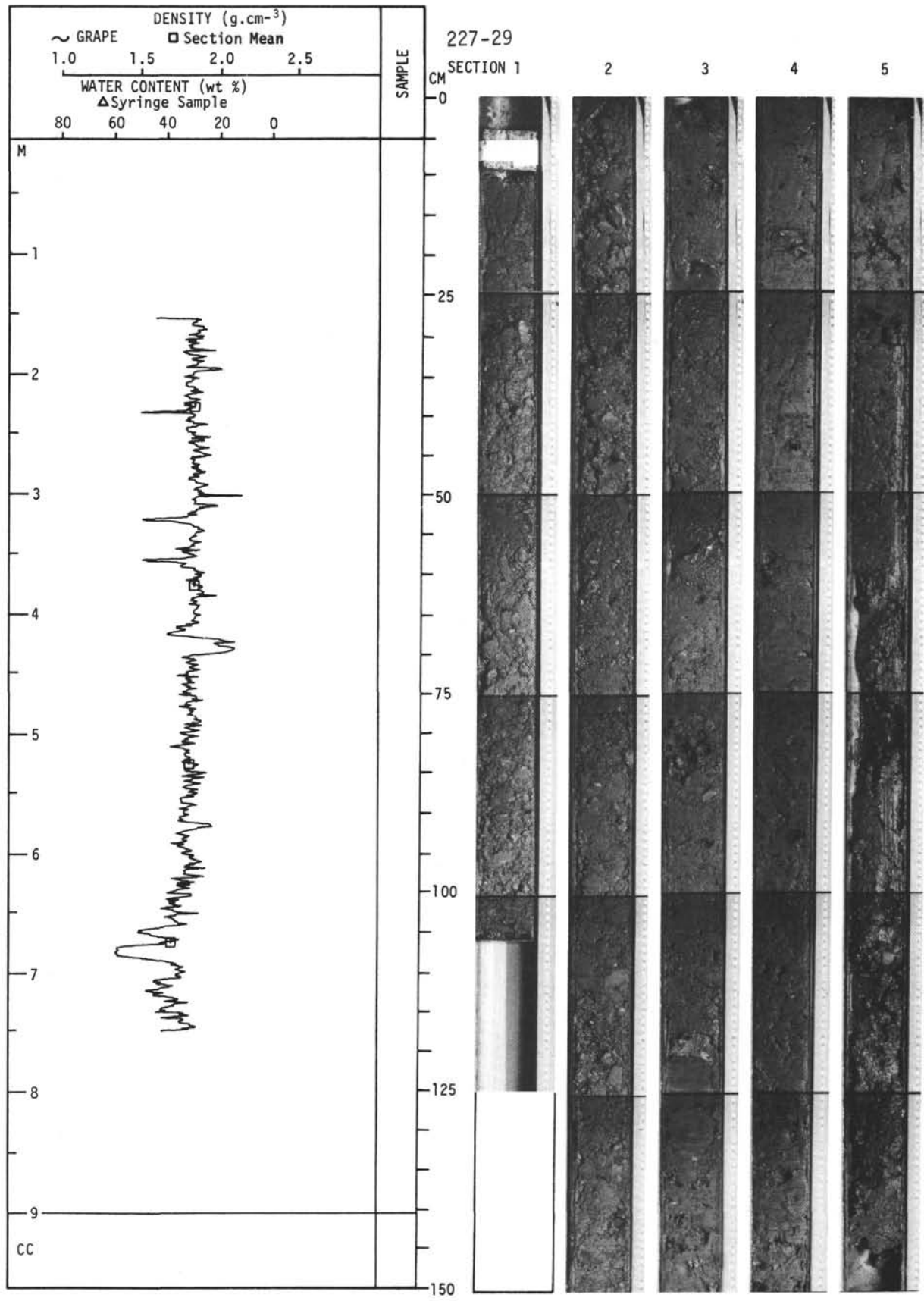
For Explanatory Notes, see Chapter 2



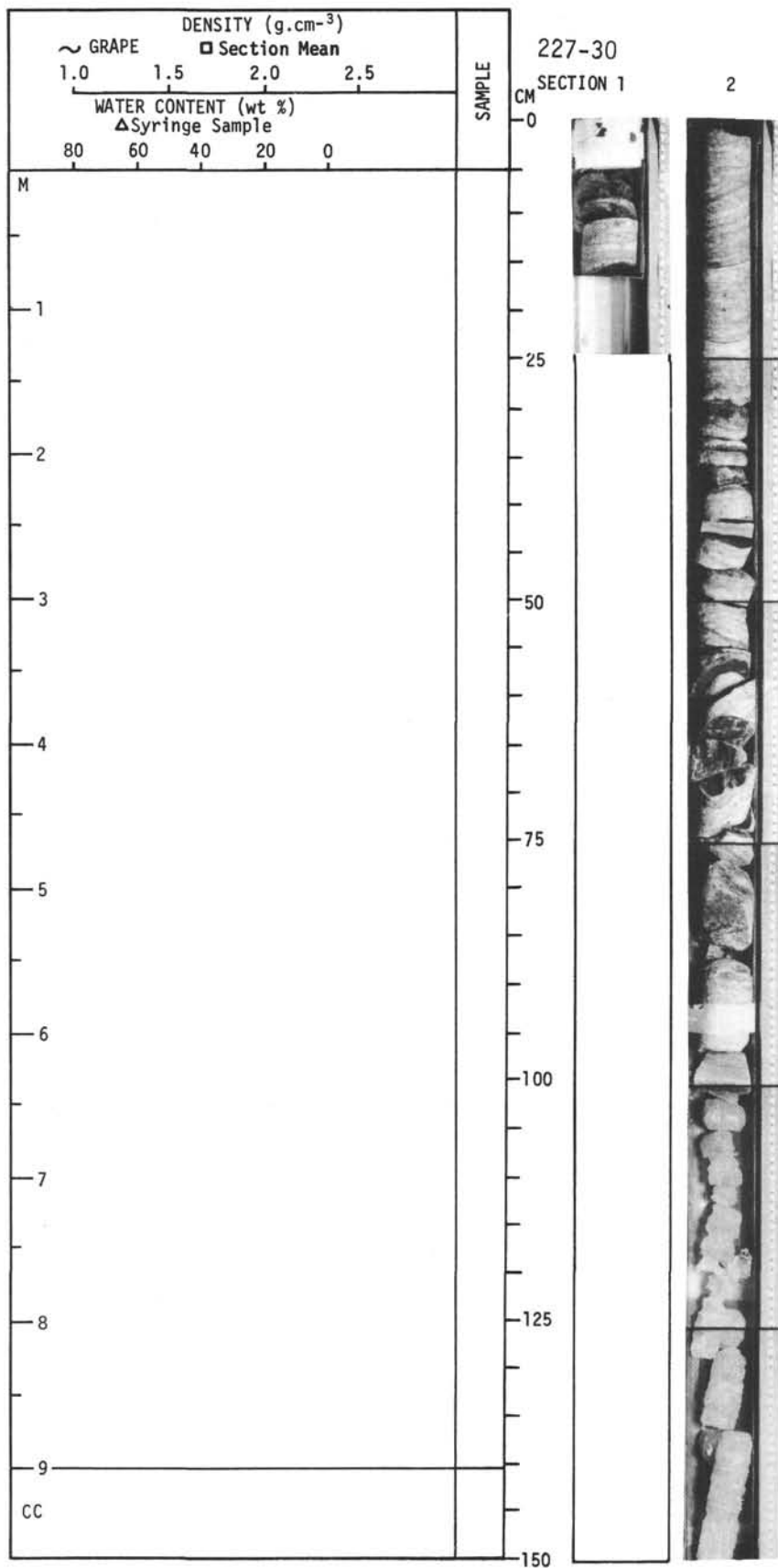
For Explanatory Notes, see Chapter 2



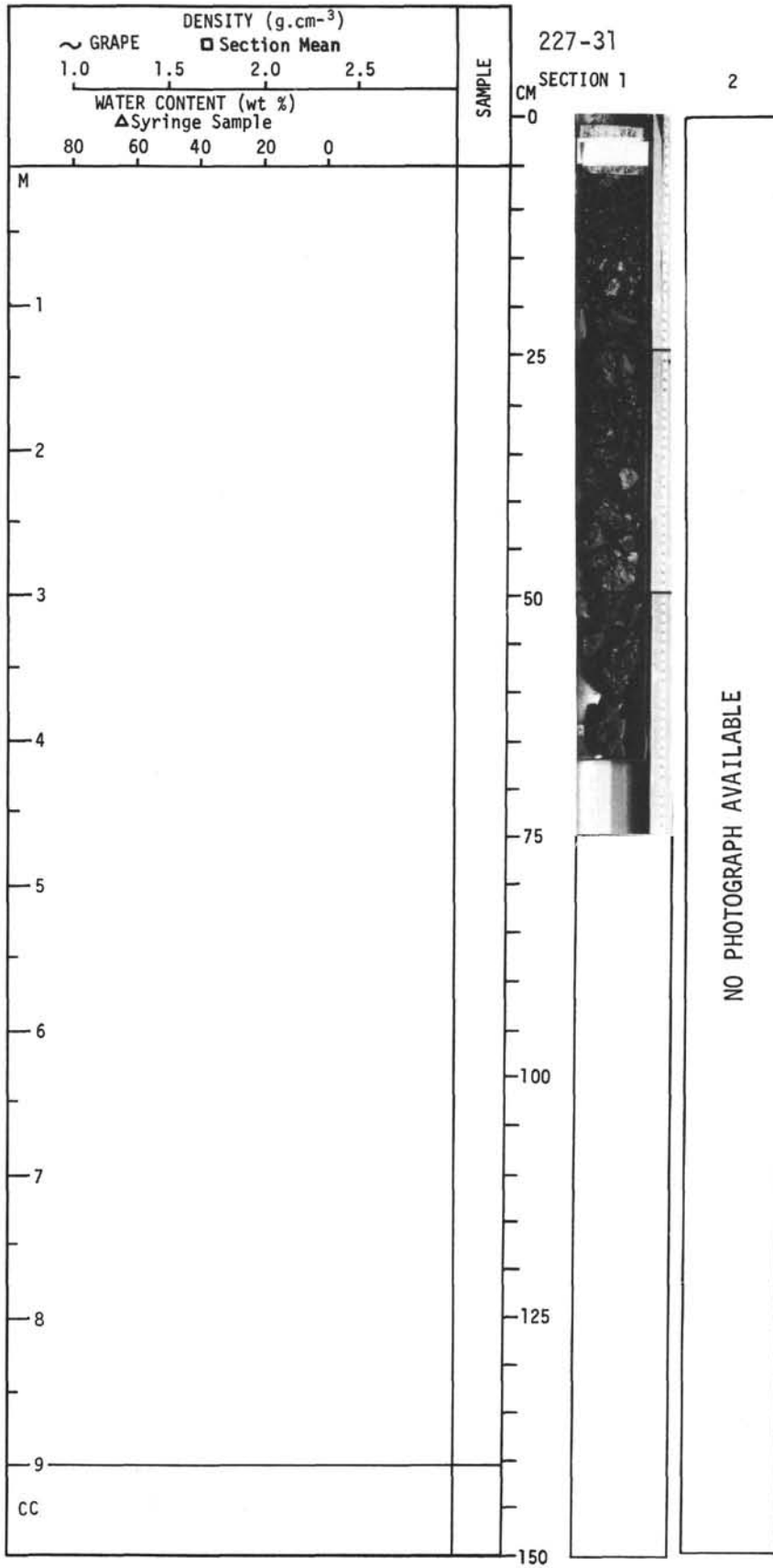
For Explanatory Notes, see Chapter 2



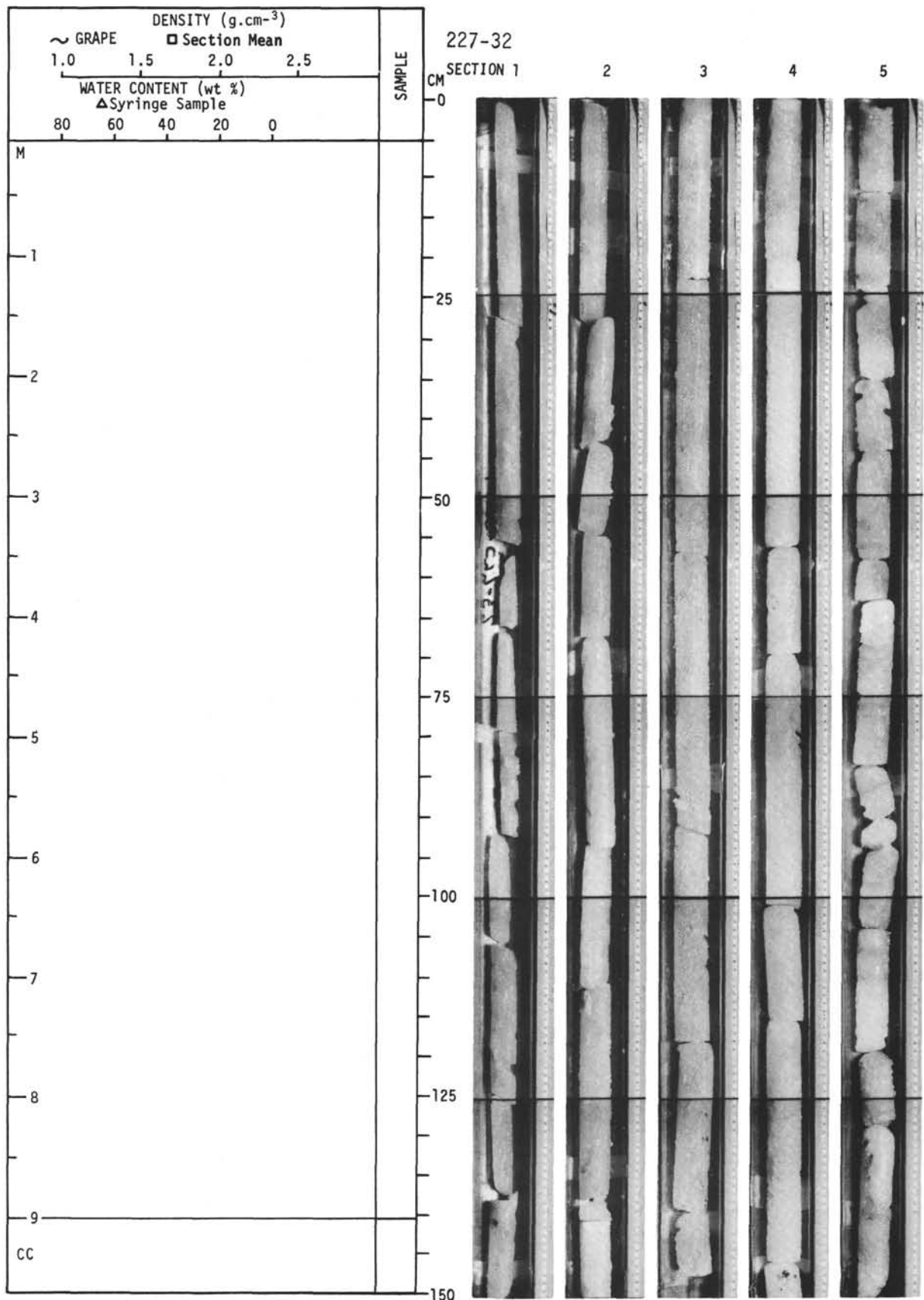
For Explanatory Notes, see Chapter 2



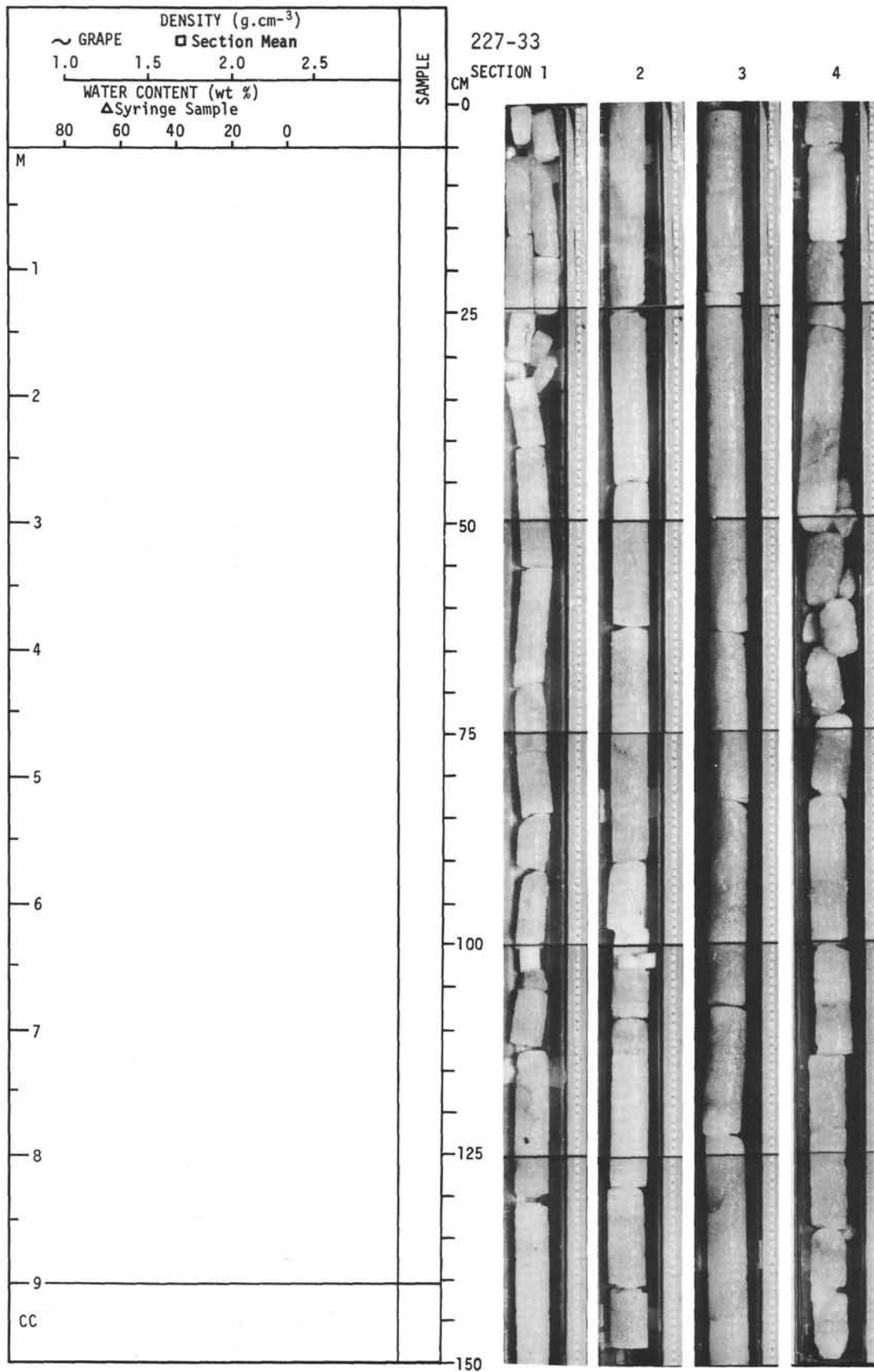
For Explanatory Notes, see Chapter 2



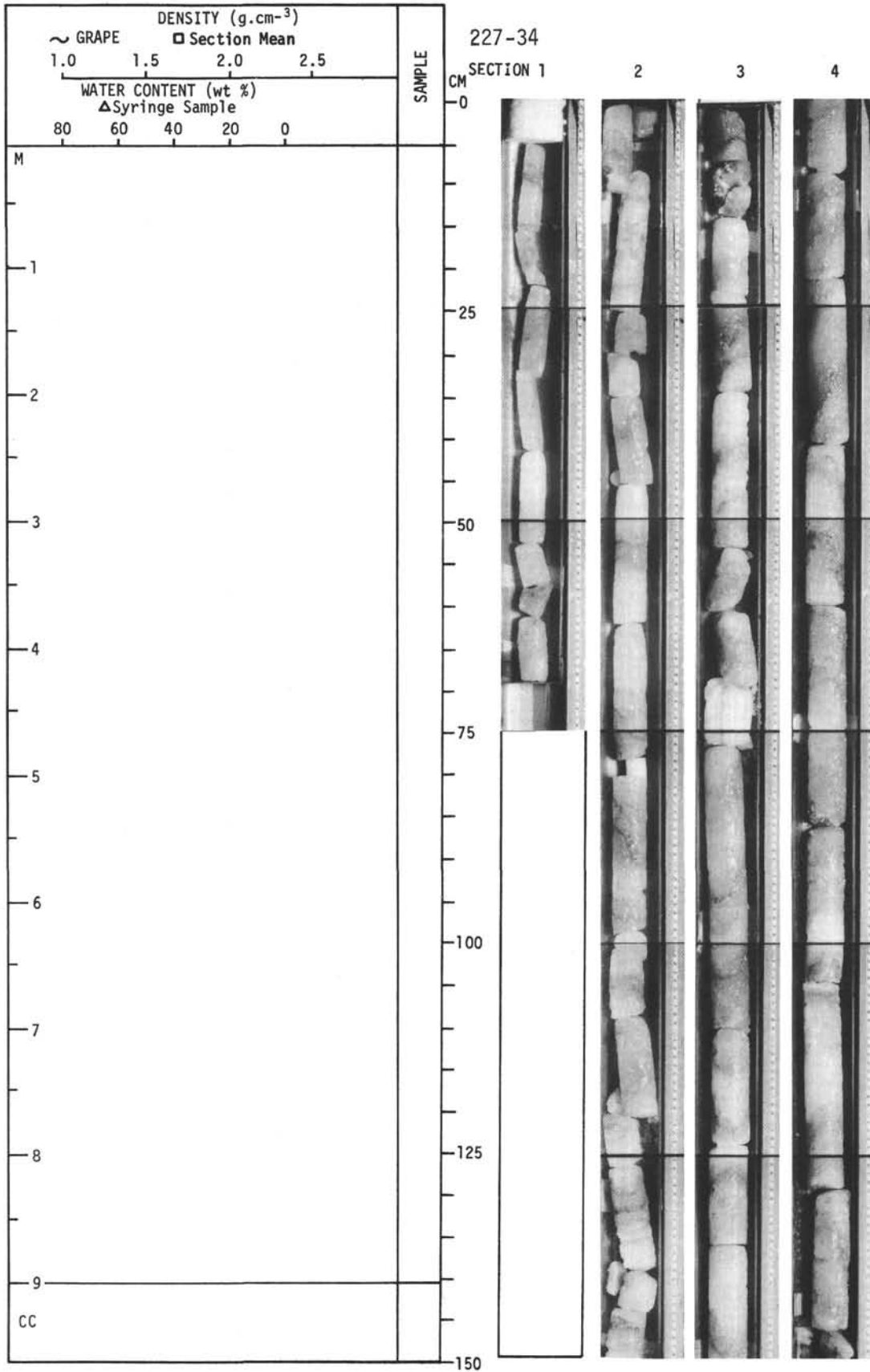
For Explanatory Notes, see Chapter 2



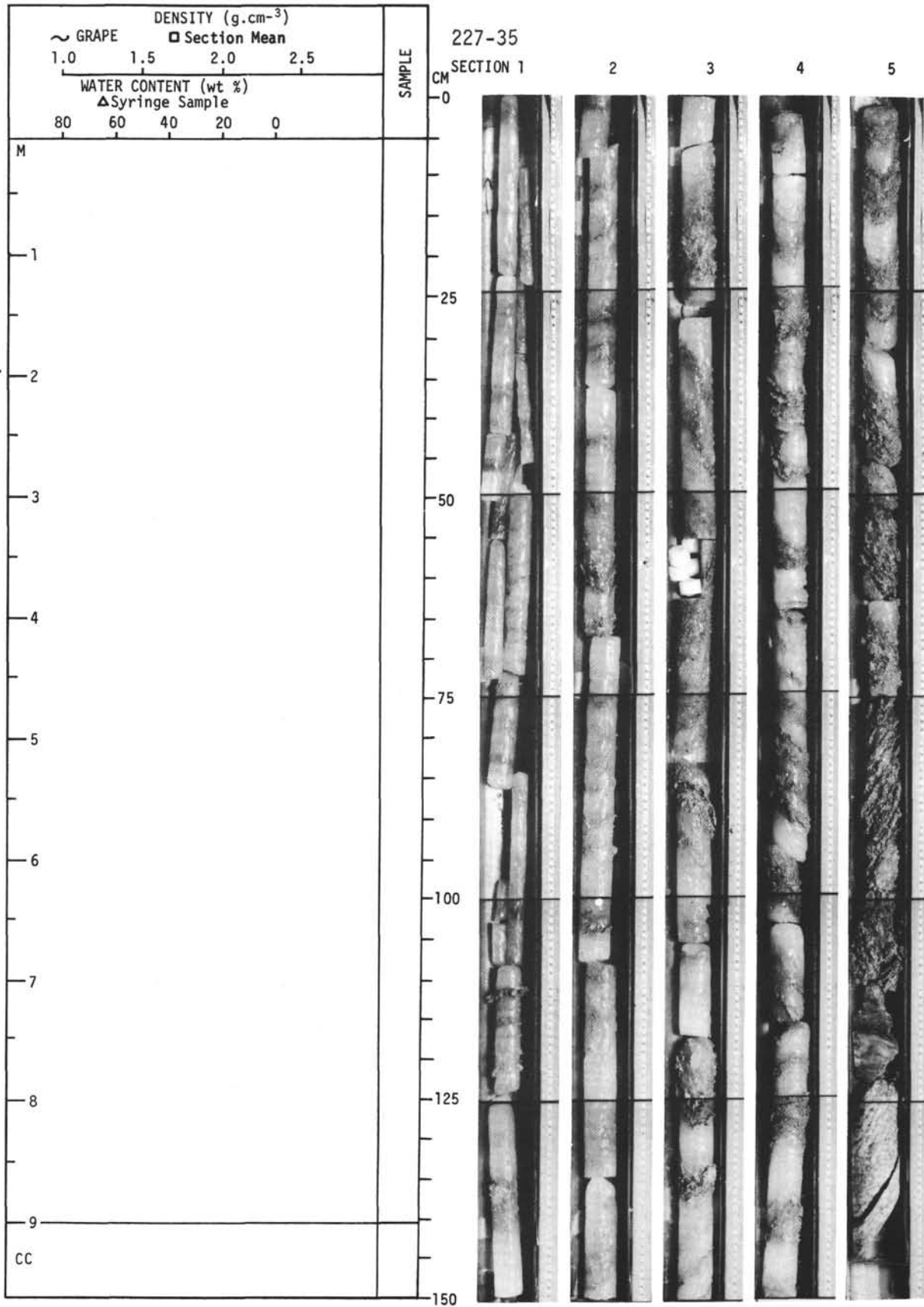
For Explanatory Notes, see Chapter 2



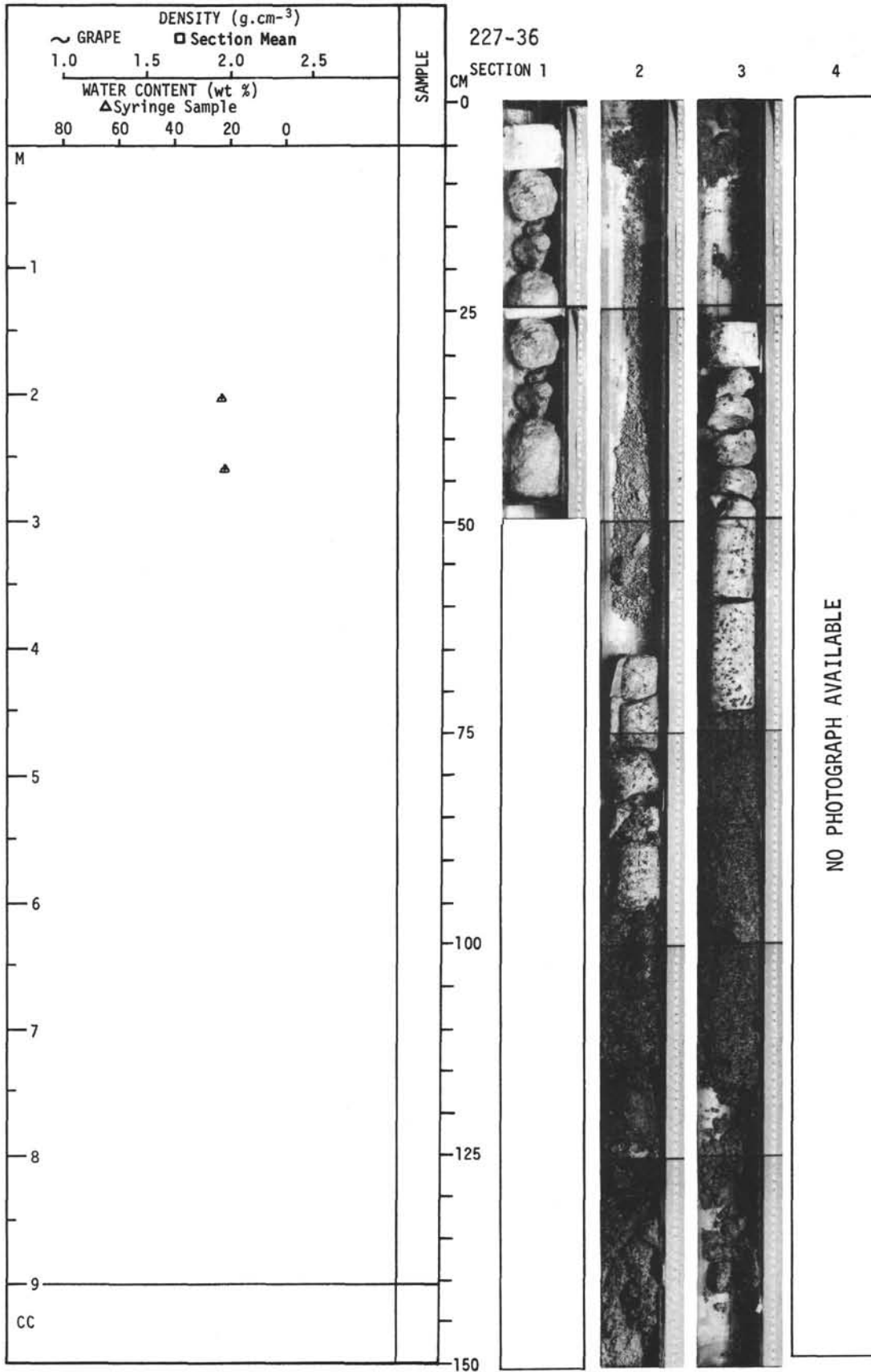
For Explanatory Notes, see Chapter 2



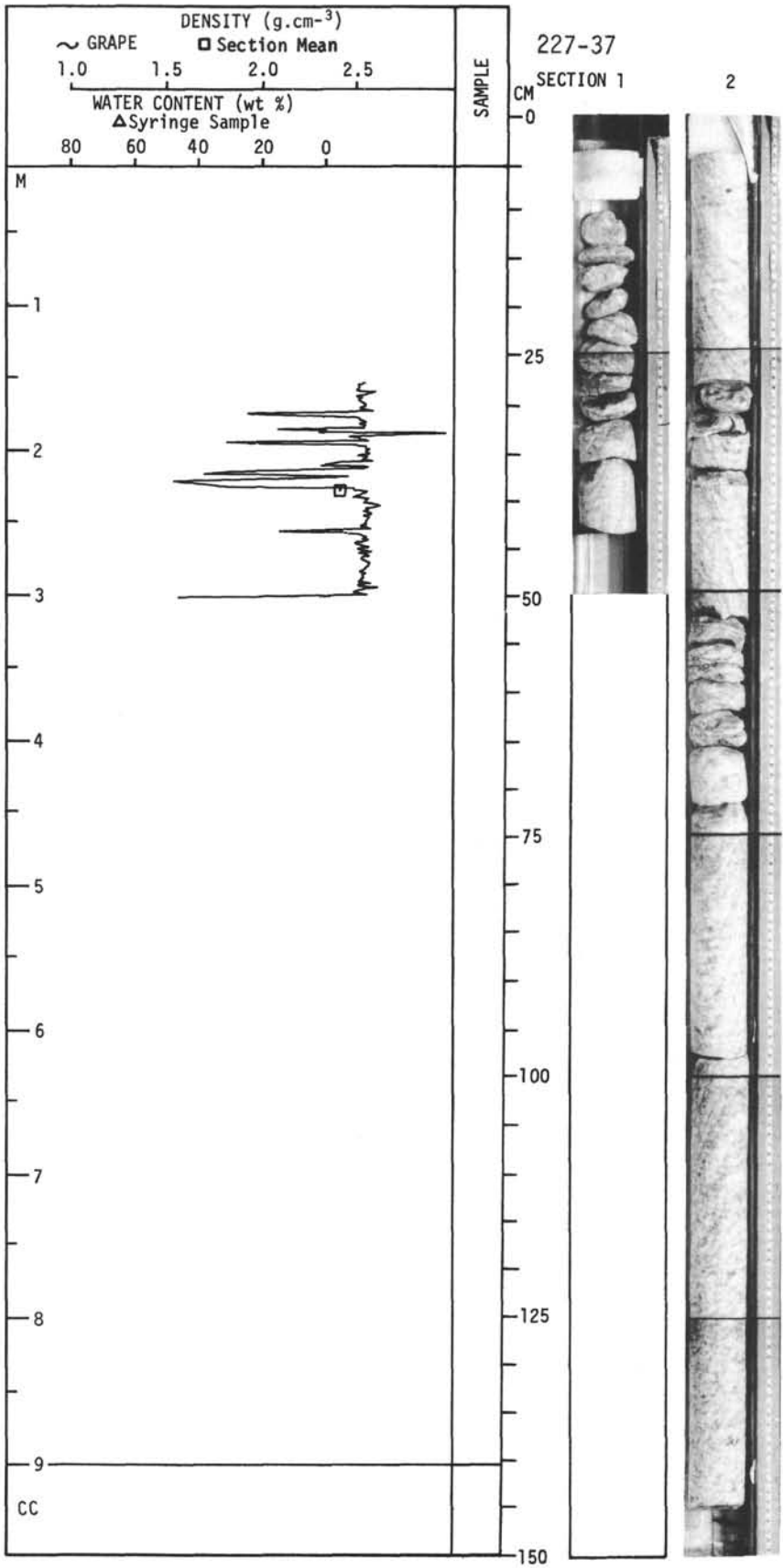
For Explanatory Notes, see Chapter 2



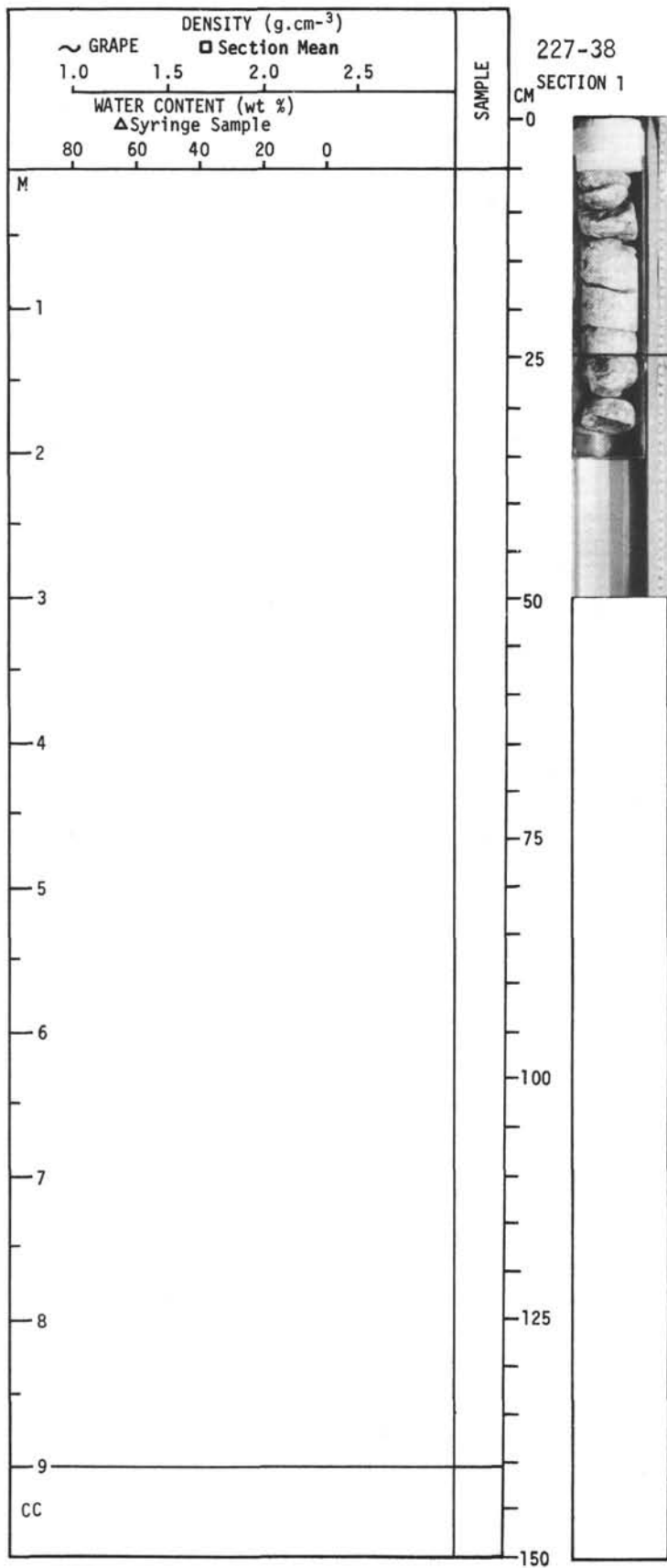
For Explanatory Notes, see Chapter 2



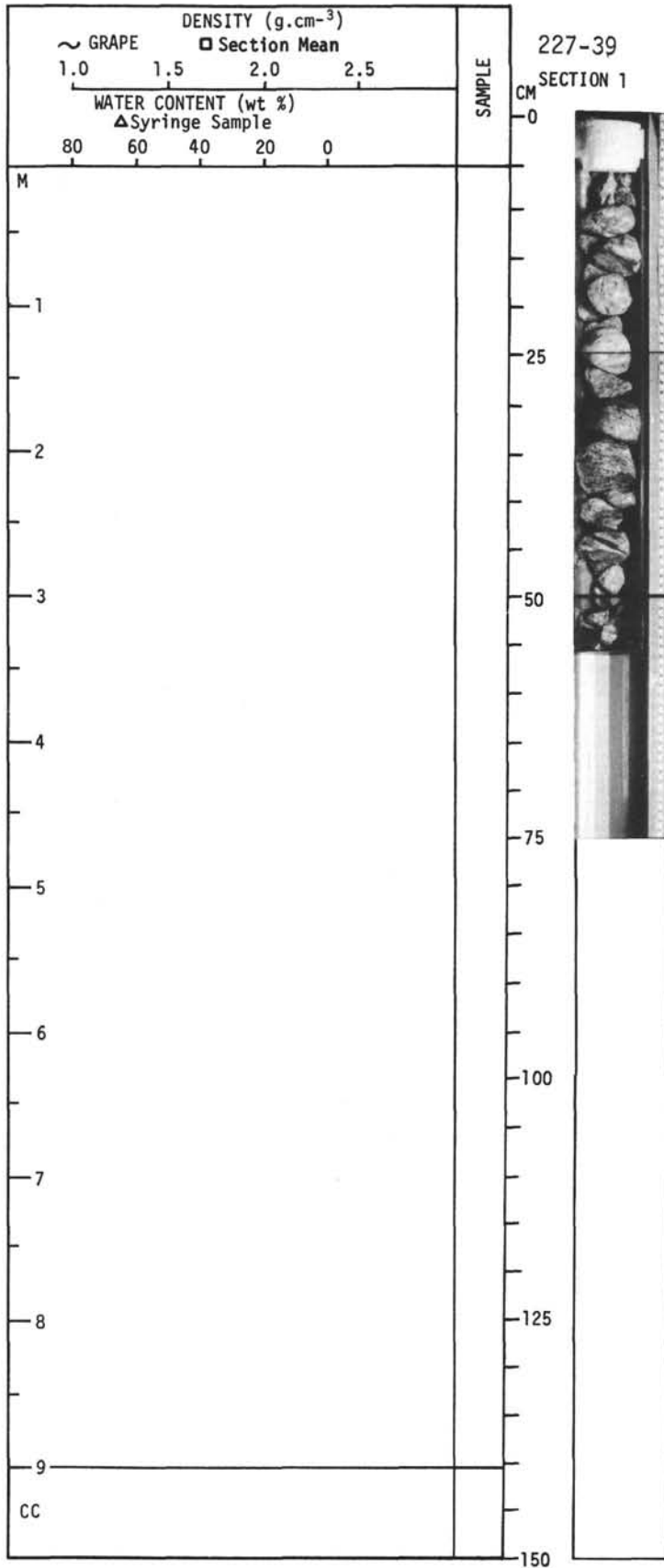
For Explanatory Notes, see Chapter 2



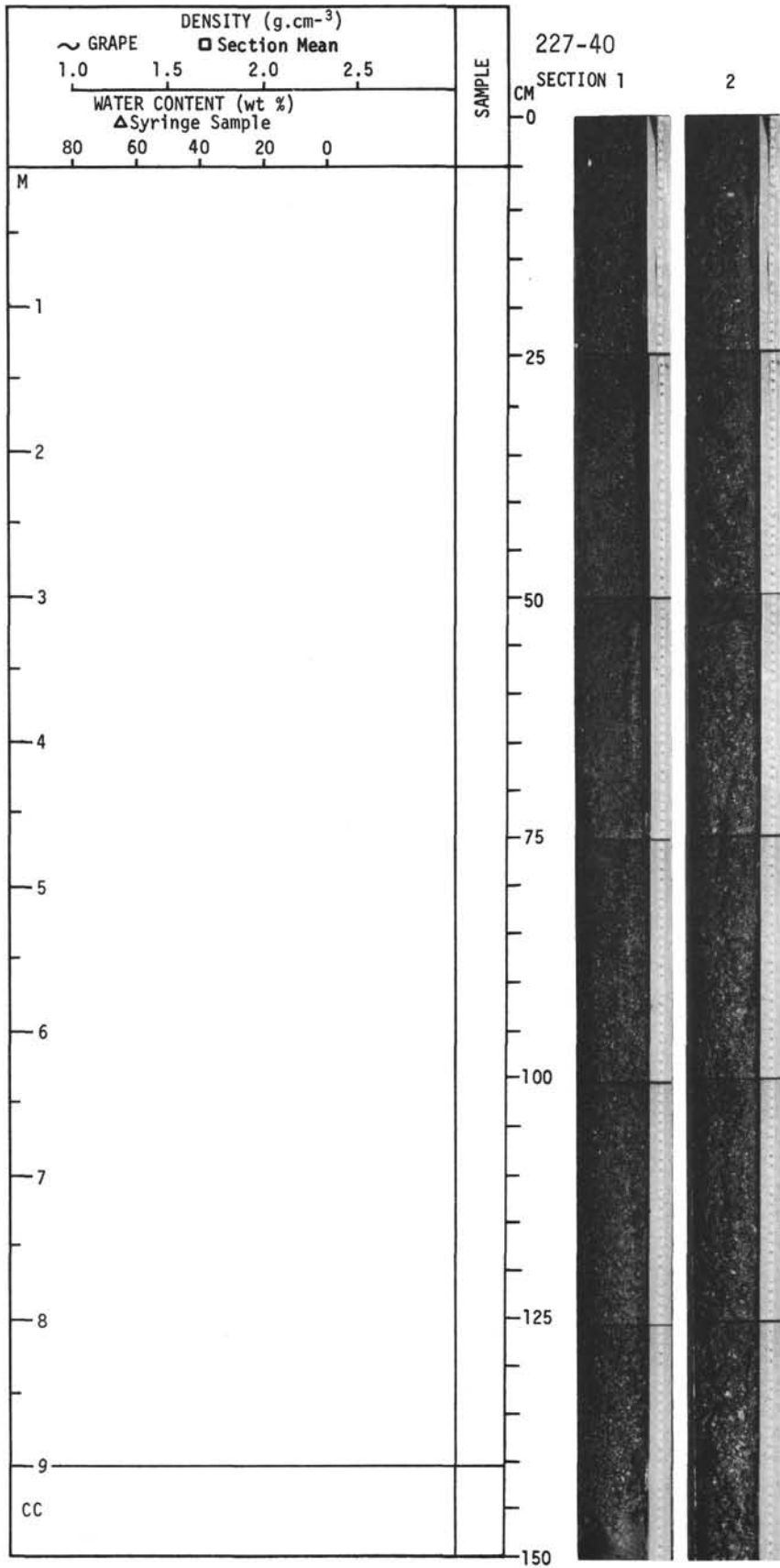
For Explanatory Notes, see Chapter 2



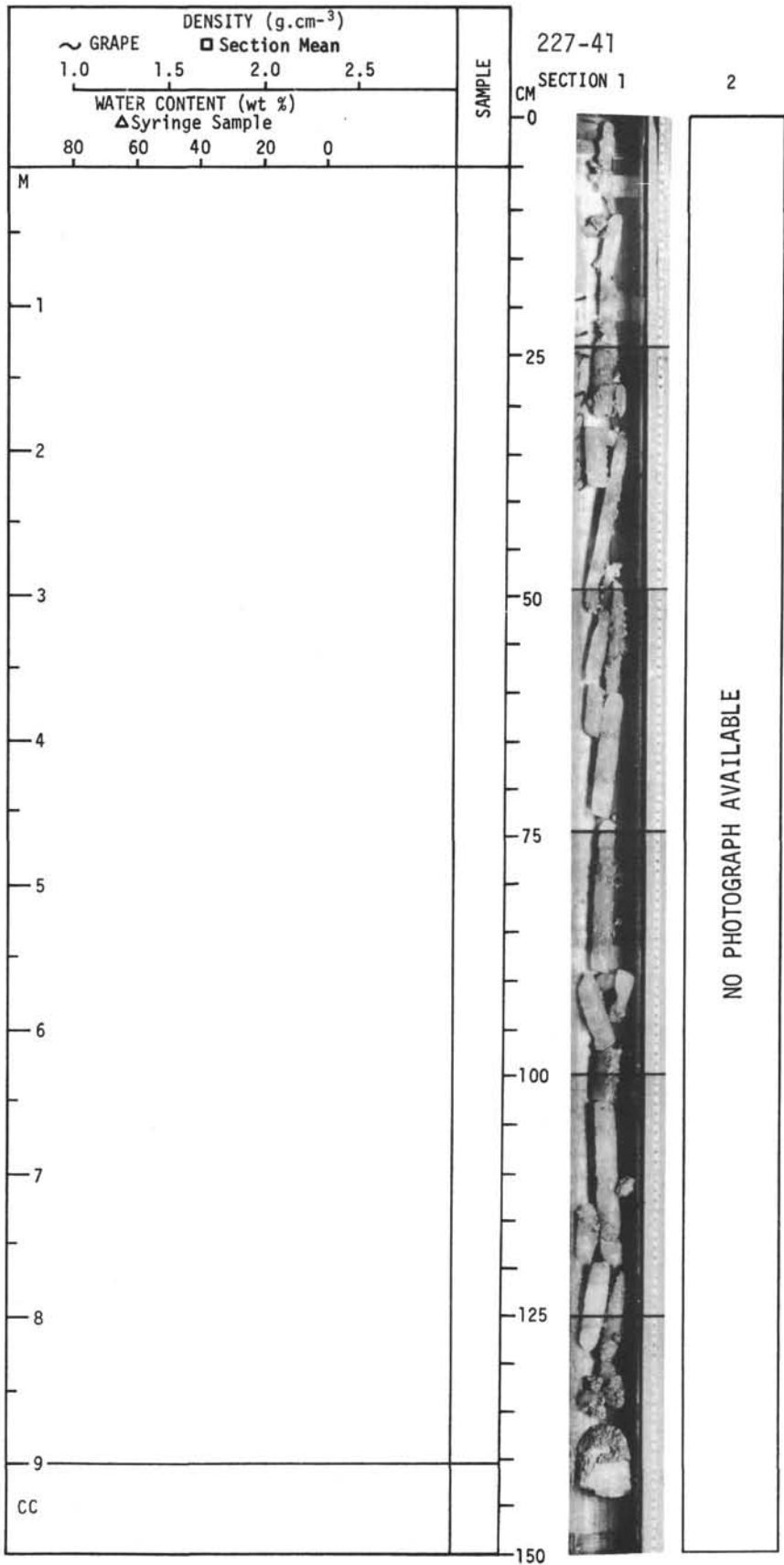
For Explanatory Notes, see Chapter 2



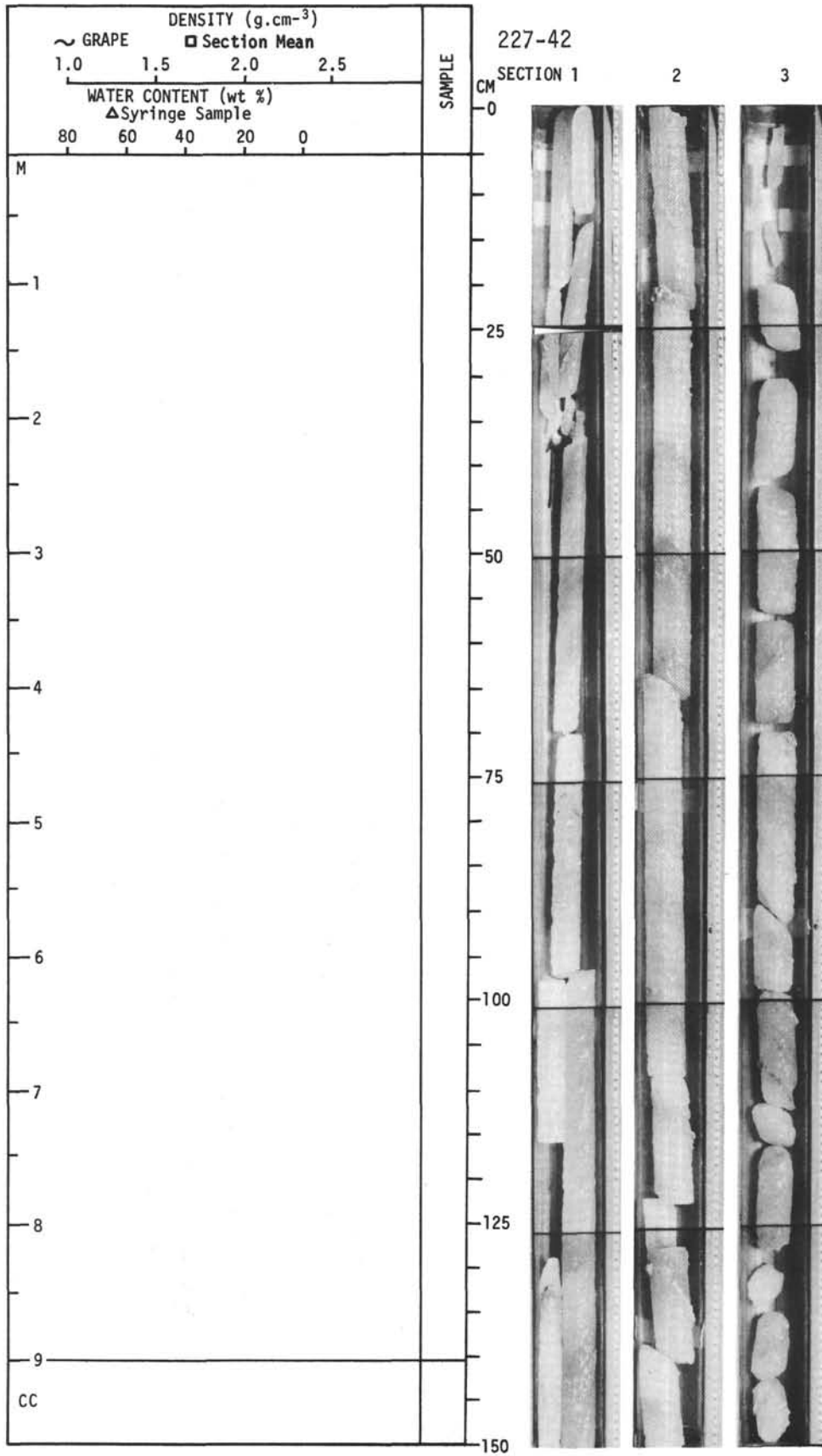
For Explanatory Notes, see Chapter 2



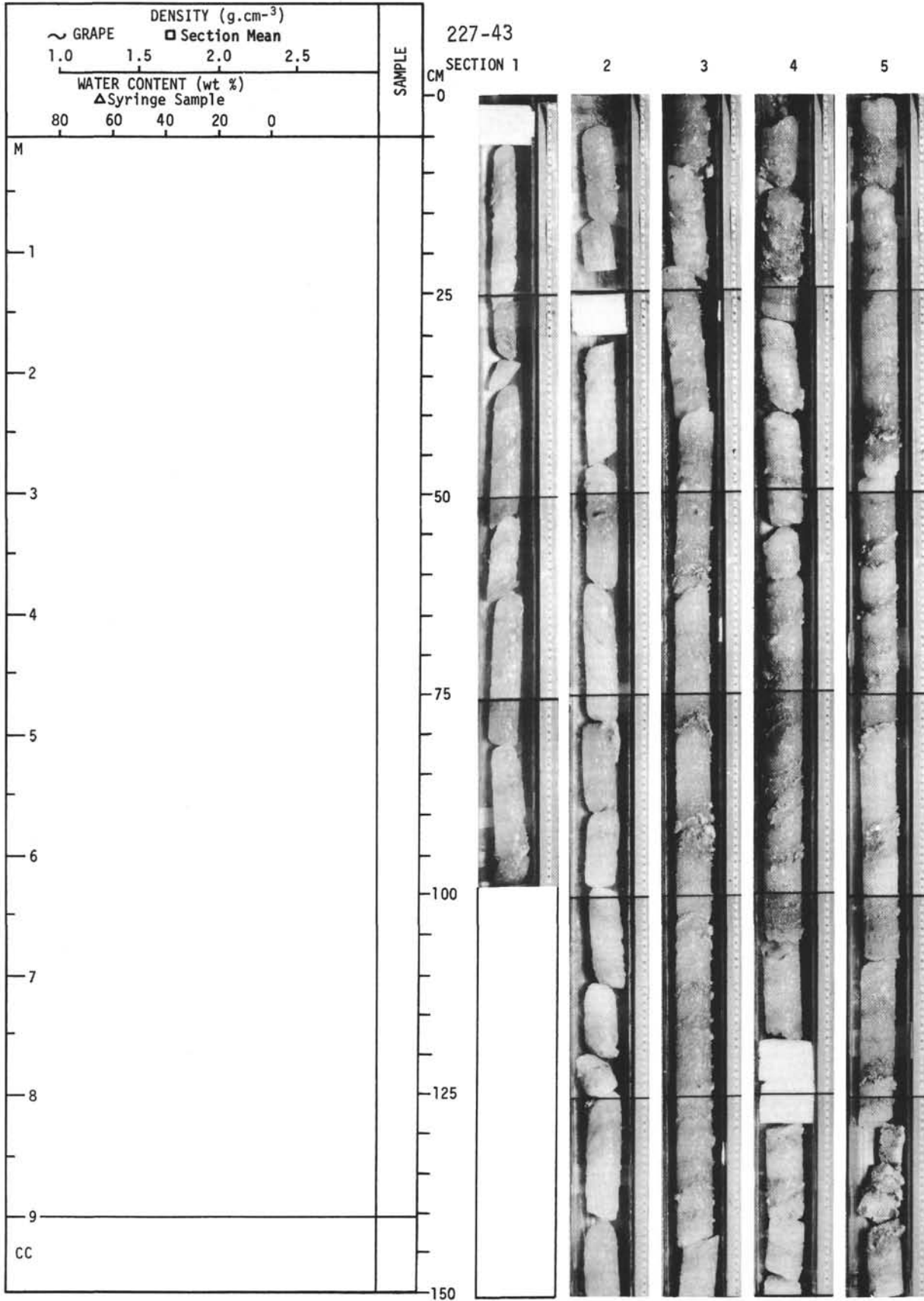
For Explanatory Notes, see Chapter 2



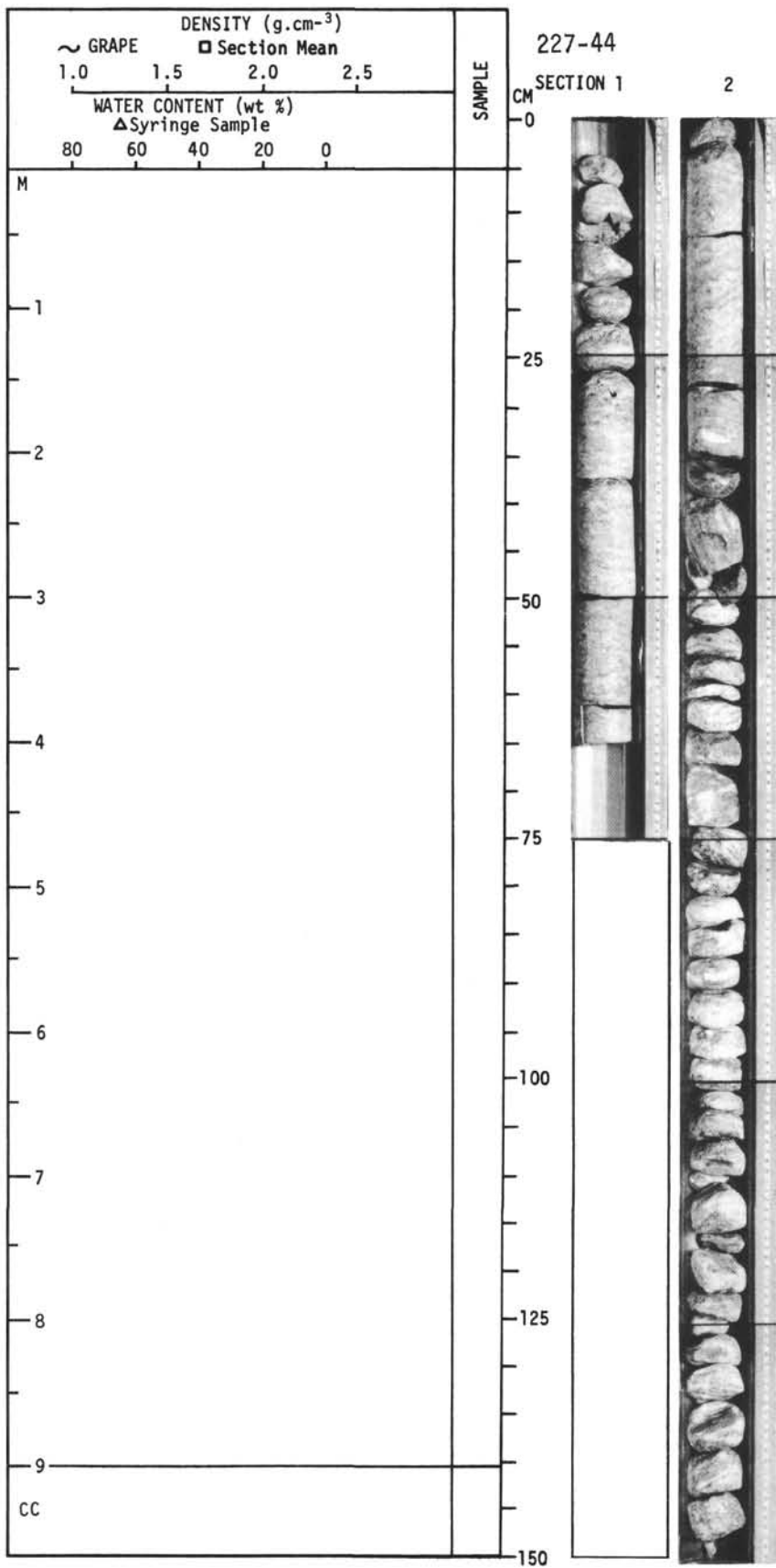
For Explanatory Notes, see Chapter 2



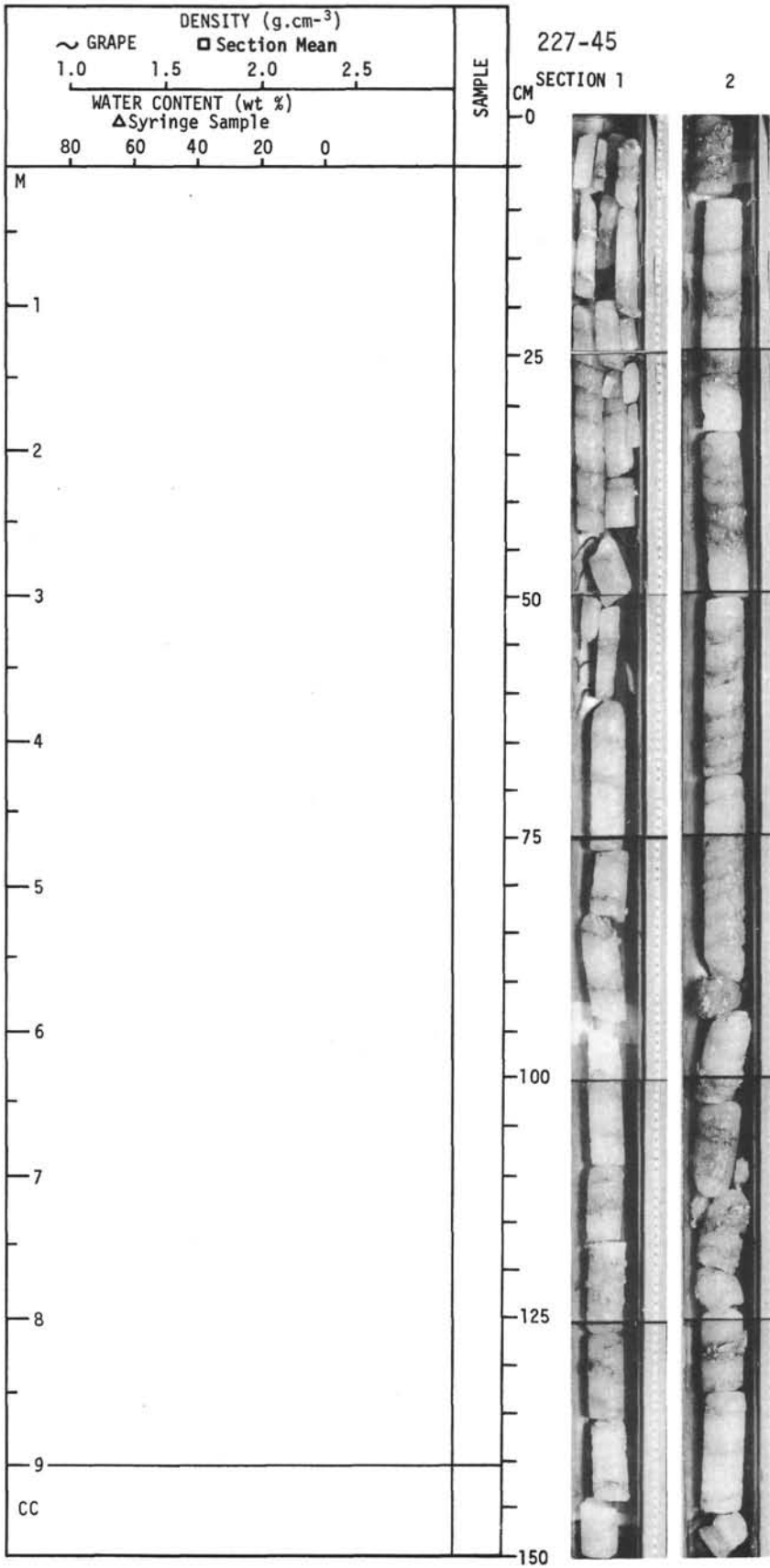
For Explanatory Notes, see Chapter 2



For Explanatory Notes, see Chapter 2



For Explanatory Notes, see Chapter 2



For Explanatory Notes, see Chapter 2